University of Alberta

Left Ventricular Ejection Fraction and Volume Calculations Using Three-Dimensional Echocardiography

by

Peter William Wood

A thesis submitted to the Faculty of Graduate Studies and Research

in partial fulfillment of the requirements for the degree of

Master of Science

in

Experimental Medicine

Department of Medicine

Spring 2014

Edmonton, Alberta

Abstract

In a review encompassing 18 single- and multi-centre studies comparing echocardiography with magnetic resonance imaging, it was determined that three-dimensional echocardiography has greatly improved the calculation of left ventricular (LV) volumes. However, there is still a systematic underestimation of volume measurements, and experimental studies have yet to be performed. This project sought to assess the accuracy of current semi-automatic contour finding algorithms using an anatomically correct dynamic heart phantom. The contour algorithm resulted in an underestimation of up to 31% of the true volume. With manual correction this reduced to 21%. None of the semi-automatic contours followed completely the true ventricular border. The manual method of discs (MOD) technique was proposed as a method which may improve accuracy in patients with asymmetric ventricles; the largest difference was 9% of the true volume. Therefore, while currently available LV contouring algorithms further underestimate volumes in asymmetrical chambers, MOD is an accurate alternative.

Acknowledgments

First and foremost, I would like to thank Prof. Harald Becher for introducing me to the world of research and giving me the opportunity to start down a new and exciting career path. Without his support, belief and guidance, this opportunity would have never presented itself.

Furthermore, I would like to thank his research team Dr. Patrick Gibson, Dr. Hayrapet Kalashian, Eila Mirhadi, Allen He and Nerys Jones for all their assistance during my time in the department. They are a well-oiled machine without which I would have been unable to accomplish this thesis.

Prof. Robert Haennel provided some wise words and guidance throughout my time here and it is with his navigation that I found my true path.

Prof. Pierre Boulanger and Dr. Kumaradevan Punithakumar were a dynamic team of researchers to collaborate with, and they allowed me to be a part of projects with a high level of innovation and technology that I'd believed to be science fiction before joining them. Dr. Punithakumar was also a great help with the technical analysis and data processing during my experimental procedures.

The Canadian Heart and Stroke Foundation supported me financially throughout my MSc through an endowment supplied to Prof. Becher, which I am truly grateful for. Their involvement and support allows investigators to explore possibilities that put Canadian institutions at the forefront of world cardiovascular research.

Finally, I would like to thank all my friends (far and near – in particular Mr. Piers) and family for their exhaustive support throughout my personal and professional endeavors. In particular, my mother and father Alice and Russell Wood for their love and support in all the decisions and transitions I have made in my life, and my sister and brother Annabelle and Thomas Wood for always being there. Without these people in my life, I would be a ship without sails and wouldn't have a place to come home to.

Table of Contents

List of Tables

List of Figures

List of Abbreviations

2D ECHO	Two-dimensional echocardiography
3D ECHO	Three-dimensional echocardiography
3DQ	Subprogram of Philips QLAB v8.1 software for left ventricular volume calculation using Simpson's biplane rule
3DQadv	Subprogram of Philips QLAB v8.1 software for left ventricular volume calculation using a three-dimensional voxel counting method
4D-MSPECT	Four-dimensional myocardial single photon emission computed tomography software
A1	Analysis 1
A2	Analysis 2
ASE	American Society of Echocardiography
BA	Bland-Altman
Bt	Beat
CMR	Cardiac magnetic resonance imaging
CT	Computed tomography
CV	Coefficient of variability
D1	Dataset 1
D2	Dataset 2
D3	Dataset 3
D4	Dataset 4
D5	Dataset 5
DHP	Dynamic heart phantom
ECG	Electrocardiogram
EDV	End-diastolic volume
ESV	End-systolic volume
GE	General Electric
gSPECT	Gated single photon emission computed tomography
ICC	Intra-class correlation
LV	Left ventricle
LVEF	Left ventricular ejection fraction
MD	Mean difference
Method A1	Semi-automated volumetric method – without manual correction

Method A2	Semi-automated volumetric method + manual correction on end-systolic and end-diastolic volumes, before processing the entire three-dimensional dataset
Method A3	Semi-automated volumetric method + manual correction at all time points after processing the entire three-dimensional dataset
Method B	Simpson's biplane method of discs on optimised orthogonal 2D planes of a 3D dataset
Method C	Method of three-dimensional volume calculation involving manual tracing of a stack of short axis discs
MOD	Method of discs
MRI	Magnetic resonance imaging
PCC	Pearson's correlation coefficient
PH	Philips
Pl	Plane
QGS	Quantitative gated single photon emission computed tomography software
RAPU	Remote advanced playback unit
RNV	Radionuclide ventriculography
SD	Standard deviation
SI	Siemens
SSFP	Steady state free procession
TGE	Turbo gradient echo
UN	Unknown
VSA	Visual show automation

1 Introduction to Echocardiographic Assessment of Left Ventricular Function: Ejection Fraction and Volume Calculations

Left ventricular ejection fraction (LVEF) is currently one of the most valued and validated tools for determining patient outcome in cardiology (1). There is strong evidence associating a decline in ejection fraction with an increase in mortality (2). Since LVEF guides treatment options for people both with a clinical diagnosis of heart disease and without (such as those referred for chemotherapy), accurate LVEF calculations are of critical prognostic importance (3). The formula for calculating left ventricular ejection fraction is:

$$LVEF = \frac{EDV - ESV}{EDV} \times 100$$

where EDV is end-diastolic volume and ESV is end-systolic volume.

In other words, LVEF is equal to stroke volume as a percentage of EDV. It is clear that accurate volume calculations are paramount to an accurate ejection fraction. Furthermore, volume measurements have been reported to be important diagnostic indicators of such diseases as dilated cardiomyopathy, indicated by volumes exceeding that of the normal range (4,5).

A normal left ventricle (LV) has an ellipsoid shape (6). This known geometry has been used to devise many methods of volume calculation by echocardiography, each with varying degrees of accuracy (7).

With the first echocardiography scanners, when only diameters of the cavities could be measured, Quinones, Dumesnil, Baran and Nanda and Teichholz methods were used (8-11). These diameter measurements using M-mode, and later two-dimensional (2D) echocardiograms, allowed LV volumes and LVEF to be calculated by different formulas assuming an ellipsoid shaped ventricle. While innovative at the time, the Quinones method, for example, could not adapt to other LV morphologies. Due to this and other proven inaccuracies in ventricles with abnormal shapes and regional wall motion abnormalities, these methods are not recommended anymore by the American and European Societies of Echocardiography (4,5).

Reference:

(1) Klem I, Shah DJ, White RD, Pennell DJ, van Rossum AC, Regenfus M, et al. Prognostic value of routine cardiac magnetic resonance assessment of left ventricular ejection fraction and myocardial damage: an international, multicenter study. Circulation: Cardiovasc Imaging 2011 Nov;4(6):610-619.

(2) Curtis JP, Sokol SI, Wang Y, Rathore SS, Ko DT, Jadbabaie F, et al. The association of left ventricular ejection fraction, mortality, and cause of death in stable outpatients with heart failure. J Am Coll Cardiol 2003 August 20;42(4):736-742.

(3) Ewer MS, Lenihan DJ. Left Ventricular Ejection Fraction and Cardiotoxicity: Is Our Ear Really to the Ground? J Clin Oncol 2008 March 10;26(8):1201-1203.

(4) Lang RM, Bierig M, Devereux RB, Flachskampf FA, Foster E, Pellikka PA, et al. Recommendations for Chamber Quantification: A Report from the American Society of Echocardiography's Guidelines and Standards Committee and the Chamber Quantification Writing Group, Developed in Conjunction with the European Association of Echocardiography, a Branch of the European Society of Cardiology. J Am Soc Echocardiogr 2005 12;18(12):1440-1463.

(5) Lang RM, Bierig M, Devereux RB, Flachskampf FA, Foster E, Pellikka PA, et al. Recommendations for chamber quantification. Eur J Echocardiogr 2006 Mar;7(2):79-108.

(6) Otto CM. Textbook of Clinical Echocardiography. Fifth ed. Waltham, MA, USA: Elsevier Inc.; 2013.

(7) Dorosz JL, Lezotte DC, Weitzenkamp DA, Allen LA, Salcedo EE. Performance of 3-dimensional echocardiography in measuring left ventricular volumes and ejection fraction: a systematic review and meta-analysis. J Am Coll Cardiol 2012 May 15;59(20):1799-1808.

(8) Quinones MA, Waggoner AD, Reduto LA, Nelson JG, Young JB, Winters WL,Jr, et al. A new, simplified and accurate method for determining ejection fraction with two-dimensional echocardiography. Circulation 1981 Oct;64(4):744-753.

(9) Dumesnil JG, Dion D, Yvorchuk K, Davies RA, Chan K. A new, simple and accurate method for determining ejection fraction by Doppler echocardiography. Can J Cardiol 1995 Dec;11(11):1007-1014.

(10) Baran AO, Rogal GJ, Nanda NC. Ejection fraction determination without planimetry by two-dimensional echocardiography: A new method. J Am Coll Cardiol 1983 6;1(6):1471-1478.

(11) Teichholz LE, Kreulen T, Herman MV, Gorlin R. Problems in echocardiographic volume determinations: echocardiographic-angiographic correlations in the presence of absence of asynergy. Am J Cardiol 1976 Jan;37(1):7-11.

2 Current Echocardiographic Methods for Assessment of Left Ventricular Function

There are currently three methods of left ventricular (LV) function assessment recommended by the American and European governing bodies for echocardiography: two-dimensional echocardiography (2D ECHO), contrast 2D ECHO, and three-dimensional echocardiography (3D ECHO). Furthermore, a fourth method exists, contrast 3D ECHO, which requires a larger evidence base before it will be introduced into common echocardiographic practice (Table 2.1).

2.1 Two-Dimensional Echocardiography

2D ECHO is achieved using a phased array transducer that transmits an ultrasound beam that sweeps across a sector; the same beam also receives ultrasound signals from backscattering. The sector width can be modified by the echocardiographer, however, the default width is 90 degrees (1). The ultrasound image is achieved by transforming the received ultrasound signals into video signals where brightness displays the amplitude (2). The phased array transducer achieves this via an array of piezoelectric crystals that vibrate and generate an acoustic signal when electrical energy is applied to them. 2D ECHO provides multiple cross section views of the heart. 2D ECHO LV volume calculations are performed on two orthogonal views, the four chamber (4CV) and the two chamber (2CV) views (Fig. 2.1). In order to obtain the 4CV and 2CV, the echocardiographer places the probe on the area of the chest where the apex of the heart can be felt. These views are at 90 degrees of transducer rotation to each other and provide 2D assessment of the septal, lateral, apical and basal territories in the 4CV and anterior, inferior, apical and basal territories in the 2CV.

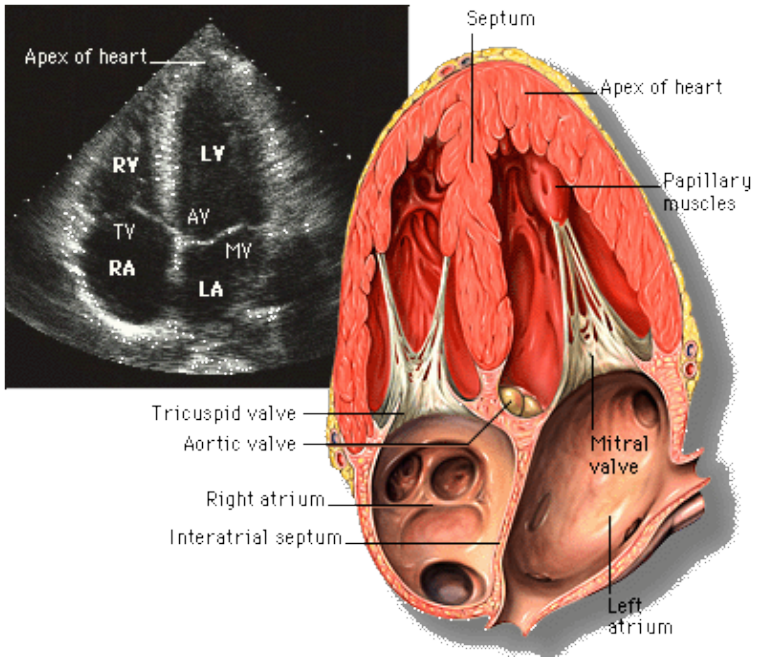

a

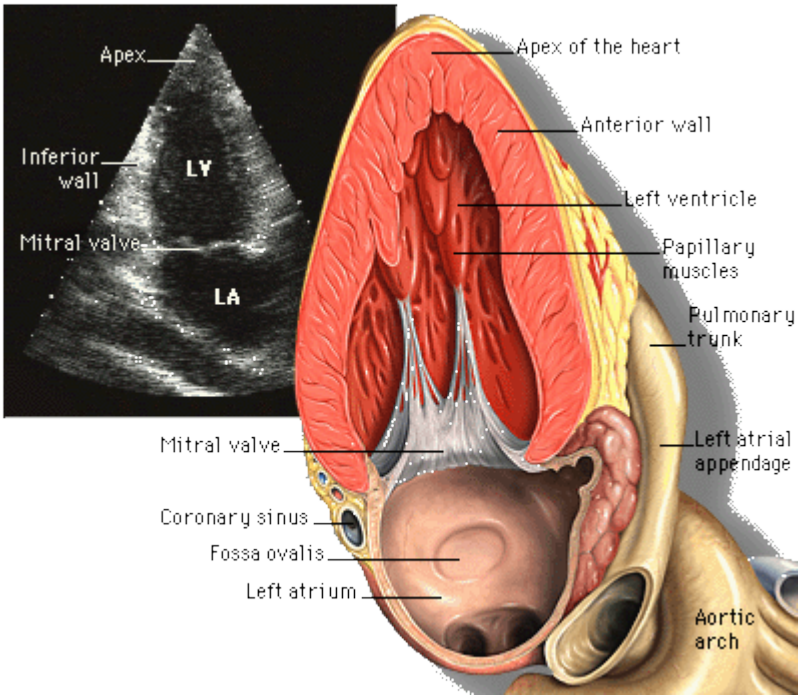

b

Figure 2.1 Comparison of apical four chamber (a) and apical two chamber (b) views of the left ventricle in a human study. Image cited from the Atlas of Echocardiography, Yale University (3).

The method for calculating LV volume recommended by the American Society of Echocardiography and European Association of Echocardiography is the Simpson's biplane method (or method of discs, or modified Simpsons rule) (4,5)**.** This method

calculates volume based on the sum of 20 stacked discs each of which has a volume determined by manually delineated borders and an assumed ellipsoid shape of the ventricle (Fig 2.2). The Simpson's biplane formula allows for an integrated calculation of volumes from both the 4CV and 2CV, reducing the amount of geometrical assumption performed by the calculation to a minor extent.

The formula is:

$$V = \frac{\pi}{4} \sum_{i=1}^{20} \alpha_i \beta_i \frac{L}{20}$$

where α_i and β_i are the diameters of the discs in the 4CV and 2CV, respectively, 20 is the number of discs in each 2D stack, and L is the longest ventricular length of the two views (6).

The area is delineated by the user along the endocardial border of the ventricle, including the papillary muscles (4,5) (Fig. 2.2). This differs from magnetic resonance imaging where the papillary muscles are excluded from the total volume calculated (7). In order to obtain the volumes from the 2CV and 4CVs, the operator has to trace the border of the myocardium to the cavity (Fig. 2.3). The two orthogonal views for measurement of the LV volumes have to cut through the apex and the ring of the mitral valve. This is a source for potential errors as the echocardiographers have to find the longest axis of the LV in each view by moving the ultrasound transducer across the chest (4,5).

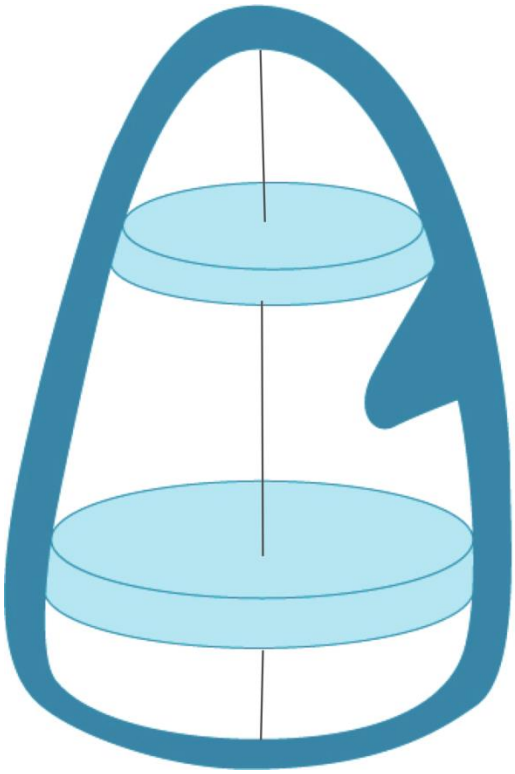

Figure 2.2 Illustration representing the principle of the Simpson's biplane method of discs technique where a two-dimensional tracing assumes an ellipsoid shape. Image cited from 123sonography.com (8).

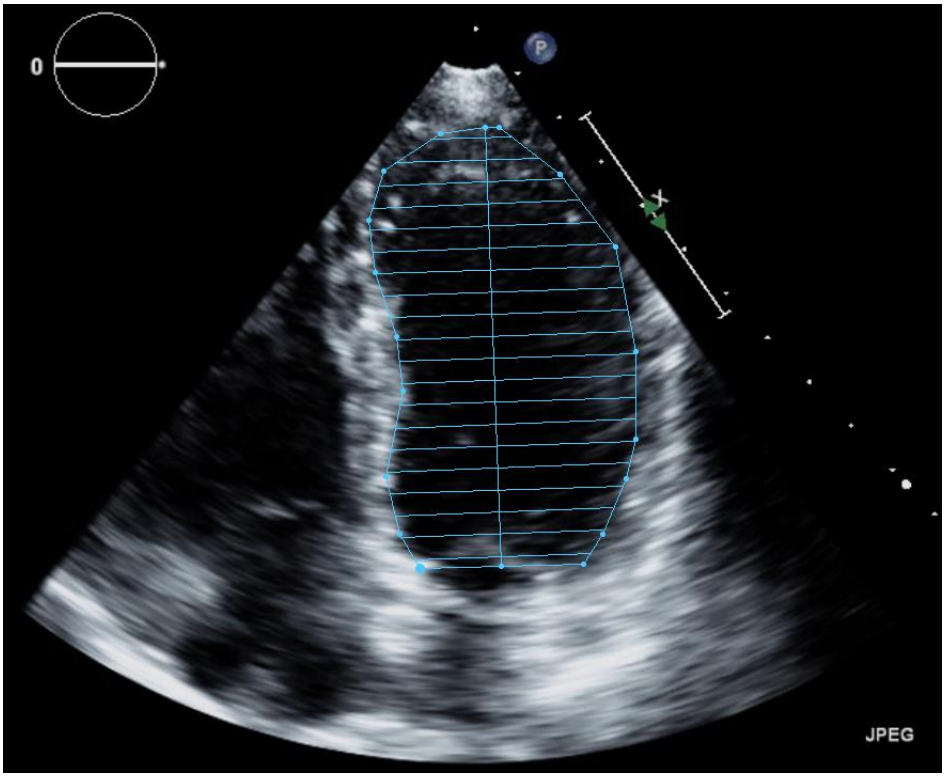

Figure 2.3 Two-dimensional echocardiography apical four chamber view of the left ventricle used for Simpson's biplane measurement for volume calculation.

Table 2.1 Advantages and limitations of echocardiographic techniques used for ventricular functional assessment

Method	Assessment Type	Geometrical Assumption	Advantages	Limitations
Linear	M mode	Yes	• Quick and easy to perform	• Assumes an ellipsoid shaped ventricle • Needs perpendicular parasternal imaging • Depends on acoustic window • Therefore least accurate method
2D	Simpson's biplane	Yes	• More accurate and reproducible than M mode.	• Assumes an ellipsoid shaped ventricle • Needs unforeshortened orthogonal views • Depends on acoustic window and operator experience • Endocardium often not fully visualised in a single frame used for manual tracing.
2D Contrast	Simpson's biplane	Yes	• More accurate and reproducible than 2D • Less susceptible to poor image quality	• As 2D; but less susceptible to poor image quality
3D Biplane	Simpson's biplane	Yes	• 2 orthogonal planes from the same beat • Avoids off-axis views and foreshortening	• Assumes an ellipsoid shaped ventricle. • Depends on acoustic window and operator experience • Full volume recordings require stable heart rhythm and breath hold (usually 4 beats) otherwise stitching artefacts • Real-time acquisition reduces image quality • Lower spatial and temporal resolution than 2D
3D	Voxel count	Partial	• Avoids off-axis views and foreshortening • Automatic border delineation following minimal landmark allocations • More accurate than 2D and 3D biplane	• Depends on acoustic window and operator experience • Full volume recordings require stable heart rhythm and breath hold (usually 4 beats) otherwise stitching artefacts • Real-time acquisition reduces image quality • Lower spatial and temporal resolution than 2D • Has problems fitting to some abnormal LV shapes (i.e. apical infarcts)
3D Contrast	Voxel count	Partial	• Best agreement with CMR and CT angiography	• Few studies available • Artefacts from apical contrast destruction and attenuation • Lowest spatial and temporal resolution • Not all software packages can perform LV assessment with the addition of contrast

LV = left ventricle; 2D = two-dimensional; 3D = three-dimensional; CMR = cardiac magnetic resonance imaging; CT = computed tomography

2.2 Two-Dimensional Contrast Echocardiography

Echocardiography has limitations which affect its accuracy and reproducibility. In any diagnostic ultrasound image, quality can be significantly limited by the attenuation of the sending and receiving signals. In echocardiography, this can manifest as an inability to accurately delineate the endocardial border, or, more severely, as a complete absence of one of the ventricular walls (9,10) (Fig. 2.4). These attenuation effects are largely due to the air in the lungs and bone reflection (ribs) (2). The first causes a reduction in image clarity and quality, whereas the second causes shadowing over those structures that lay behind the rib bone.

Ultrasound contrast agents have been developed to enhance the signal intensity and quality of the internal ventricular chamber blood volume against that of the myocardium. Thus, instead of identifying the endocardial border by muscle definition, the border is enhanced by the opacified blood in the chamber.

The method for volume and ejection fraction calculation with this imaging technique remains Simpson's biplane method, with the same methodology as standard 2D ECHO.

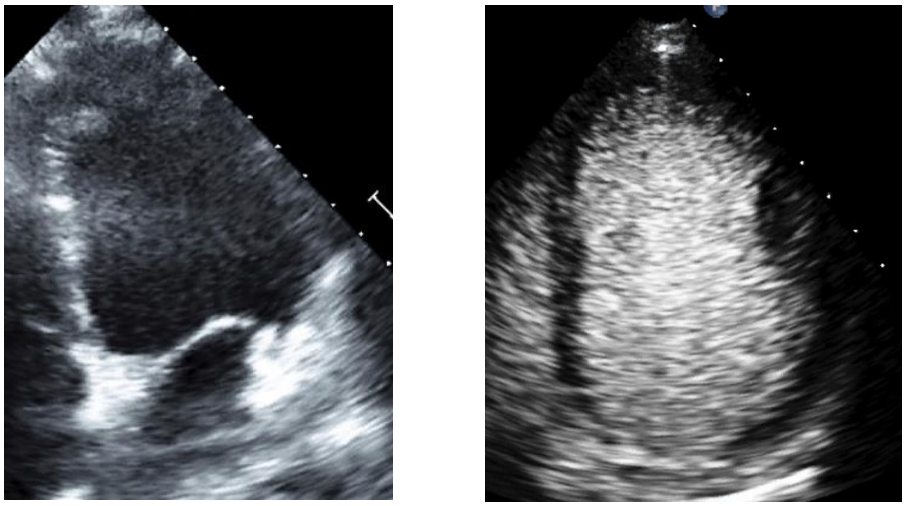

a **b**

Figure 2.4 Example of a patient with a poor acoustic window in the four chamber view using noncontrast two-dimensional echocardiography (a). The patient is injected with a microbubble contrast agent enhancing left ventricular opacification significantly, allowing easy identification of the left ventiruclar endocardial border for volume calculation (b).

When ultrasound contrast agents are used, the transmit power that the echocardiography scan heads deliver can be reduced. Under these conditions, the signals from heart structures such as the myocardium get weaker (=look darker, see Fig. 2.4b). The contrast in the cavity causes bright echoes, because the microbubbles resonate in the sound field when transmit power is low. The only disadvantage associated with contrast enhanced left ventricular opacification is that the strong sound scatters in the proximal image can affect the identification of basal segments in the distal image, in particular, the mitral annulus (10).

2.3 Three-Dimensional Echocardiography

The most promising advancement in ultrasound for LV function assessment in recent years has certainly been that of the development of 3D ECHO. The principle of this technique allows for a volume to be acquired instead of the multiple 2D planes required to cognitively approximate the shape of the ventricular chamber by the reading physician. The matrix array transducer, which allows for the acquisition of a 3D dataset, transmits from multiple lines crystals (3000 total crystals on the transducer head) instead of with a single array of crystals (as with the 2D phase array transducer) (11) (Fig. 2.5 & 2.6).

The acquired 3D ECHO image is viewed via three two-dimensional planes (two orthogonal long axis views and a short axis view). The analysis software allows the user to steer through each plane and visualise any structure of interest within the dataset. For volume calculations, this requires optimal alignment of the orthogonal long axis views so that foreshortening and volume inaccuracy is avoided (12) (Fig. 2.7).

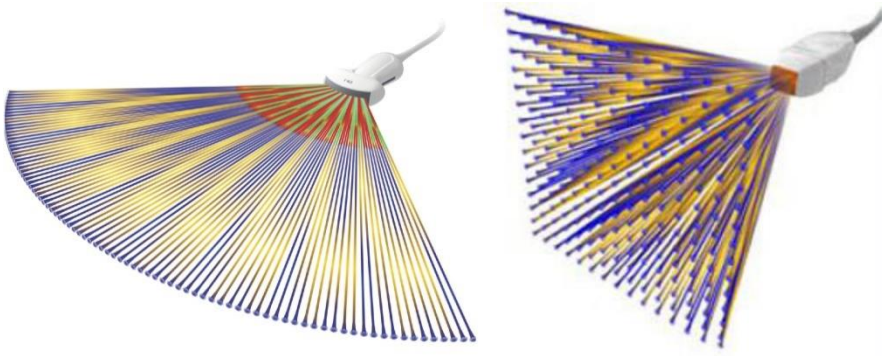

a **b**

Figure 2.5 Image depicting the dispersion of ultrasound beams in a two-dimensional (a) and three-dimensional (b) transducer. Images sourced from the Philips Ultrasound website: http://www.healthcare.philips.com/us_en/products/ultrasound/technologies/xmatrix.wpd (13).

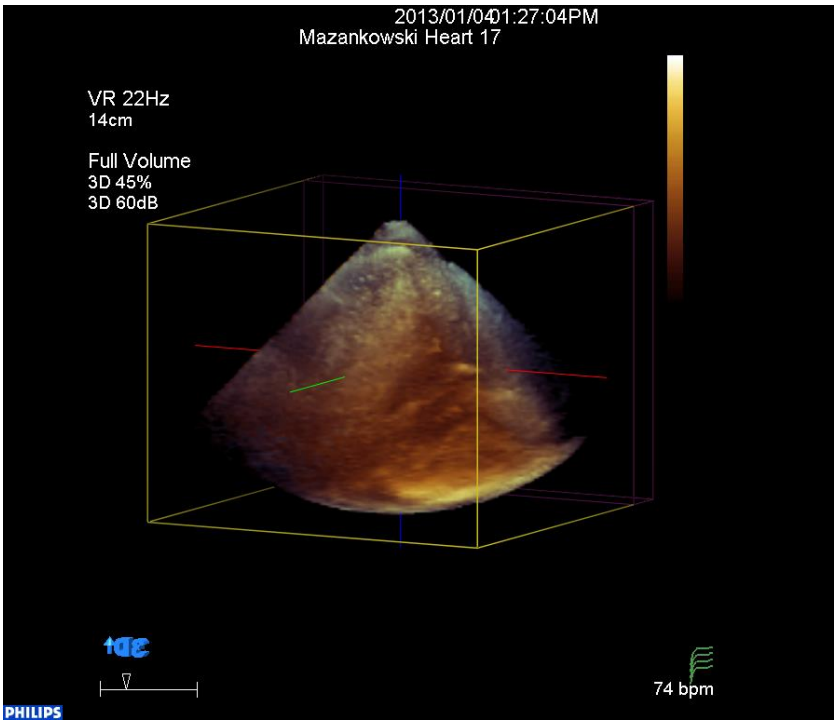

Figure 2.6 Example of a three-dimensional pyramidal ultrasound volume containing the entire structure of the heart within.

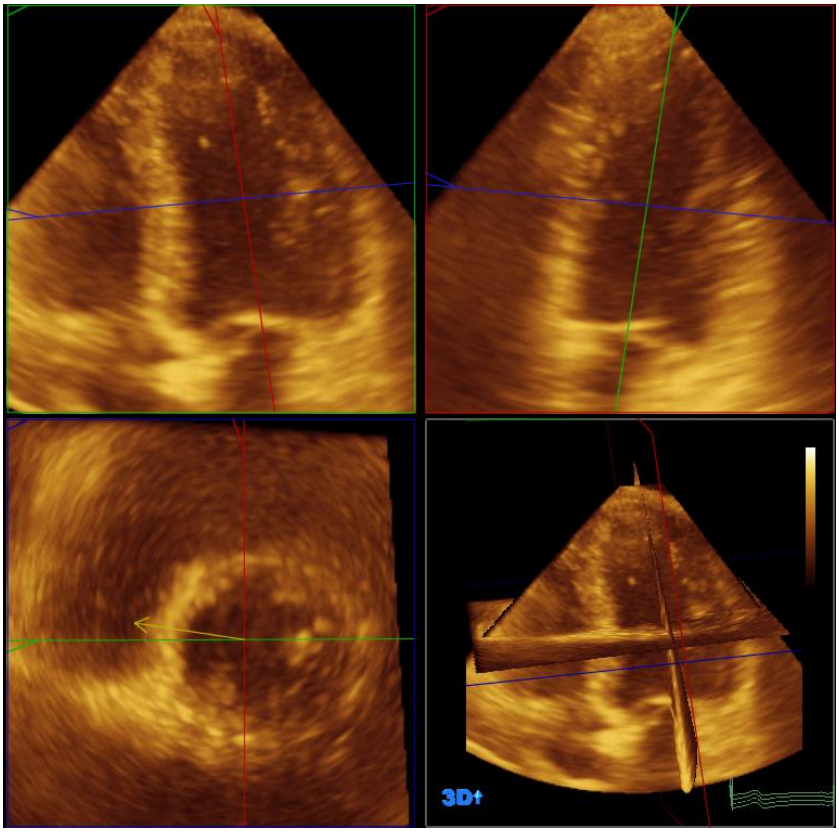

Figure 2.7 Example of the Philips QLAB quad screen displaying the three-dimensional ultrasound dataset of an adult patient. The red, blue and green axes, when rotated, allow viewing of the data.

With all the benefits that 3D ECHO adds to diagnostic cardiology, it has one large limitation – the image quality is not as high as that of its 2D counterpart. This is observed in both spatial (the ability to distinguish between two points) and temporal (the amount of information recorded over time) resolution. In order to counteract this limitation, the manufacturers of 3D ultrasound machines have designed a strategy that involves "stitching" together two or more (usually 4) subvolumes of ultrasound datasets (Fig. 2.8). This works because a smaller sector of ultrasound transmission uses the same number of scan lines to image a smaller area, increasing the amount of information in the sector. The recorded image of the first sector is played on a loop while the transducer transmits ultrasound to send and receive the second sector; usually four sectors are stitched together (12). Unfortunately, coupled with this method for improving image quality is another limitation related to movement of the patient or transducer. If the patient or transducer moves during image acquisition, then the stitched information will not line up correctly with the previous subvolume loops, and a "stitch" artefact will occur (12). In order to record

the entire LV in real-time, the ultrasound pyramidal volume transmitted and received needs to cover a sector of 90 degrees.

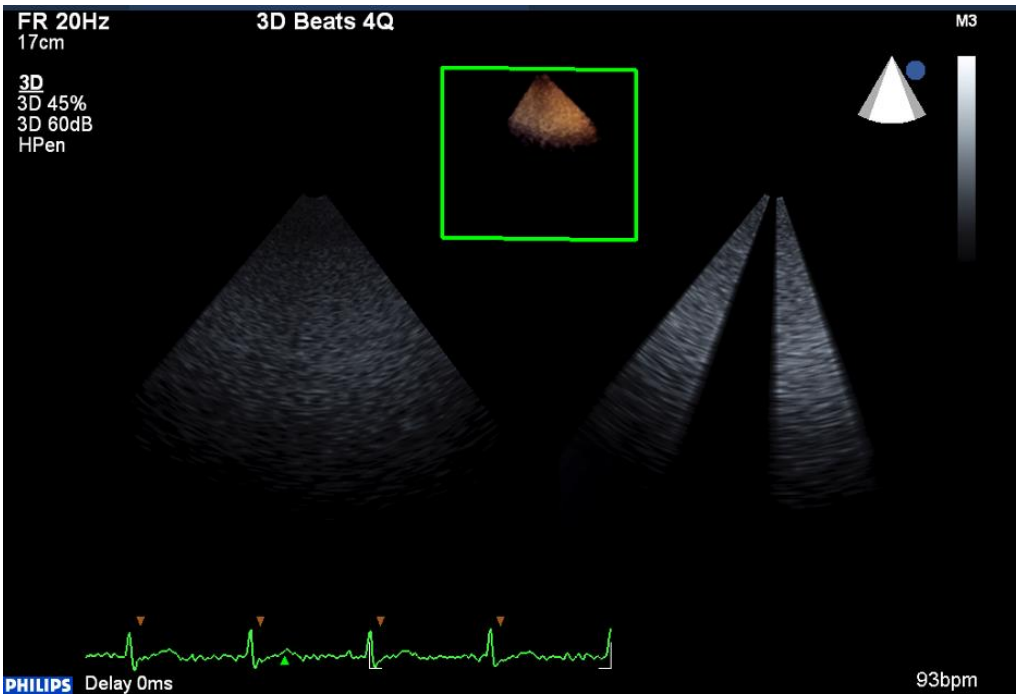

Figure 2.8 Image demonstrating the "stitching" of several ultrasound subvolumes, which allows a higher temporal resolution without loss of spatial resolution. Two of the four subvolumes being stitched together are evident on the right hand view.

In order to obtain volumes from 3D datasets several methods have been established: 1. application of the Simpson's biplane method is still available, implemented on two optimally aligned long axis views of a 3D dataset (Fig 2.9); 2. a true volumetric method which is also initiated by border identification in two long axis views from a 3D dataset (Fig 2.10); 3. and a 3D method of discs, which applies manual tracing of a stack of multiple short axis planes – similar to the technique used in magnetic resonance imaging (Fig 2.11). The most frequently used method for volume calculation has been the volumetric method, which, along with the semi-automatic calculation of end-diastolic and end-systolic volumes, generates a volume curve of the entire cardiac cycle (12). The volumes are calculated by counting the amount of voxels (known volume) within the contoured chambers giving a true 3D volume calculation. These algorithms have been demonstrated to be the most accurate and reproducible ultrasound techniques in comparison with the current reference standard cardiac magnetic resonance imaging (CMR) (12,14). The manual method of discs technique utilises the same methodology as in CMR, whereby the LV is sliced into 16 discs with the 3D dataset allowing direct area tracing of the short

axis slices – the individual short axis volumes are calculated and summed to give the total chamber volume.

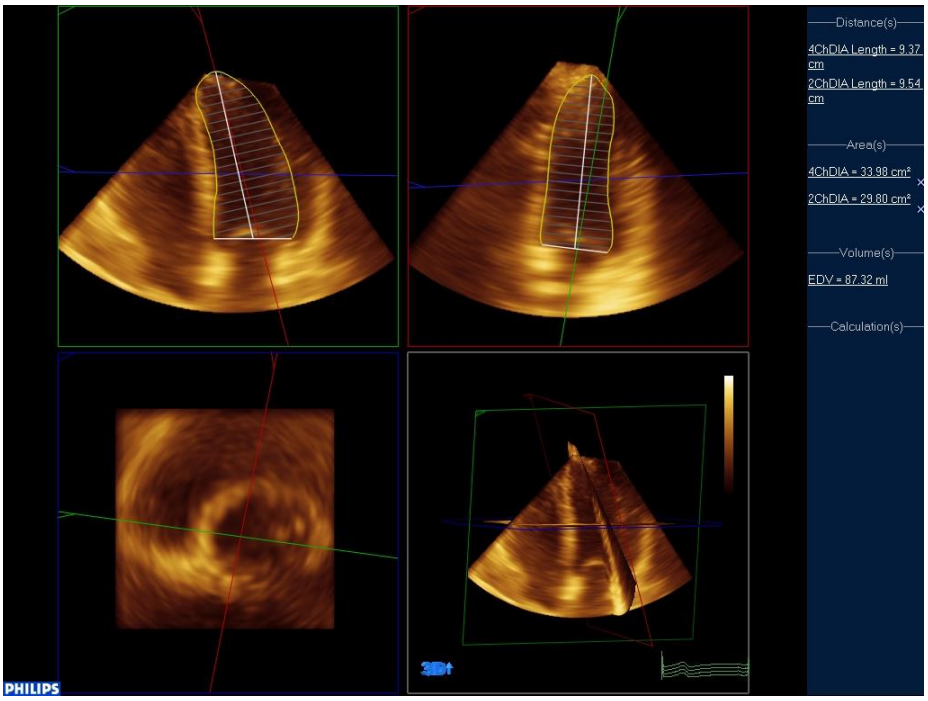

Figure 2.9 Snapshot of the Simpson's biplane method performed on a three-dimensional dataset. Depth 15cm. Volume rate 20Hz.

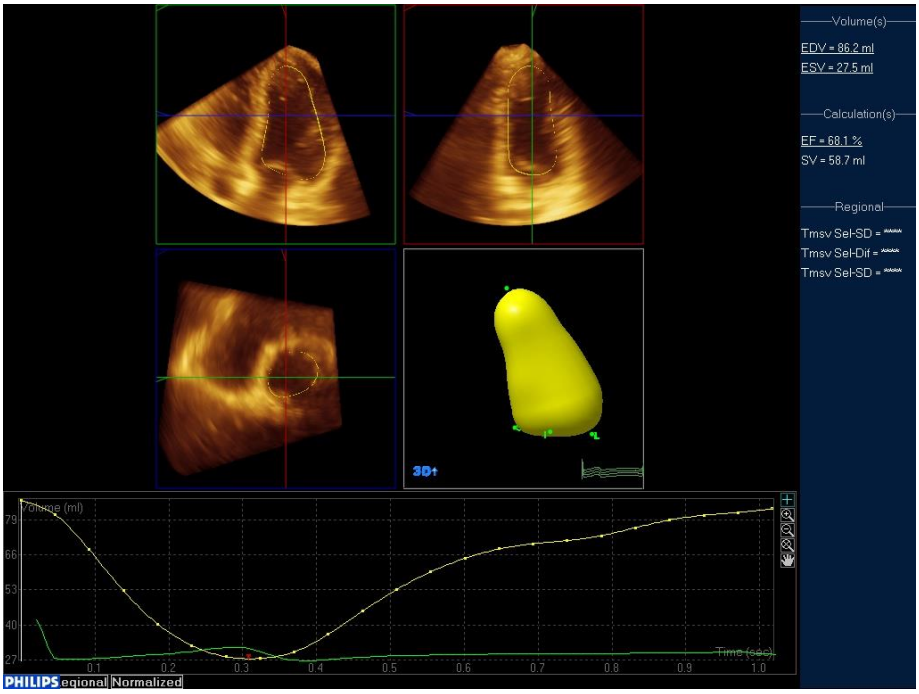

Figure 2.10 Snapshot of the true volumetric method whereby the user identifies the border through marker placements, and the volume is calculated automatically through voxel counting. Depth 15cm. Volume rate 20Hz.

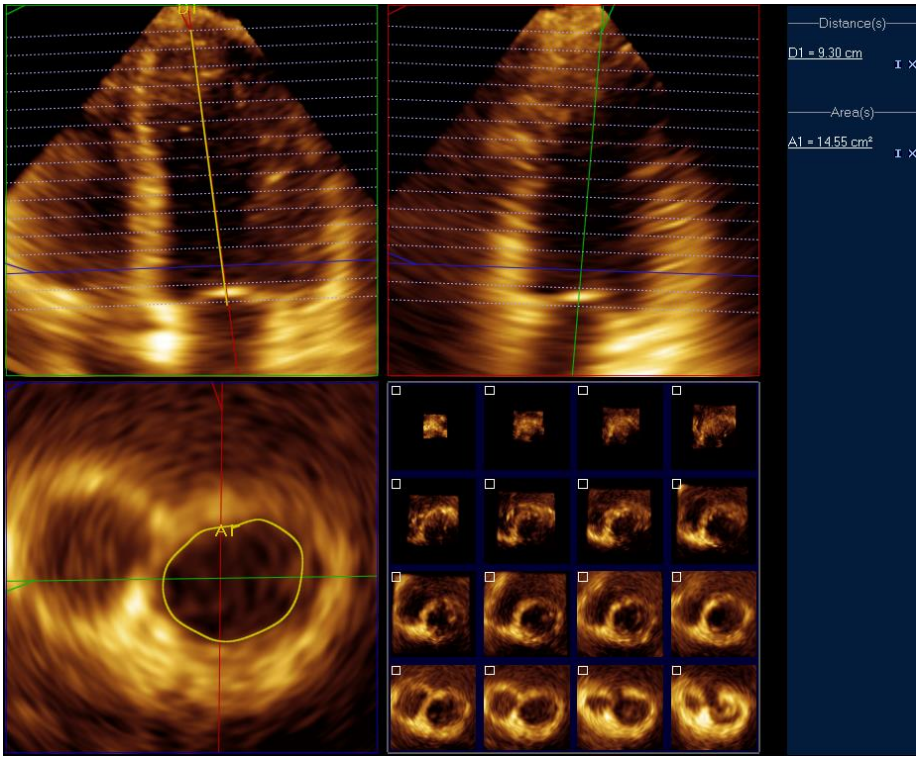

Figure 2.11 Snapshot of the manual method of discs volume measurement technique whereby the three-dimensional left ventricular cavity is sliced into 16 discs allowing for direct manual tracing of the short axis slices — the total volume equalling the sum of the volume of the individual discs. Note that the individual disc volumes cannot be calculated by the software and must be performed manually. Depth 15cm. Volume rate 20Hz.

2.4 Three-Dimensional Contrast Echocardiography

Three-dimensional contrast echocardiography incorporates the use of full volume 3D ECHO image acquisition with a contrast agent infusion for improved left ventricular opacification (Fig. 2.12). The combination of these two technologies have so far reported to correlate less than that of native 3D ECHO, most likely due to the lower frame-rates and higher stitching artefacts (15). These are likely because the 3D protocols have not been designed towards contrast imaging, and the lower power outputs required would cause the lower temporal resolutions. One promising potential advantage for contrast administration would be during the manual method of discs technique. The improved border delineation that contrast would offer should only improve the accuracy and reproducibility of the method further, presumably bringing it close to a reference method. Furthermore, for those users who choose to adopt the Simpson's biplane method in the 3D datasets, contrast should also improve border delineation, increasing the accuracy of this method without the potential for chamber foreshortening. However, there is still a

decreased ability to identify the mitral annulus, making delineation of the basal territory more difficult.

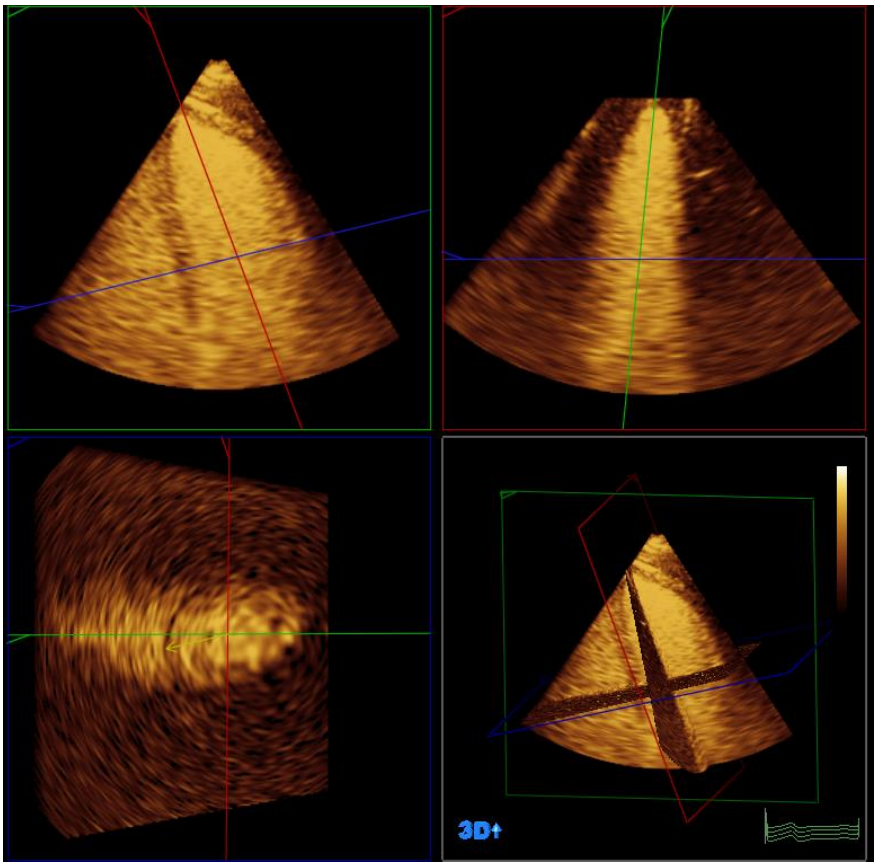

Figure 2.12 Snapshot of a three-dimensional contrast ultrasound image. Note the difficulty in identifying the mitral annulus. The volume rate for this image was 12Hz.

Reference:

(1) Hoskins P, Martin K, Thrush A. Diagnostic Ultrasound: Physics and Equipment. 2nd ed. Cambridge, UK: Cambridge Medicine; 2010.

(2) Otto CM. Textbook of Clinical Echocardiography. Fifth ed. Waltham, MA, USA: Elsevier Inc.; 2013.

(3) Yale University. Atlas of Echocardiography. 1999; Available at: http://www.yale.edu/imaging/echo_atlas/contents/index.html. Accessed 10/12, 2013.

(4) Lang RM, Bierig M, Devereux RB, Flachskampf FA, Foster E, Pellikka PA, et al. Recommendations for Chamber Quantification: A Report from the American Society of Echocardiography's Guidelines and Standards Committee and the Chamber Quantification Writing Group, Developed in Conjunction with the European Association of Echocardiography, a Branch of the European Society of Cardiology. J Am Soc Echocardiogr 2005 12;18(12):1440-1463.

(5) Lang RM, Bierig M, Devereux RB, Flachskampf FA, Foster E, Pellikka PA, et al. Recommendations for chamber quantification. Eur J Echocardiogr 2006 Mar;7(2):79-108.

(6) Schiller NB, Shah PM, Crawford M, DeMaria A, Devereux R, Feigenbaum H, et al. Recommendations for quantitation of the left ventricle by two-dimensional echocardiography. American Society of Echocardiography Committee on Standards, Subcommittee on Quantitation of Two-Dimensional Echocardiograms. J Am Soc Echocardiogr 1989 Sep-Oct;2(5):358-367.

(7) Zomorano JL, Bax JJ, Rademakers RE, Knuuti J. The ESC Textbook of Cardiovascular Imaging. Dordrecht, The Netherlands: Springer; 2010.

(8) Binder T, Wiesbauer F, Goliasch G, Hubler O, Erbschwendner S, Wagner MS, et al. 123sonography.com. Available at: http://123sonography.com/node/853. Accessed 10/12, 2013.

(9) Hoffmann R, von Bardeleben S, ten Cate F, Borges AC, Kasprzak J, Firschke C, et al. Assessment of systolic left ventricular function: a multi-centre comparison of cineventriculography, cardiac magnetic resonance imaging, unenhanced and contrast-enhanced echocardiography. Eur Heart J March 2005 March 2005;26(6):607-616.

(10) Burns PN, Becher H. Handbook of Contrast Echocardiography: Left ventricular function and myocardial perfusion. First ed. Secaucus, NJ, USA: Springer-Verlag New York Inc.; 2000.

(11) Sugeng L, Weinert L, Thiele K, Lang RM. Real-time three-dimensional echocardiography using a novel matrix array transducer. Echocardiogr 2003 Oct;20(7):623-635.

(12) Lang RM, Badano LP, Tsang W, Adams DH, Agricola E, Buck T, et al. EAE/ASE recommendations for image acquisition and display using three-dimensional echocardiography. Eur Heart J Cardiovasc Imaging 2012 Jan;13(1):1-46.

(13) Philips Healthcare. xMATRIX Array Technology. Available at: http://www.healthcare.philips.com/us_en/products/ultrasound/technologies/xmatrix.wpd. Accessed 10/12, 2013.

(14) Dorosz JL, Lezotte DC, Weitzenkamp DA, Allen LA, Salcedo EE. Performance of 3-dimensional echocardiography in measuring left ventricular volumes and ejection fraction: a systematic review and meta-analysis. J Am Coll Cardiol 2012 May 15;59(20):1799-1808.

(15) Takeuchi M, Otani S, Weinert L, Spencer KT, Lang RM. Comparison of Contrast-enhanced Real-time Live 3-Dimensional Dobutamine Stress Echocardiography with Contrast 2-Dimensional Echocardiography for Detecting Stress-induced Wall-motion Abnormalities. J Am Soc Echocardiogr 2006 3;19(3):294-299.

3 Echocardiography Methods for Left Ventricular Assessment: A Review of the Literature

Assessment of left ventricular (LV) function and volumes is the cornerstone of cardiac diagnostics (1). Several imaging methods are in clinical practice, and one would assume that these methods would provide the same results. In practice, however, if the same patient with stable conditions is investigated with different methods, different results are obtained, which may have an impact on patient management. This review gives an overview on comparative studies between echocardiographic modalities and cardiac magnetic resonance imaging (CMR) which is regarded as the reference method for LV volumes and ejection fraction (LVEF) (2). It will cover the normal values, comparative studies with CMR and a critical assessment of the reproducibility data. A recent paper by Dorosz et al. has provided an extensive overview and a meta-analysis on studies comparing 2D and 3D echocardiography with CMR (3). This review is complimentary as it includes contrast echocardiography and provides a more comprehensive section on reproducibility, which has a major impact for clinical use.

3.1 Review of the Literature: Methods

3.1.1 Normal Values

Normal values were selected from the guideline papers of the echocardiographic and radiological scientific societies or from articles which established the normal values. Particular importance is placed on the lower limits of LVEF, as these are clinical indicators for left ventricular impairment. The reference values are based on studies involving cohorts as low as 60 patients ranging up to 1200 (4-15).

3.1.2 Echocardiographic Techniques versus Magnetic Resonance Imaging

A PubMed review was carried out – including 18 studies, encompassing 1299 patients – comparing studies which included patients with abnormal LV function. Unlike the Dorosz paper, this review had an inclusion criterion of 30 patients per study and included contrast echocardiography as well as several more recent investigations in which Bland-Altman (BA) analysis was used as the method of calculating agreement with CMR in different patient groups (3). In these studies, both patients with normal and abnormal hearts were included. In abnormal hearts,

the differences between the different imaging methods may become even more relevant.

BA analysis provides two parameters which allow to assess the agreement between different methods that measure the same parameter – bias and limits of agreement (LOA). Bias means the measurements with a specific echocardiographic technique are systematically different from the CMR measurements, which are regarded as the reference standard. A bias can be positive (=overestimation compared to the CMR measurements) or negative (=underestimation compared to the CMR measurements). For example, a bias of 5% means that the echocardiographic method overestimates the CMR measurements on an average by 5%. The limits of agreement (LOA) represent the degree of accuracy between the echocardiographic measurements and the CMR measurements. The LOA are calculated by 2 (or 1.96) standard deviations (SD) of the differences and covers the range of values which includes 95% of all the differences between the echocardiographic and CMR measurements. For example, with a bias of – 5% and 2 SD = 10%, the range is -15 to +5%. The smaller the LOA range the better is the echocardiographic method when compared with CMR (16). In the review, studies which used other methods for assessment of the inter- and intra-observer variability, such as intra-class correlation coefficients (ICC), and coefficient of variability (CV), were also included.

3.2 Review Results

3.2.1 Normal Values

The differences in normal values are particularly large when end-diastolic and end-systolic volumes are compared (Tables 3.2 and 3.3). It should be acknowledged that if techniques are used interchangeably, an improvement or deterioration may be observed on an individual basis which does not reflect the patient's underlying pathology.

The lower limits of LVEF varied largely between modalities, such as between magnetic resonance imaging (male – 57%) and radionuclide angiography (male – 45%). This was also the case within the same modality, as between Alfaikih et al. (55%) and Nikitin et al. (66.0 – 70%) for magnetic resonance imaging steady state free procession. In the same modality, differences in LVEF differed up to 4% in age

ranges. Differences between men and women in the same age group differed up to 8% in the 3D ECHO study (Table 3.1).

The largest differences were observed in the normal values for LV volumes. EDV index upper limit values in men ranged from 56 to 112mL between modalities; ESV index upper limit values in men ranged from 20 to 89.7mL. In the same modality, up to 12mL difference was reported between different ages in EDV index, and 10mL difference between age matched males and females (Tables 3.2 & 3.3).

Table 3.1 Normal values for left ventricular ejection fraction

Paper	N	Mode	Male EF Lower Limit (%)	Female Lower Limit (%)
Alfakih et al (4)	60	MRI TGE	57.0	58.0
Alfakih et al (4)	60	MRI SSFP	55.0	54.0
Cain et al(5)	96	MRI Gradient echo**	49.0 (61-80yrs)	53.0 (61-80yrs)
Nikitin et al(6)	95	MRI SSFP	66.0 (<65yrs) 70.0 (>65yrs)	68.0 (>65yrs) 72.0 (>65yrs)
Lang et al. (ASE Guidelines) (7)	510	2D ECHO	55.0	55.0
Aune et al(8)	166	3D ECHO	49.0	49.0
Fukuda et al(8) - **Japanese**	410	3D ECHO (QLAB, Tomtec)	51.0 (60-69yrs)	53.0 (60-69yrs)
Chahal et al (10)– **European White**	499	3D ECHO	50.0 (35-44yrs) 52.0 (45-54yrs) 48.0 (55-64yrs) 47.0 (65-75yrs)	52.0 (35-44yrs) 51.0 (45-54yrs) 53.0 (55-64yrs) 55.0 (65-75yrs)
Chahal et al (10)– **Indian Asian**	479	3D ECHO	50.0 (35-44yrs) 51.0 (45-54yrs) 51.0 (55-64yrs) 53.0 (65-75yrs)	53.0 (35-44yrs) 52.0 (45-54yrs) 53.0 (55-64yrs) 55.0 (65-75yrs)
Wang et al(11)	140	gSPECT QGS	51.1	57.6
Wang et al(11)	140	gSPECT 4D-MSPECT	57.1	51.5
Nakajima et al (12)	268	gSPECT QGS	48.7	55.5
Hor et al (13)	585	RNV	49.0	49.0
Pfisterer et al (14)	1200	RNV	45.0	45.0
Jongjirasiri et al (15)	115	320-CT	47.4	53.1

ASE = American Society of Echocardiography; MRI = Magnetic Resonance Imaging; TGE = Turbo Gradient echo; SSFP = Steady State Free Procession; 2D = Two-dimensional; 3D = Three-dimensional; ECHO = echocardiography; gSPECT = gated Single Photon Emission Computed Tomography; QGS = Quantitative Gated Single Photon Emission Computed Tomography Software; 4D-MSPECT = Four-Dimensional Myocardial Single Photon Emission Computed Tomography; RNV = Radionuclide Ventriculography; 320-CT = 320 Slice Computed Tomography; **Sequence not specified.

Table 3.2 Normal values for left ventricular end-diastolic volume index from the literature

Paper	N	Mode	Male EDV Lower Limit (mL)	Male EDV Upper Limit (mL)	Female EDV Lower Limit (mL)	Female EDV Upper Limit (mL)
Alfakih et al (4)	60	MRI TGE	45.0 (40-65 yrs)	104.0 (40-65 yrs)	48.0 (40-65 yrs)	94.0 (40-65 yrs)
Alfakih et al(4)	60	MRI SSFP	53.0 (40-65 yrs)	112.0 (40-65 yrs)	56.0 (40-65 yrs)	99.0 (40-65 yrs)
Cain et al(5)	96	MRI Gradient echo**	48.0 (51-60yr) 43.0 (61-70yr) 36.0 (71-80yr)	97.0 (51-60yr) 92.0 (61-70yr) 88.0 (71-80yr)	46.0 (51-60yr) 45.0 (61-70yr) 44.0 (71-80yr)	87.0 (51-60yr) 86.0 (61-70yr) 87.0 (71-80yr)
Nikitin et al (6)	95	MRI SSFP	63.0 (<65yr) 54.0 (>65yr)	73.0 (<65yr) 67.0 (>65yr)	63.0(<65yr) 56.0(>65yr)	73.0 (<65yr) 69.0 (>65yr)
Lang et al. (ASE Guidelines) (7)	510	2D ECHO	35.0	75.0	35.0	75.0
Aune et al(8)	166	3D ECHO	46.0	86.0	42.0	74.0
Fukuda (9) - **Japanese**	410	3D ECHO (QLAB, Tomtec)	21.0 (50-59yrs) 20.0 (60-69yrs)	69.0 (50-59yrs) 68.0 (60-69yrs)	28.0 (50-59yrs) 25.0 (60-69yrs)	60.0 (50-59yrs) 57.0 (60-69yrs)
Chahal et al (10)– **European White**	499	3D ECHO	N/A	72.0 (35-44yrs) 71.0 (45-54yrs) 64.0 (55-64yrs) 62.0 (65-75yrs)	N/A	64.0 (35-44yrs) 59.0 (45-54yrs) 56.0 (55-64yrs) 52.0 (65-75yrs)
Chahal et al (10)– **Indian Asian**	479	3D ECHO	N/A	63.0 (35-44yrs) 57.0 (45-54yrs) 55.0 (55-64yrs) 56.0 (65-75yrs)	N/A	59.0 (35-44yrs) 53.0 (45-54yrs) 49.0 (55-64yrs) 60.0 (65-75yrs)
Wang et al(11)	140	gSPECT QGS	17.6	62.4	14.7	51.1
Wang et al(11)	140	gSPECT 4D-MSPECT	15.4	60.2	12.8	53.2
Nakajima et al (12)	268	gSPECT QGS	27.5	74.1	17.9	60.7
Hor et al*(13)	585	RNV	130.0	160.0	130.0	160.0
Jongjirasiri*(15)	115	320-CT	88.0	157.2	61.7	128.1

Values are indexed to body surface area. Abbreviations as in Table 3.1. *Indicates values were not indexed.

Table 3.3 Normal values for left ventricular end-systolic volume index from the literature

Paper	N	Mode	Male ESV Lower Limit (mL)	Male ESV Upper Limit (mL)	Female ESV Lower Limit (mL)	Female ESV Upper Limit (mL)
Alfakih et al* (4)	60	MRI TGE	19.7 (40-65yrs)	78.9 (40-65yrs)	22.0 (40-65yrs)	56.0 (40-65yrs)
Alfakih et al* (4)	60	MRI SSFP	26.1 (40-65yrs)	89.7 (40-65yrs)	26.8 (40-65yrs)	68.8 (40-65yrs)
Cain et al (5)	96	MRI Gradient echo**	14.0 (51-60yr) 12.0 (61-70yr) 8.0 (71-80yr)	46.0 (51-60yr) 44.0 (61-70yr) 43.0 (71-80yr)	13.0 (51-60yr) 14.0 (61-70yr) 14.0 (71-80yr)	37.0 (51-60yr) 38.0 (61-70yr) 39.0 (71-80yr)
Nikitin et al (6)	95	MRI SSFP	19.0 (<65yr) 15.0 (>65yr)	24.0 (<65yr) 20.0 (>65yr)	19.0 (<65yr) 13.0 (>65yr)	23.0 (<65yr) 20.0 (>65yr)
Lang et al. (ASE Guidelines) (50)	510	2D ECHO	12.0	30.0	12.0	30.0
Aune et al (8)	166	3D ECHO	17.0	41.0	13.0	33.0
Fukuda (9)**- Japanese**	410	3D ECHO	7.0 (50-59yrs) 7.0 (60-69yrs)	27.0 (50-59yrs) 27.0 (60-69yrs)	8.0 (50-59yrs) 7.0 (60-69yrs)	24.0 (50-59yrs) 23.0 (60-69yrs)
Chahal et al (10)**– European White**	499	3D ECHO	30.0 (35-44yrs) 32.0 (45-54yrs) 29.0 (55-64yrs) 26.0 (65-75yrs)	N / A	26.0 (35-44yrs) 26.0 (45-54yrs) 21.0 (55-64yrs) 20.0 (65-75yrs)	N / A
Chahal et al (10)**– Indian Asian**	479	3D ECHO	28.0 (35-44yrs) 24.0 (45-54yrs) 23.0 (55-64yrs) 24.0 (65-75yrs)	N / A	23.0 (35-44yrs) 21.0 (45-54yrs) 19.0 (55-64yrs) 22.0 (65-75yrs)	N / A
Wang et al (11)	140	gSPECT QGS	N / A	26.6	N / A	17.3
Wang et al (11)	140	gSPECT 4D-MSPECT	N / A	20.4	N / A	20.1
Nakajima et al (12)	268	gSPECT QGS	N / A	33.2	N / A	23.7
Hor et al* (13)	585	RNV	50.0	60.0	50.0	60.0
Jongjirasiri et al* (15)	115	320-CT	28.4	68.0	15.9	52.3

Values are indexed to body surface area. Abbreviations as in Table 3.1. *Indicates values were not indexed

3.2.2 Accuracy of Echocardiographic Methods in the Multi-centre Studies

Only two multi-centre studies have been performed to compare CMR with echocardiographic imaging modalities (marked by a † in Fig. 3.1, 3.2 and 3.3). Hoffman et al. investigated 120 patients with variable levels of left ventricular function, of which 55 patients had CMR as well as standard and contrast 2D ECHO. They showed in Bland-Altman analysis for unenhanced 2D ECHO (Simpson's biplane) left ventricular ejection fraction (LVEF) to have a good agreement (bias = 0.8%; LOA = -20.0 to 21.6%) with CMR. Contrast enhanced 2D ECHO (Simpson's biplane) showed a similar agreement (bias = 4.6%; LOAs of -12.4 to 21.6%). End-diastolic volume (EDV) and end-systolic volume (ESV) in unenhanced 2D ECHO showed a bias of -72.3mL (LOA = -150.3 to 5.7mL) and -35.7mL (LOA = -99.4 to 28mL) respectively, compared with -42.3mL (LOA = -114.6 to 30mL) and -27.2mL (LOA = -80.9 to 26.5mL) using contrast 2D ECHO. Various combinations of three readers (one onsite and two offsite) produced mean percentage errors (MPE) and confidence intervals (95%CI) for 2D ECHO (12.8, 10.9 – 14.8; 11.7, 10.1 – 13.4; 12.6, 10.4 – 14.8) and for contrast 2D ECHO (8.9, 7.5 – 10.3; 8.8, 7.5 – 10.2; 4.1, 3.1 – 5.0). These showed a clear improved agreement when contrast agents were used (17). The second multi-centre study, consisting of 92 patients with various degrees of LV function as assessed by Simpson's biplane LVEF assessment, was carried out by Mor-Avi et al. investigating the accuracy and reproducibility of three-dimensional echocardiography (3D ECHO) (5 beat volume acquisition; QLAB, Philips Ultrasound Ltd., Bothell, Washington, USA). The bias (LOAs) were -3% (LOA = ± 22%), -67mL (LOA = ± 90mL) and -41mL (LOA = ± 90mL) for LVEF, EDV and ESV respectively. The degree of bias in the volume calculations were attributed to the less experienced centres in 3D ECHO utilization, which highlights the importance of adequate training in the utilization of 3D ECHO for LV function assessment (18).

3.2.3 Accuracy of Echocardiographic Methods in the Single-Centre Studies

There were 16 single-centre studies which satisfy the inclusion criteria of this review; three of which included ≥ 100 patients (highlighted by a box in Fig. 3.1, 3.2 and 3.3). Whereas native and contrast echocardiography can be performed with all state of the art scanners, there are currently only four commercially available systems for 3D ECHO with inclusive analysis software (Philips, GE, Siemens and Toshiba). In addition, there is one commercially available software package for offline analysis (TomTec).

No studies have been performed to compare measurements obtained on scanners from different manufacturers. The single centre studies included a total of 1087 patients and healthy volunteers. The bias and limits of agreement for measurements of LVEF, EDV and ESV are shown in Figure 3.1, 3.2 and 3.3 (17-34). The findings in single and multi-centre studies can be concluded as follows:

1. 2D contrast echocardiography is superior to 2D non-contrast echocardiography regarding agreement of volume and LVEF measurements. The volumes measured with 2D contrast echocardiography are closer to the corresponding CMR measurements than those obtained with non-contrast echocardiography. Contrast 2D echocardiography is particularly useful in patients with poor acoustic windows (17,20,21).

2. Most studies showed the superiority of non-contrast 3D over non-contrast 2D echocardiography (17-34). In particular, the measured volumes deviated less from the CMR measurements using non-contrast 3D echocardiography compared to non-contrast 2D echocardiography. Only one study specifically focused on patients with LV aneurysms and seemed to show similar results compared to the other studies (23).

3. There are several studies exploring different recording and analysis protocols for non-contrast 3D ECHO. The most frequently used technique for 3D ECHO volume measurements is voxel count. The borders of the LV cavity are traced semi-automatically and the voxels (known volume) inside the traced volume are counted. The difference between the analysis software from different manufacturers is the number of 2D slices which are used for the initial tracing of the endocardium. Whereas QLAB uses two orthogonal views, TomTec uses at least three planes; however, after segmentation, all further measurements are performed via voxel count. Jacobs et al. showed better results using the 3D voxel counting method compared to biplane Simpson data obtained from a 3D dataset (22). Voxel count was also superior to a multiplane measurement of LVEF (24,26). There was no significant difference in LVEF estimation between the QLAB and TomTec voxel methods (30,32). However, the TomTec volume measurements were closer to CMR than the QLAB measurements (25).

4. Most 3D studies used a multi-beat acquisition: that means that the 3D dataset is acquired by small datasets which are acquired during four or more consecutive beats and electronically stitched together. A study by Macron et al. investigated the impact of single beat acquisition (which is associated with limited temporal and spatial resolution) versus multibeat 3D ECHO image acquisition. The single beat acquisition resulted in significantly smaller and more variable measurements of ejection fraction (bias 5%) compared to four beat acquisitions (33). Thavendiranathan et al. used a real-time scanner (Siemens, CA, USA) which provided high volume rates and showed good agreement with CMR. They also were able to scan patients with atrial fibrillation. The authors went on to report the effect of adding various amounts of adjustments to the endocardial border of the contour algorithm, demonstrating a closer relationship with CMR in LVEF measurements when the contour finding algorithm is moved slightly outside the initially traced contour so as to include the small LV trabeculations (34).

5. No final judgement can be made about the comparison between 2D contrast and 3D non contrast and contrast studies. No study yet fulfilled the inclusion criteria for this review, but there is a European multi-centre study completed that will be available within a year. Caiani et al. compared 3D ECHO with 2D ECHO (Simpson's biplane) and CMR in a population of 46 patients, of which a subset of 14 consented for contrast infusion during 3D ECHO acquisition. The LVEF was not different with both methods, but the agreement of EDV and ESV became worse when a contrast agent was used: the bias (LOA) for contrast EDV was -34mL compared to -5.7mL for native 3D ECHO. It was suggested by the authors that this negative impact of values relative to the reference method may have been due to bubble destruction, resulting from the high density of scan lines required for full volumetric acquisition (27). In a recent study by Thavendiranathan and colleagues, the reproducibility of non-contrast 3D echocardiography exceeded that of 2D and 3D contrast echocardiography. But this study included only patients with good image quality, and no CMR measurements were performed (35).

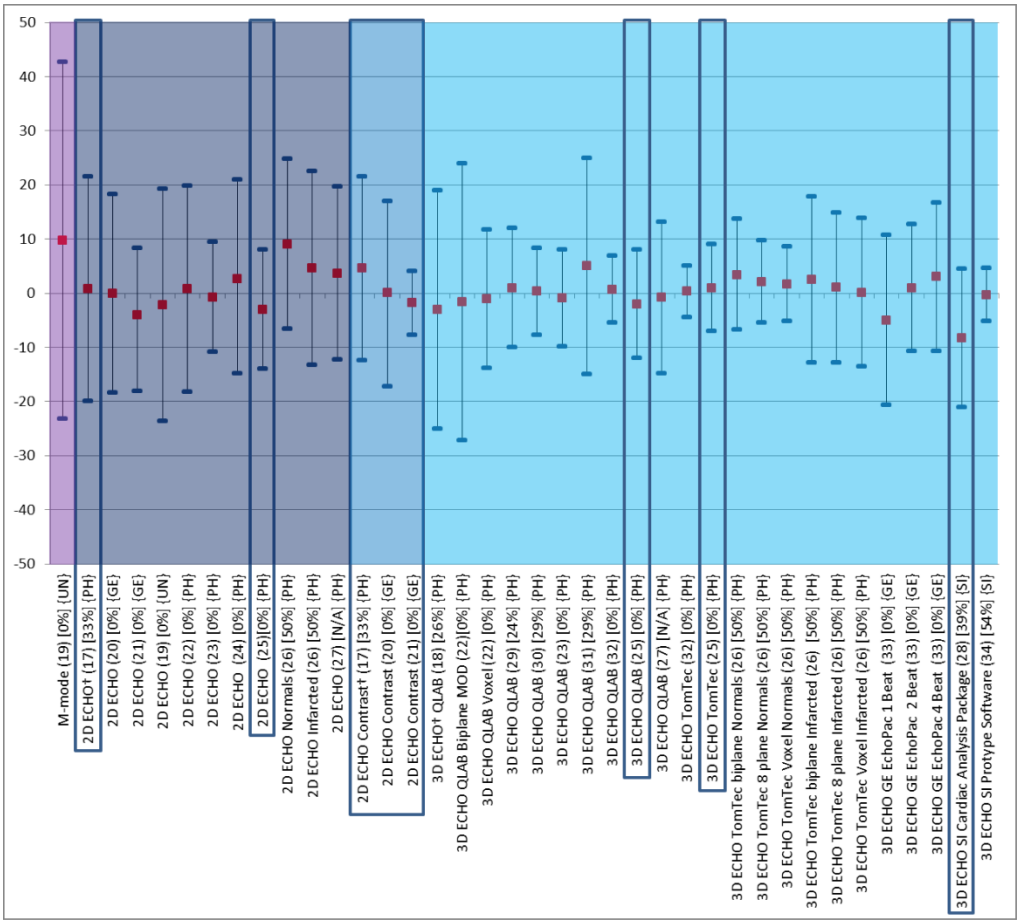

Figure 3.1 Comparison of echocardiographic techniques with cardiac magnetic resonance imaging for measurement of ejection fraction (%). Bias and limits of agreement: the closer the dots are to the mid-line, the smaller the bias. Red square box indicates bias compared to magnetic resonance imaging. Blue line at each end of the plots indicates the lower and upper limits of agreement calculated by Bland-Altman. 2D ECHO = two-dimensional echocardiography; 3D ECHO = three-dimensional echocardiography; NSR = Normal Sinus Rhythm; MOD = method of disks. QLAB = Philips online and offline LV volume calculation tool. TomTec = offline left ventricular volume calculation tool. UN = Unknown; PH = Philips; GE = General Electric; SI = Siemens; † Indicates multi-centre studies. Values in square brackets are the percentage of patients without disease within each study.

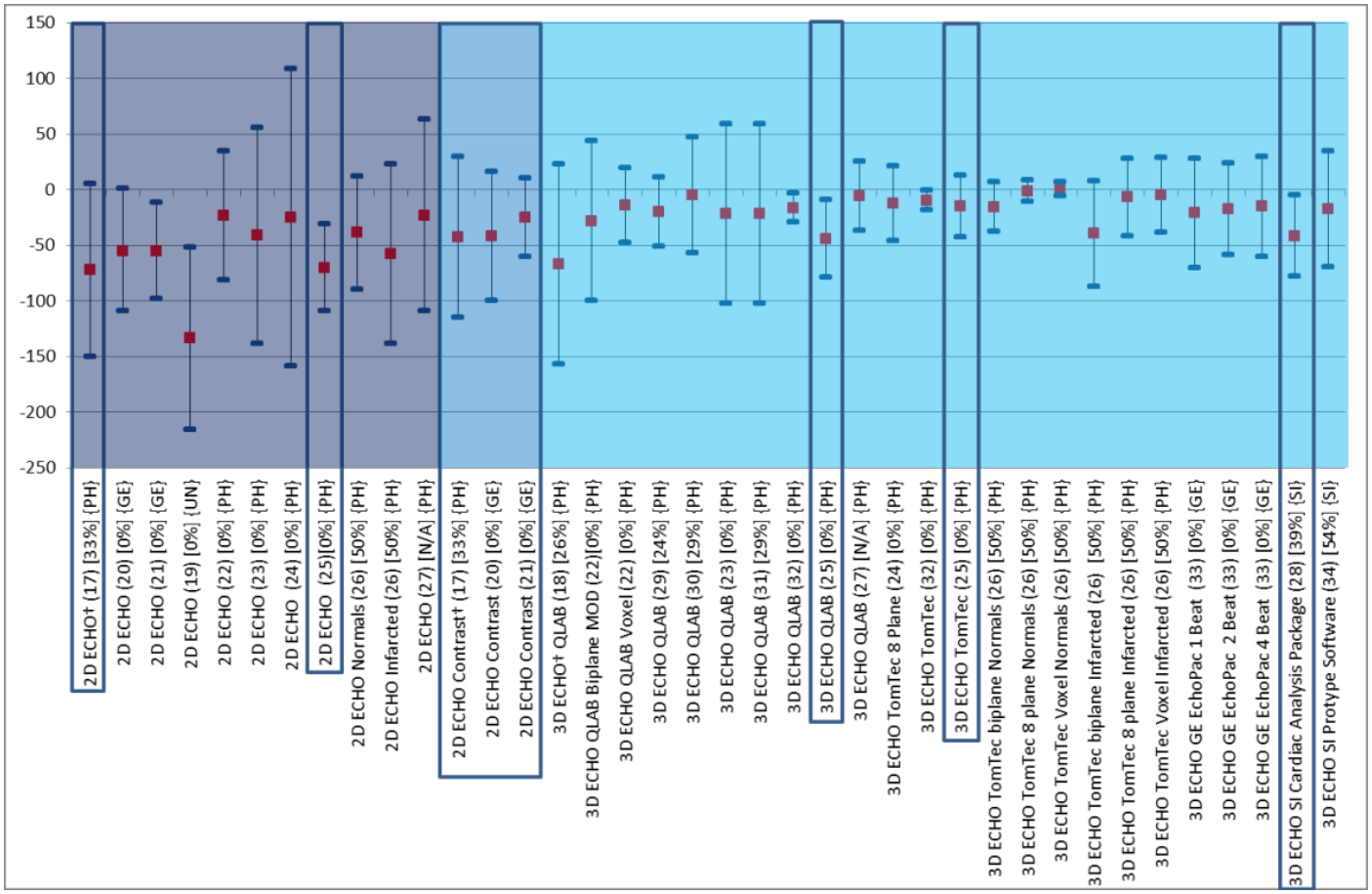

Figure 3.2 Comparison of echocardiographic techniques with cardiac magnetic resonance imaging for measurement of end-diastolic volume (mL). The closer the red boxes are to the mid-line, the smaller the bias. Abbreviations as in Figure 3.1.

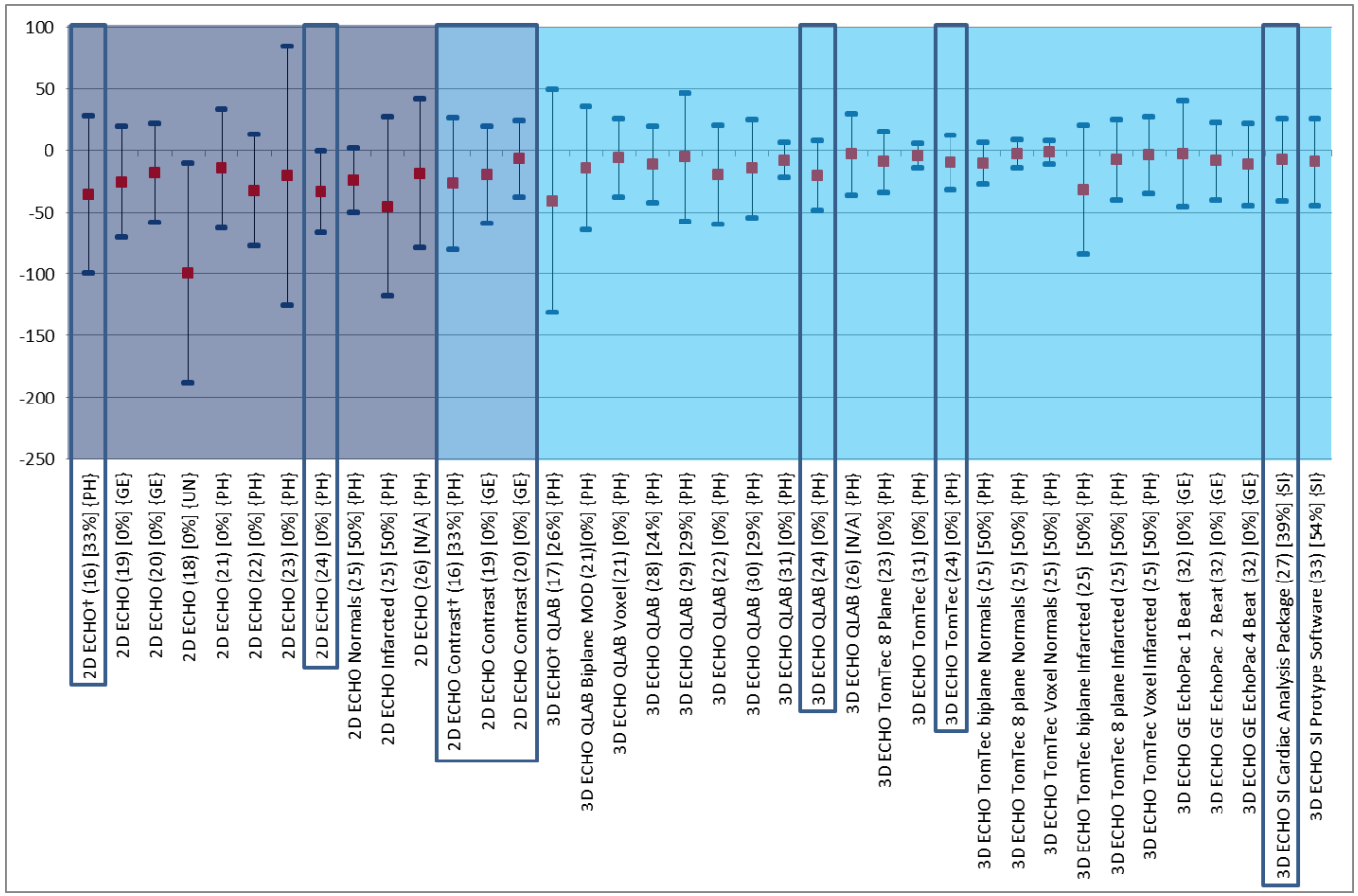

Figure 3.3 Comparison of echocardiographic techniques with cardiac magnetic resonance imaging for measurement of end-systolic volume (mL). The closer the red boxes are to the mid-line, the smaller the bias. Abbreviations as in Figure 3.1.

3.2.4 The Observer Variability of the Echocardiographic Methods and Other Cardiac Tools for Assessing Left Ventricular Function in the Comparative Studies

Different methods of statistical analysis were used to assess the reproducibility of tests between two different observers and of repeat tests for the same observer; these are as follows, intra-class correlation coefficients (ICC), Bland-Altman method (BA), coefficient of variability (CV) and percentage difference of the mean (MD) (16,36). Pearsons correlation coefficient was also used in one paper. Generally, using ICC as the statistical test for assessing reproducibility, 3D ECHO was more reproducible than 2D ECHO. With Bland Altman (BA) analysis there was an obvious difference between the two methods, although, BA was not used very often for comparison in 3D ECHO. The most frequently used test for 3D ECHO was MD, defined as the absolute difference between corresponding repeated measurements expressed in percent of their mean, which showed an improvement of 3D ECHO as compared with 2D ECHO (Table 3.4 &3.5).

The reproducibility of CMR measurements is better than that measured with non-contrast 2D ECHO in most studies. But with contrast echocardiography, there are only minor differences, in particular for LVEF; in the multi-centre study of Hoffman et al., contrast 2D ECHO had a better variability using ICC than did CMR (0.91 vs 0.86, respectively) when the onsite reader and two offsite readers were compared (17). The inter- and intra-observer variability of CMR measurements is dependent on the expertise of the readers (37). The inter-observer variability of LVEF measurements can be improved from 7.2% to 3.7% after training (37). In table 3.6, the studies are listed in which the reproducibility was reported for CMR. The variability of computed tomography (CT) and radionuclide ventriculography (RNV) reported by separate studies are listed in table 3.7; all of which reported excellent variability except one study which reported a correlation coefficient of 0.6 for LVEF by RNV (38-43). This is not surprising as CT utilizes the same methods for border delineation and volume calculation as CMR, using images with higher spatial resolution (40).

Table 3.4 Two-dimensional echocardiography, inter-observer and intra-observer comparison

Technique	Study Reference	Statistic	Interobserver			Intraobserver		
			LVEF	EDV	ESV	LVEF	EDV	ESV
Simpson's Biplane	Malm et al* (21)	BA	±15.4%	±25.7mL	±20mL	±18.91%	N / A	N / A
Simpson's Biplane	Jacobs et al (22)	MD BA	14 ± 17 ± 18%	19 ± 20 ± 42mL	24 ± 21 ± 20 mL	13 ± 11 ± 12%	13 ± 21 ± 46 mL	24 ± 24 ± 24 mL
Simpson's Biplane	Caiani et al (27)	CV ICC	14.2†	26.4†	37.7†	N / A	0.91	0.92
Simpson's Biplane	Gutierrez-Chico et al (24)	ICC	0.94	0.58	0.83	0.92	0.80	0.89
Simpson's Biplane	Hoffman et al (17)	ICC	0.79	N / A	N / A	N / A	N / A	N / A
Simpson's Biplane Contrast	Hoffman et al (17)	ICC	0.91	N / A	N / A	N / A	N / A	N / A
Simpson's Biplane Contrast	Malm et al* (21)	BA	±6.4%	±20.7mL	±15.2mL	N / A	N / A	N / A
Offline, 3D ECHO Biplane (TomTec)	Gutierrez-Chico et al (24)	ICC	0.96	0.97	0.99	0.97	0.98	0.97

ICC = Intra-class Correlation, CV = Coefficient of Variability (% ± 2SD), BA= Bland-Altman (Bias ± 2SD); MD = Mean Difference expressed as a percentage of the mean (% ± 2SD); EDV = End-diastolic volume; ESV = End-systolic volume; LVEF = Ejection fraction, CI = confidence interval. * Bias not made available. † Standard Deviation not reported.

Table 3.5 Three-dimensional echocardiography inter-observer and intra-observer comparison of the literature with varying methods of statistical analysis

Technique	Study Reference	Statistic	Interobserver			Intraobserver		
			LVEF	EDV	ESV	LVEF	EDV	ESV
5 Bt (QLAB)	Mor-Avi et al (18)	CV	N / A	8 ± 16	13 ± 28	N / A	5 ± 10	10 ± 22
4 Bt (QLAB)	Jacobs et al (22)	MD	5 ± 4	10 ± 8	11 ± 6	10 ± 5	10 ± 6	11 ± 5
		BA	3 ± 4%	14 ± 20 mL	7 ± 10 mL	6 ± 6%	13 ± 14 mL	6 ± 6 mL
4 Bt (TomTec)	Sugeng et al (30)	MD	10.5 ± 16.6	11.2 ± 17.2	14.2 ±23.6	5.6 ±6.8	3.9 ± 4	5.6 ±7.8
4 Bt, (QLAB)	Soliman et al (32)	MD	9.7 ± 8.8	12.2 ± 10.1	13.6 ± 11.2	7.3 ± 9.1	7.2 ± 8.1	9.1 ± 7.2
4Bt (TomTec)	Soliman et al (32)	MD	7.1 ± 6.9	6.4 ± 7.8	7.8 ± 9.7	6.6 ± 7.4	4.7 ± 3.2	6.1 ± 5.8
1 Bt (EchoPAC)	Macron et al (32)	MD	8.6 ± 23.2	9.2 ± 11.2	11.9 ± 16.8	6.8 ± 8.8	3.4 ± 7.4	8.0 ± 10.2
2 Bt (EchoPAC)	Macron et al (33)	MD	6.6 ± 7.8	4.6 ± 8.4	9.0 ± 13.8	4.5 ± 7.8	3.2 ± 6.6	3.2 ± 4.8
4 Bt (EchoPAC)	Macron et al (33)	MD	9.2 ± 9.6	5.6 ± 7.2	9.6 ± 14.8	6.4 ± 12.8	3.1 ± 5.4	4.2 ± 10.6
1 Bt, Online	Chang et al (28)	ICC		0.99	0.99		0.99	0.99
		BA	N/A	-1.62mL ± 8.78	-0.32mL ± 10.0	N/A	-7.91mL ± 33.06	-1.62mL ± 6.85
4 Pl (TomTec)	Gutierrez-Chico et al (24)	ICC	0.98	0.99	0.99	0.99	0.99	0.99
8 Pl (TomTec)	Gutierrez-Chico et al (24)	ICC	0.99	0.99	0.99	0.99	0.99	0.99
4 Bt (TomTec)	Qi et al (31)	PCC	0.98	0.995	0.998	0.948	0.947	0.982
3 to 5 Bt (Siemens)	Thavendiranathan et al (34)	MD	1 ± 16	9 ± 14	9 ± 16	2 ± 20	5 ± 20	3 ± 22

PCC = Pearson's Correlation Coefficient. Bt = Beat, Pl = Plane. Other abbreviations as in Table 3.4.

Table 3.6 Cardiac magnetic resonance imaging, inter-observer and intra-observer comparison, obtained from studies in which cardiac magnetic resonance imaging and echocardiographic methods are compared

Technique	Study Reference	Statistic	Interobserver			Intraobserver		
			LVEF	EDV	ESV	LVEF	EDV	ESV
CMR	Hoffman et al (17)	ICC	0.86; 95% CI 0.80 – 0.92	N / A	N / A	N / A	N / A	N / A
CMR	Mor-Avi et al (18)	MD	N / A	5 ± 8	7 ± 14	N / A	4 ± 10	4 ± 8
CMR	Sugeng et al (30)	MD	8.5 ± 19.4	6.3 ± 11.4	7.7 ± 13.2	6.2 ± 12.4	2.4 ± 4.6	6.3 ± 9.2
CMR	van Geuns et al (39)	MD	5.6 ± 6.0	3.7 ± 3.1	4.8 ± 4.0	0.2 ± 6.2	0.2 ± 1.0	1.4 ± 2.3
CMR	Thavendiranathan et al (34)	MD	1 ± 4	1 ± 12	2 ± 10	1 ± 4	0 ± 8	0 ± 12

CMR = Cardiac magnetic resonance imaging. Other abbreviations as in Table 3.4.

Table 3.7 Computed tomography and radionuclide ventriculography, inter-observer and intra-observer comparison

Technique	Study Reference	Statistic	Interobserver			Intraobserver		
			LVEF	EDV	ESV	LVEF	EDV	ESV
CT Multirow	Raman et al (38)	ICC	0.98	0.98	0.99	N / A	N / A	N / A
CT 64-Slice	Annuar et al (39)	ICC	0.99 ± 0.01	N / A	N / A	N / A	N / A	N / A
CT 64-Slice	Maffei et al (40)	CV	4.4	2.3	3.8	1.3	1.0	1.3
CT 64-Slice	Sarwar et al (41)	PCC	0.75	0.91	0.87	N / A	N / A	N / A
RNV	Xie et al (42)	PCC	0.98	0.98	0.98	0.99	0.99	0.99
RNV	Sibille et al (43)	CV	0.6	1.1	1.7	N / A	N / A	N / A

CT = computed tomography, RNV = radionuclide ventriculography. Other abbreviations as in Table 3.4.

3.3 Review Discussion

Normal Values

It is important to have a reference point from which to compare values. In a perfect world, one normal range should apply for all cardiac imaging tools in calculating ejection fraction and volumetric measurements. However, it is becoming apparent that due to the differences in methodology and algorithms between diagnostic modalities, a fixed value is not possible, and so it is necessary to develop a range of normal values corresponding to specific modalities. This may even be the case for various software packages used in the same diagnostic tool (Tables 3.1, 3.2, and 3.3).

In circumstances such as monitoring of treatment with potentially cardiotoxic drugs (Herceptin), accurate assessment of LVEF is crucial. However, if measurements are used interchangeably between different tests, which may be occurring in current practice, then interpretation may become difficult and the information could be misleading. A normal ejection fraction for CMR may correspond with a mildly compromised ventricle in 2D ECHO, and so on (Table 3.1). Thus, the difference between these measurements may be the difference between whether a patient does, or does not, qualify for therapeutic intervention. In ejection fraction and volume calculations, the variances in the literature were not only restricted to the different imaging modalities, but the different imaging sequences and software packages as well; furthermore, the normal values differed according to age and ethnicity (Tables 3.1 – 3.3).

Echocardiographic Techniques versus Magnetic Resonance Imaging

There is no systematic difference in the measured ejection fraction between the echocardiographic methods and CMR (Fig. 3.1). As already reported for the normal values, there are major differences in volumes between echocardiographic methods and CMR. With the use of contrast agents, these differences in volume measurement have reduced, however, this is still not to the level where results can be considered interchangeable. Regarding volumes, 3D echocardiography has been demonstrated to show a large improvement towards the values of CMR, and as such, is the most accurate ultrasound technique for determining left ventricular function, although the total number of patients included in trials is still small and very good acoustic windows are needed (39). The most promising technique in

echocardiography is certainly contrast 3D, however, the excellent results demonstrated by the Jenkins group in 2009 could not be reproduced by Caiani et al., and so further investigation is required (40). Table 2.1 (*see Chapter 2.1*), summarizes the advantages and limitations of the different echocardiographic methods.

CMR has been regarded the reference standard for measurement of LV volumes and ejection fraction because of its high image quality and volumetric data (41). There are well performed ex-vivo studies which have demonstrated the validity of CMR measurements (42). The bias and 95% limits of agreement between the dog heart mold data and different methods for LV volume determination were between 4.94mL ± 12.11 and 1.71mL ± 18.11. High image quality with good segmentation of blood and tissue as well as a volumetric dataset are the prerequisites for accurate measurements of LV volumes.

One of the difficulties facing LV function assessment is that LVEF may be a moving target, as a beat to beat variability has been reported to be up to 5.8% ± 1.7% (43). LVEF varies with BP, inotropic state and heart rate. In order to obtain reliable comparison of LVEF measurements from two different methods, it is mandatory to examine the patient under the same hemodynamic conditions. The effect of the beat to beat variation can only be minimized by taking multiple measurements and averaging the results (43,44). However, in reality this is often not carried out due to time constraints and high clinical loads.

The reproducibility of the echocardiography techniques showed a marked improvement with the introduction of contrast 2D ECHO and 3D ECHO in both intra-observer and inter-observer methods and comes close to CMR. However, we think there is not yet enough data to provide benchmarks for quality assessment. The differing tests used for variability assessments make it difficult for a reliable assessment to be made – particularly as some studies do not include either intra- or inter-observer calculations. Considering the importance of accurate assessment of LV function, it is remarkable that there has been only a limited body of comprehensive studies which attempt to define the differences between the various imaging methods. In particular, the data on the reproducibility is not satisfactory. The scientific societies should encourage studies or registries to broaden the database and to provide guidelines on how to perform validation studies. The Bland-Altman analysis appears to be an ideal test to analyse differences between methods

or between observers. Based on the available studies, the different imaging techniques for assessment of LV ejection fraction and volumes are not interchangeable. If follow-up measurements are necessary, they should be performed with the same method.

In the current review only 2 of the 18 studies reviewed as validation studies for echocardiography were multi-centre studies. Most of the data is from single centre studies, which are subject to referral bias. Thus, the reproducibility may be overestimated. Further investigation from larger cohorts is needed.

Is visual assessment an alternative?

Visual assessment of LV function on 2D echocardiograms has been used in many hospitals; for example, by estimating the LVEF in 5% steps (such as 30-35%) or just classifying the LV function as normal, mildly, moderately or severely impaired. The reason for using a visual rather than a quantitative assessment is the extra time needed to calculate LV volumes and the difficulty of tracing the endocardial borders on still frames. It is believed that no studies using visual assessment have been published in contrast echocardiography, where endocardial borders usually are well seen. Although visual assessment of global LV function has been reported to be 'reasonable' among experienced readers, the actual inter-observer variability was 5.8% and the intra-class correlation coefficient was 0.78 (45). This does not allow the use of visual assessment for follow-up studies of LVEF and volumes. In CMR, a comparison of visual and quantitative assessment of LVEF showed a major underestimation (8.4%) with visual assessment. Therefore, it was recommended to use quantitative analysis for accurate assessment of LV function (46).

Reference:

(1) Otto CM. Textbook of Clinical Echocardiography. Fifth ed. Waltham, MA, USA: Elsevier Inc.; 2013.

(2) Zomorano JL, Bax JJ, Rademakers RE, Knuuti J. The ESC Textbook of Cardiovascular Imaging. Dordrecht, The Netherlands: Springer; 2010.

(3) Dorosz JL, Lezotte DC, Weitzenkamp DA, Allen LA, Salcedo EE. Performance of 3-dimensional echocardiography in measuring left ventricular volumes and ejection fraction: a systematic review and meta-analysis. J Am Coll Cardiol 2012 May 15;59(20):1799-1808.

(4) Alfakih K, Plein S, Thiele H, Jones T, Ridgway JP, Sivananthan MU. Normal human left and right ventricular dimensions for MRI as assessed by turbo gradient echo and steady-state free precession imaging sequences. J Magn Reson Im 2003;17(3):323-329.

(5) Cain PA, Ahl R, Hedstrom E, Ugander M, Allansdotter-Johnsson A, Friberg P, et al. Age and gender specific normal values of left ventricular mass, volume and function for gradient echo magnetic resonance imaging: a cross sectional study. Br Med Comm: Med Im 2009;9(2).

(6) Nikitin NP, Huan Loh P, de Silva R, Witte KKA, Lukaschuk EI, Parker A, et al. Left ventricular morphology, global and longitudinal function in normal older individuals: A cardiac magnetic resonance study. Int J Cardiol 2006 3/22;108(1):76-83.

(7) Lang RM, Bierig M, Devereux RB, Flachskampf FA, Foster E, Pellikka PA, et al. Recommendations for Chamber Quantification: A Report from the American Society of Echocardiography's Guidelines and Standards Committee and the Chamber Quantification Writing Group, Developed in Conjunction with the European Association of Echocardiography, a Branch of the European Society of Cardiology. J Am Soc Echocardiogr 2005 12;18(12):1440-1463.

(8) Aune E, Bækkevar M, Rødevand O, ErikOtterstad J. Reference values for left ventricular volumes with real-time 3-dimensional echocardiography. Scandinavian Cardiovascular Journal 2010;44(1):24-30.

(9) Fukuda S, Watanabe H, Daimon M, Abe Y, Hirashiki A, Hirata K, et al. Normal Values of Real-Time 3-Dimensional Echocardiographic Parameters in a Healthy Japanese Population; – The JAMP-3D Study –. Circulation Journal 2012;76(5):1177-1181.

(10) Chahal NS, Lim TK, Jain P, Chambers JC, Kooner JS, Senior R. Population-Based Reference Values for 3D Echocardiographic LV Volumes and Ejection Fraction. J Am Coll Cardiol: Cardiovasc Imaging 2012 Dec;5(12):1191-1197.

(11) Wang SY, Cheng MF, Hwang JJ, Hung CS, Wu YW. Sex-specific normal limits of left ventricular ejection fraction and volumes estimated by gated myocardial perfusion imaging in adult patients in Taiwan: a comparison between two quantitative methods. Nuc Med Comm 2011;32(2):113-120.

(12) Nakajima K, Kusuoka H, Nishimura S, Yamashina A, Nishimura T. Normal limits of ejection fraction and volumes determined by gated SPECT in clinically normal patients without cardiac events: a study based on the J-ACCESS database. Eur J Nuc Med Mol Im 2007;34(7):1088-1096.

(13) Hor G, Schicha H, Standke R. Normal values in equilibrium radionuclide ventriculography. Results of a multicenter study. Nuklearmedizin 1990;29(5):186-94.

(14) Pfisterer ME, Battler A, Zaret BL. Range of normal values for left and right ventricular ejection fraction at rest and during exercise assessed by radionuclide angiocardiography. Eur Heart J 1985 August 01;6(8):647-655.

(15) Jongjirasiri S, Sritara C, Waeosak P, Laothamatas J. Normal data of left ventricular parameters in non-hypertensive patients using 320-slice cardiac CT: a study on intra- and interobserver variability. J Med Assoc Thai 2011;94(9):1053-60.

(16) Myles PS, Cui J. I. Using the Bland–Altman method to measure agreement with repeated measures. Br J of Anaesth 2007 September 01;99(3):309-311.

(17) Hoffmann R, von Bardeleben S, ten Cate F, Borges AC, Kasprzak J, Firschke C, et al. Assessment of systolic left ventricular function: a multi-centre comparison of cineventriculography, cardiac magnetic resonance imaging, unenhanced and contrast-enhanced echocardiography. Eur Heart J March 2005 March 2005;26(6):607-616.

(18) Mor-Avi V, Jenkins C, Kühl HP, Nesser H, Marwick T, Franke A, et al. Real-Time 3-Dimensional Echocardiographic Quantification of Left Ventricular Volumes: Multicenter Study for Validation With Magnetic Resonance Imaging and Investigation of Sources of Error. J Am Coll Cardiol: Cardiovasc Im 2008 7;1(4):413-423.

(19) Bellenger NG, Burgess MI, Ray SG, Lahiri A, Coats AJS, Cleland JGF, et al. Comparison of left ventricular ejection fraction and volumes in heart failure by echocardiography, radionuclide ventriculography and cardiovascular magnetic resonance. Are they interchangeable? Eur Heart J 2000 August 01;21(16):1387-1396.

(20) Mistry N, Halvorsen S, Hoffmann P, Müller C, Bøhmer E, Kjeldsen SE, et al. Assessment of left ventricular function with magnetic resonance imaging vs. echocardiography, contrast echocardiography, and single-photon emission computed tomography in patients with recent ST-elevation myocardial infarction. Eur J Echocardiogr 2010 October 01;11(9):793-800.

(21) Malm S, Frigstad S, Sagberg E, Larsson H, Skjaerpe T. Accurate and reproducible measurement of left ventricular volume and ejection fraction by contrast echocardiography: A comparison with magnetic resonance imaging. J Am Coll Cardiol 2004 9/1;44(5):1030-1035.

(22) Jacobs LD, Salgo IS, Goonewardena S, Weinert L, Coon P, Bardo D, et al. Rapid online quantification of left ventricular volume from real-time three-dimensional echocardiographic data. Eur Heart J February 2006 February 2006;27(4):460-468.

(23) Marsan NA, Westenberg JJ, Roes SD, van Bommel RJ, Delgado V, van der Geest RJ, et al. Three-dimensional echocardiography for the preoperative

assessment of patients with left ventricular aneurysm. Ann Thorac Surg 2011 Jan;91(1):113-121.

(24) Gutierrez-Chico JL, Zamorano JL, Perez de Isla L, Orejas M, Almeria C, Rodrigo JL, et al. Comparison of left ventricular volumes and ejection fractions measured by three-dimensional echocardiography versus by two-dimensional echocardiography and cardiac magnetic resonance in patients with various cardiomyopathies. Am J Cardiol 2005 Mar 15;95(6):809-813.

(25) Jenkins C, Chan J, Hanekom L, Marwick TH. Accuracy and feasibility of online 3-dimensional echocardiography for measurement of left ventricular parameters. J Am Soc Echocardiogr 2006 Sep;19(9):1119-1128.

(26) Chukwu EO, Barasch E, Mihalatos DG, Katz A, Lachmann J, Han J, et al. Relative importance of errors in left ventricular quantitation by two-dimensional echocardiography: insights from three-dimensional echocardiography and cardiac magnetic resonance imaging. J Am Soc Echocardiogr 2008 Sep;21(9):990-997.

(27) Caiani EG, Corsi C, Zamorano J, Sugeng L, MacEneaney P, Weinert L, et al. Improved Semiautomated Quantification of Left Ventricular Volumes and Ejection Fraction Using 3-Dimensional Echocardiography with a Full Matrix-array Transducer: Comparison with Magnetic Resonance Imaging. J Am Soc Echocardiogr 2005 8;18(8):779-788.

(28) Chang S, Lee S, Kim E, Hahm S, Jang SY, Park S, et al. Feasibility of Single-Beat Full-Volume Capture Real-Time Three-Dimensional Echocardiography and Auto-Contouring Algorithm for Quantification of Left Ventricular Volume: Validation with Cardiac Magnetic Resonance Imaging. J Am Soc Echocardiogr 2011 8;24(8):853-859.

(29) Pouleur AC, le Polain de Waroux JB, Pasquet A, Gerber BL, Gerard O, Allain P, et al. Assessment of left ventricular mass and volumes by three-dimensional echocardiography in patients with or without wall motion abnormalities: comparison against cine magnetic resonance imaging. Heart 2008 Aug;94(8):1050-1057.

(30) Sugeng L, Mor-Avi V, Weinert L, Niel J, Ebner C, Steringer-Mascherbauer R, et al. Quantitative Assessment of Left Ventricular Size and Function: Side-by-Side Comparison of Real-Time Three-Dimensional Echocardiography and Computed Tomography With Magnetic Resonance Reference. Circulation 2006 August 15;114(7):654-661.

(31) Qi X, Cogar B, Hsiung MC, Nanda NC, Miller AP, Yelamanchili P, et al. Live/real time three-dimensional transthoracic echocardiographic assessment of left ventricular volumes, ejection fraction, and mass compared with magnetic resonance imaging. Echocardiogr 2007 Feb;24(2):166-173.

(32) Soliman OI, Krenning BJ, Geleijnse ML, Nemes A, van Geuns RJ, Baks T, et al. A comparison between QLAB and TomTec full volume

reconstruction for real time three-dimensional echocardiographic quantification of left ventricular volumes. Echocardiogr 2007 Oct;24(9):967-974.

(33) Macron L, Lim P, Bensaid A, Nahum J, Dussault C, Mitchell-Heggs L, et al. Single-beat versus multibeat real-time 3D echocardiography for assessing left ventricular volumes and ejection fraction: a comparison study with cardiac magnetic resonance. Circ Cardiovasc Imaging 2010 Jul;3(4):450-455.

(34) Thavendiranathan P, Liu S, Verhaert D, Calleja A, Nitinunu A, Van Houten T, et al. Feasibility, Accuracy, and Reproducibility of Real-Time Full-Volume 3D Transthoracic Echocardiography to Measure LV Volumes and Systolic Function: A Fully Automated Endocardial Contouring Algorithm in Sinus Rhythm and Atrial Fibrillation. J Am Coll Cardiol: Cardiovascular Imaging 2012 3;5(3):239-251.

(35) Thavendiranathan P, Grant AD, Negishi T, Plana JC, Popovic ZB, Marwick TH. Reproducibility of echocardiographic techniques for sequential assessment of left ventricular ejection fraction and volumes: application to patients undergoing cancer chemotherapy. J Am Coll Cardiol 2013 Jan 8;61(1):77-84.

(36) Forthover RN, Lee SL, Hernandez M. Biostatistics: A Guide to Design, Analysis, and Discovery. Second ed.: Academic Press; 2007. p. 50-51, 60-62, 425.

(37) Karamitsos TD, Hudsmith LE, Selvanayagam JB, Neubauer S, Francis JM. Operator induced variability in left ventricular measurements with cardiovascular magnetic resonance is improved after training. J Cardiovasc Magn Reson 2007;9(5):777-783.

(38) Raman SV, Shah M, McCarthy B, Garcia A, Ferketich AK. Multi–detector row cardiac computed tomography accurately quantifies right and left ventricular size and function compared with cardiac magnetic resonance. Am Heart J 2006 3;151(3):736-744.

(39) Annuar BR, Liew CK, Chin SP, Ong TK, Seyfarth MT, Chan WL, et al. Assessment of global and regional left ventricular function using 64-slice multislice computed tomography and 2D echocardiography: A comparison with cardiac magnetic resonance. Eur J Radiol 2008 1;65(1):112-119.

(40) Maffei E, Messalli G, Martini C, Nieman K, Catalano O, Rossi A, et al. Left and right ventricle assessment with Cardiac CT: validation study vs. Cardiac MR. Eur Radiol 2012;22(5):1041-1049.

(41) Sarwar A, Shapiro MD, Nasir K, Nieman K, Nomura CH, Brady TJ, et al. Evaluating global and regional left ventricular function in patients with reperfused acute myocardial infarction by 64-slice multidetector CT: A comparison to magnetic resonance imaging. Journal of Cardiovascular Computed Tomography 2009 0;3(3):170-177.

(42) Xie F, Hankins J, Mahrous HA, Porter TR. Detection of coronary artery disease with a continuous infusion of definity ultrasound contrast during adenosine stress real time perfusion echocardiography. Echocardiogr 2007 Nov;24(10):1044-1050.

(43) Sibille L, Bouallegue FB, Bourdon A, Micheau A, Vernhet-Kovacsik H, Mariano-Goulart D. Comparative values of gated blood-pool SPECT and CMR for ejection fraction and volume estimation. Nucl Med Commun 2011;32:121-128.

(44) Yamani H, Cai Q, Ahmad M. Three-dimensional echocardiography in evaluation of left ventricular indices. Echocardiogr 2012;29(1):66-75.

(45) Jenkins C, Moir S, Chan J, Rakhit D, Haluska B, Marwick TH. Left ventricular volume measurement with echocardiography: a comparison of left ventricular opacification, three-dimensional echocardiography, or both with magnetic resonance imaging. Eur Heart J 2009 January 01;30(1):98-106.

(46) Zamorano JL, Bax JJ, Rademakers FE, Knuuti J. Evaluation of systolic and diastolic LV function. The ESC Textbook of Cardiovascular Imaging New York: Springer; 2010. p. 307-320.

(47) Childs H, Ma L, Ma M, Clarke J, Cocker M, Green J, et al. Comparison of long and short axis quantification of left ventricular volume parameters by cardiovascular magnetic resonance, with ex-vivo validation. J Cardiovasc Magn Reson 2011 Aug 11;13:40-429X-13-40.

(48) Lin C, Kuo C, Wang C, Yeh Y, Wu L, Hsu L, et al. Left Ventricular Systolic Function is Sensitive to Cycle-Length Irregularity in Patients with Atrial Fibrillation and Systolic Dysfunction. Acta Cardiol Sin 2012;28:103-110.

(49) Bull SC, Main ML, Stevens GR, Goldman JH, Constable SA, Becher H. Cardiac toxicity screening by echocardiography in healthy volunteers: a study of the effects of diurnal variation and use of a core laboratory on the reproducibility of left ventricular function measurement. Echocardiogr 2011 May;28(5):502-507.

(50) Blondheim DS, Beeri R, Feinberg MS, Vaturi M, Shimoni S, Fehske W, et al. Reliability of Visual Assessment of Global and Segmental Left Ventricular Function: A Multicenter Study by the Israeli Echocardiography Research Group. J A Soc Echocardiogr 2010 3;23(3):258-264.

(51) Holloway CJ, Edwards LM, Rider OJ, Fast A, Clarke K, Francis JM, et al. A comparison of visual and quantitative assessment of left ventricular ejection fraction by cardiac magnetic resonance. Int J Cardiovasc Imaging 2011 Apr;27(4):563-569.

4 Three-Dimensional Echocardiography Volume Quantification: The First Experimental Study in a Dynamic Heart Phantom

Need for Experimental Studies

The review has shown that three-dimensional echocardiography (3D ECHO) is the most promising technique for assessing volumes and ejection fraction. However, there are still limitations in accuracy and reproducibility (compared to cardiac magnetic resonance imaging). This is thought to be the due to the limited image quality of echocardiography. There is also concern that the tools for assessing left ventricular (LV) volumes might not be optimal. The best way to investigate this is to perform novel experimental studies in a dynamic heart phantom.

Need for a New Dynamic Heart Phantom

In our laboratory, a commercially available, anthropomorphic dynamic heart phantom was established which allows for performing of 3D ECHO studies for the first time. This phantom provides optimal recordings of LV shapes similar to those observed in patients after major apical myocardial infarction or during ischemia in the left anterior descending artery territory in stress echocardiography. This creates ideal conditions to investigate the different methods for volume measurements while excluding the effects of limited acoustic windows.

The anthropomorphic heart phantom allows for the assessment of ultrasound techniques and methods in a controlled clinical setting. It is believed that this is the first study to use a dynamic heart phantom for 3D ECHO volume assessment, scrutinising the most available methods for clinical LV assessment. So far, studies have mostly tested 3D techniques using static phantom models to assess the accuracy of volume measurements and to determine the primary sources of error associated with them (35,63). These phantom models were egg and balloon shaped, comprised of Zerdine and Latex materials, and were of a simplified ellipsoid shape. The accuracy and reproducibility in these studies were good, and this was also demonstrated in clinical studies (44,57,64,65). The results of this study in volumes with symmetric ventricles with an ellipsoid shape are in agreement with these reports.

Some groups have used dynamic heart phantoms for strain analysis, using hydraulic phantoms instead of a mechanically driven one. However, these phantoms cannot challenge contour finding algorithms as they do not provide changes anatomically representative to an infarcted ventricle (i.e. apical “bulging”). Heyde et al. and Lesniak Plewinska introduced inclusions into their ventricles, to mimic infarcted

territories, however, these were not anatomically representative of true pathological abnormalities and were not tested with automatic contour finding software (66,67). Furthermore, the phantoms presented by Heyde et al., Lesniak-Plewinska et al., Jia et al. and Claessens et al. are based on an ellipsoid chamber which increases and decreases its volume (66-69). The chamber keeps its ellipsoid shape during the cardiac cycle, which facilitates interpolation between manually chosen contours of the smallest and largest volume. The phantoms were designed for performing strain studies using speckle tracking imaging. LV volumes were not calculated during these studies.

Objective

The objective of the experimental studies was to compare the accuracy and reproducibility of LV volume measurements in a dynamic heart phantom with optimum image quality in five different three-dimensional echocardiographic methods.

Hypothesis 1: The semi-automatic methods for volume calculation will demonstrate difficulties in following the asymmetrical shape of the phantom heart LV.

Hypothesis 2: Inability of the semi-automatic contour detection algorithms to fit to the asymmetrical border of the phantom LV will cause inaccuracies in volume calculation, even in the context of excellent image quality.

Hypothesis 3: The manual method of discs technique will provide the most accurate measurement of the LV volumes in the phantom model due to the complete lack of geometrical assumption inherent in its methodology.

4.1 Methods

Hydrogel Anthropomorphic Heart

The hydrogel anthropomorphic heart consists of a polyvinyl alcohol (PVA) based anatomically accurate left and right ventricular structure, specifically designed for ultrasound interrogation (Fig. 4.1). The hydrogel structure not only allows for two- and three-dimensional imaging but also allows for m-mode and speckle tracking. During the moulding process, the material was mixed with an iodine solution,

allowing for use in cardiac computed tomography studies, and graphite, for generation of ultrasound speckle. The hydrogel structure mimics the density and ultrasonic properties of real myocardium, allowing for clinically relevant testing methods. At the base of the heart, four ports allow filling and emptying of both ventricular chambers.

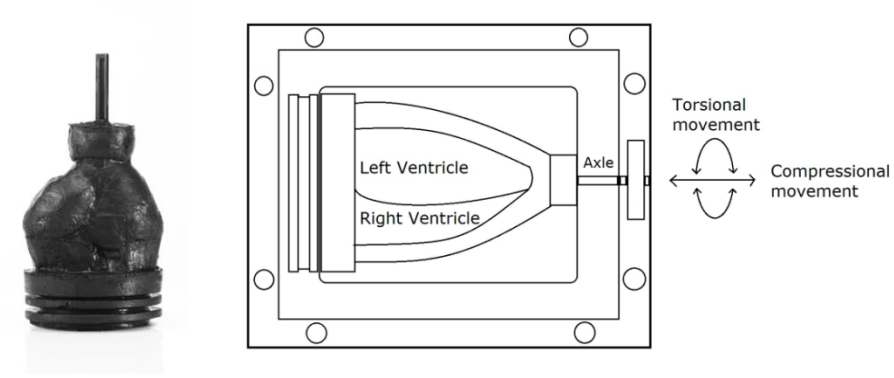

a **b**

Figure 4.1 Hydrogel Anthropomorphic Heart (a) – image selected from Shelley Medical Imaging Technologies brochure for dynamic heart phantoms; schematic of hydrogel anthropomorphic heart demonstrating the torsional and compressional forces applied to the heart (b).

Dynamic Heart Phantom

The Dynamic Heart Phantom (DHP) (Shelley Medical Imaging Technologies) consists of the hydrogel anthropomorphic heart attached to a control hub designed to govern its motion, applying both torsional and compressive forces (Fig. 4.2). It is contained within a completely transparent Plexiglas casing, and within the centre of the containment lies the hydrogel heart fixed to a cradle (consisting of the same material as the casing). At its apical end, it is connected to an axle, which is supported by another piece of the cradle. Both apical and basal cradle plates are fixed to a third plate lying along the base of the support structure. This plate is fixed to a long floating plate which lies along the base of the containment structure. The purpose of this floating baseplate is to allow movement during contraction so as to prevent damage to the phantom structure. Superiorly, there is a viewing window consisting of a thin plastic film designed to mimic the epidermis, allowing full penetration of the ultrasound beam. This viewing window is limited in its view of the phantom and only allows short axis and long axis views from its position. The entire

containment system is filled with distilled water to prevent microbial build up (which could cause clouding of the water and potential damage to the DHP).

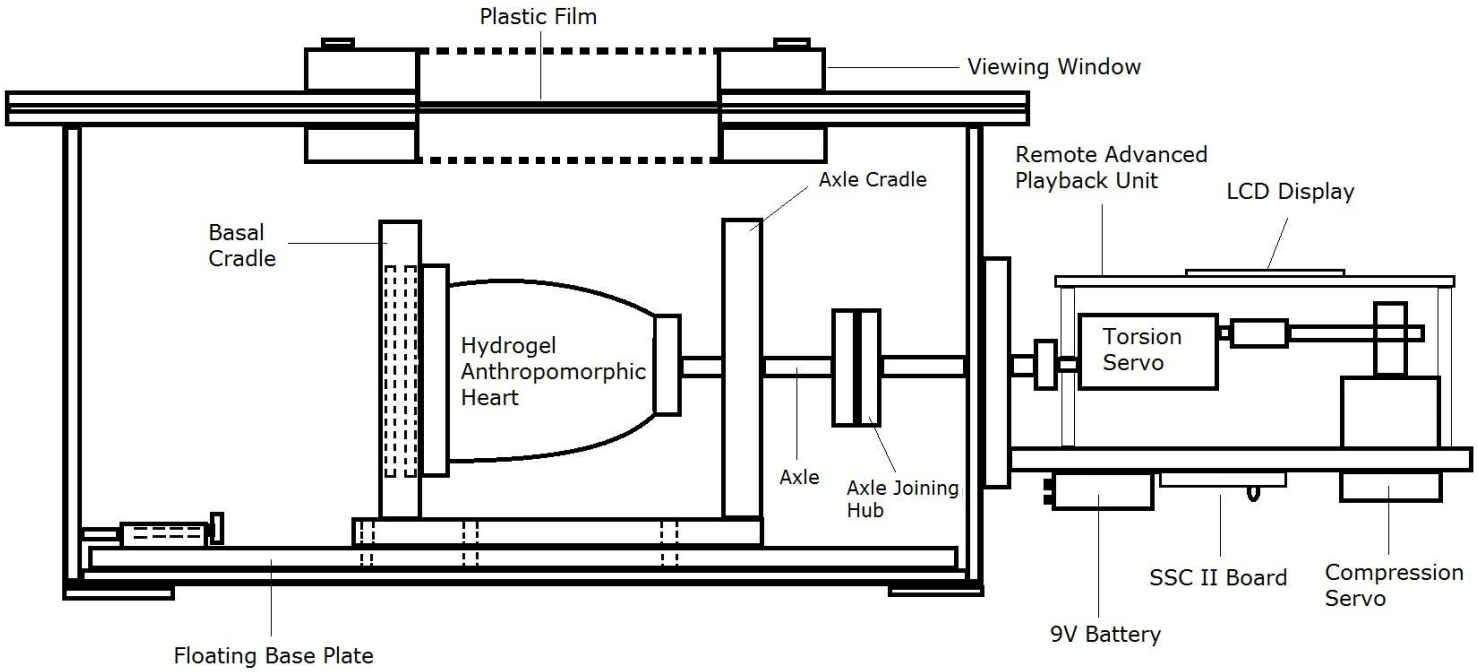

Figure 4.2 Side view schematic of Dynamic Heart Phantom System; adapted from a schematic designed by Shelley Medical Imaging Technologies.

The Servos

The forces applied to the DHP occur in simultaneous compressional and torsional phases, allowing the simulation of a live beating heart. However, the outer layer of the hydrogel heart is not rigid enough to prevent outward deformation of the chambers during compression; this prevents the larger reductions of cavity volumes which would be synonymous with a healthy cardiac output. That is to say that the ejection fraction of the DHP is only 15%. Thus, this dynamic phantom heart model can only be representative of a patient suffering from severe heart failure.

The hydrogel heart contracts via the combined forces of two separate servos (motors) attached by an axial linkage system between the two components; this system transfers the combined forces into the main axle which transmits the kinetic energy into the DHP. A lubricant is applied along the axle at junction points in which it passes through two Plexiglas interfaces. The two servos are powered by a 5V DC 2.6A input into a transformer converting the current into a 110V AC source. A 9V format 522 battery is also used to power the mini SSC II board. This small circuit board is designed to relay power from the main servo source and information from the remote advanced playback unit (RAPU) assisting in coordination of mechanical output. Of note, it is very important not to confuse the two power supplies for the RAPU and servos, as this will cause overload and damage the system.

Remote Advanced Playback Unit (RAPU)

The RAPU is a circuit board designed to deliver the desired programming information to the servos, following through the translational pathway to the DHP (Fig. 4.3). The programming information is stored in a 4GB Kingston data storage disk which rests in a port upon the RAPU. The RAPU board contains several different access ports for which different information is designed to be transferred for various purposes. This includes two audio jacks, a device serial port, control serial port, DMX output port, USB port and an infrared receiver for remote control. The board also contains a LCD display and four terminal buttons for menu control. The buttons and menu controls allow scrolling through different program options and are also important for initialising the interface

with the programming PC. The power supply for the RAPU is a 6V DC, 500mA input into an 110V AC source.

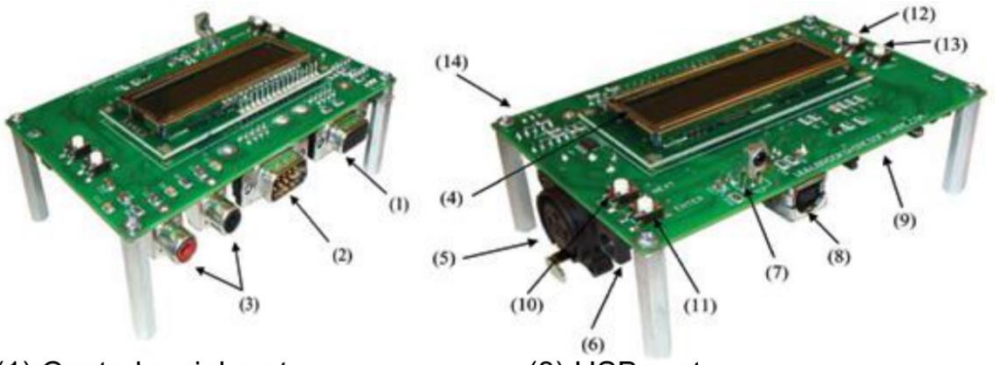

(1) Control serial port
(2) Device serial port
(3) Audio RCA jacks
(4) LCD screen
(5) DMX output port
(6) Power connector
(7) Infrared receiver
(8) USB port
(9) SD/SDHC slot
(10) Next key
(11) Enter key
(12) +VOL key
(13) -VOL key
(14) TTL port

Figure 4.3 Remote advanced playback unit schematic. Image downloaded from Brookshire Software LLC website: www.brookshiresoftware.com

Visual Show Automation (VSA)

The visual show automation (VSA) is the software which is installed on a standard PC computer with the RAPU and is used for programming the desired routines for the DHP. The VSA software divides its programming methods into two components, one for compression and the other for torsion. For the following experiments, only a fixed pre-programmed compression and torsion was used. The compression and torsion movements are programmed using a dial measured in degrees which is linked live to the DHP through a USB cable; as the dial position is altered, a movement command is communicated live to the DHP.

For compressional movement, there is a limit of 90 degrees (both clockwise and counter clockwise) (Fig. 4.4). Importantly, the torsional degree of motion only allows 20.5 degrees on either side of the programming dial; extending beyond this parameter will push the device past its safety threshold and burn out the gears of the torsional servo. Currently, there is no software restriction preventing this from happening, and so great care must be made during the writing of the routine for the torsional component. A VSA protocol was written up for the programming of the DHP system (Appendix A).

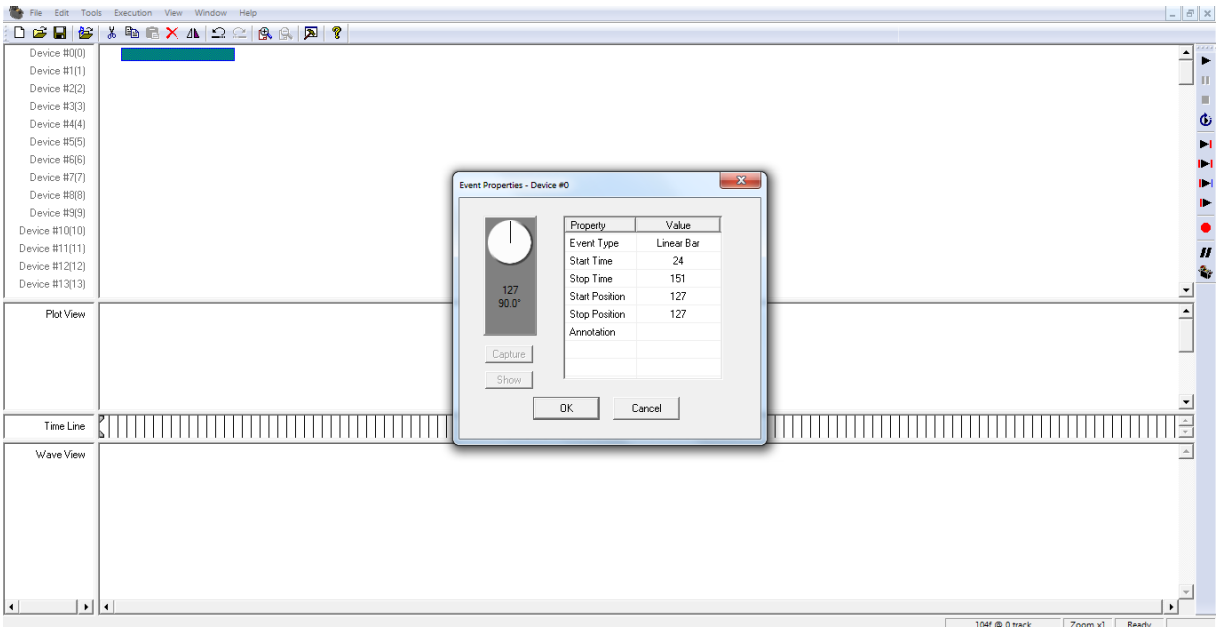

Figure 4.4 Screenshot of the visual show automation software demonstrating the programming option for compression and torsion parameter selection. The dial is manually dragged from 0 to 20.5 degrees while connected to the dynamic heart phantom, to program the desired compressional or torsional value. Exceeding the recommended limit of programming could result in damage of the servo gears. The system was pre-programmed before the experiment and this routine was maintained throughout all the experiments.

Electrocardiogram (ECG) Output

The ECG output in the supplied programs comes pre-programmed and so is automatically generated once the system is turned on. The phantom system was supplied with an audio cable containing a red input connector (Fig. 4.5a) and an open connection at the other end. This open connection requires a BNC female 1/4 inch audio phone plug adapter (purchased separately) (Fig 4.5b). This phone plug inserts into the ECG audio jack on all available ultrasound scanners. Once this jack is connected and the phantom is turned on, the preprogramed routines (i.e. anna 5 and 6 – provided by Shelley Medical Imaging Technologies) generate an ECG automatically allowing for 3D ultrasound acquisition (Fig. 4.6).

a **b**

Figure 4.5 Red audio output plug which connects to the RAPU audio RCA jack (a) and BNC ¼ inch audio phone plug adaptor which connects to the audio ECG input of the ultrasound scanner (b).

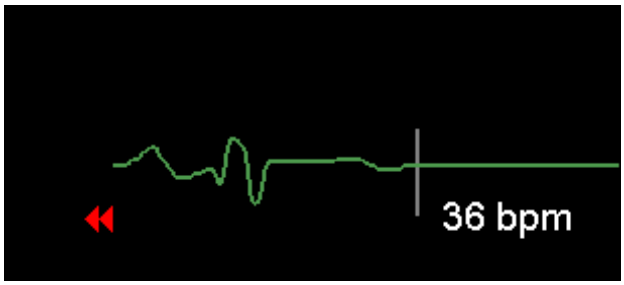

Figure 4.6 Image of the electrocardiogram from the Philips IE33 scanner, generated as an audio file by the dynamic heart phantom.

The DHP (Fig. 4.2) runs on a pre-programmed routine with the ECG cable fed into the audio input of the Philips IE33 ultrasound scanner which is separate from the standard ECG cable port used for patients; the generated heart rate was 36 beats per minute.

Measuring the True Volumes

The true volumes of the left ventricle and the volume changes were measured before the echocardiographic recordings. The anthropomorphic heart was removed from the apparatus and completely emptied and filled with distilled water using a laboratory measuring cylinder to the top of the two ports exiting the LV. The volume of both ports was then calculated from their length (7cm) and diameter (1cm) and subtracted from total amount of fluid required to fill the LV and the ports, in order to assess the absolute

resting volume of the LV (68.0mL ± 0). The two ports, which exit the left ventricle, were then connected to two Tygon tubes (diameter 1.27 cm) filled with distilled water. The two tubes were attached to a vertical stand. The tubes were initially filled to a mid-level position where a mark was made. With a 1mL syringe, water was added to the tubes by 1mL and marked at each interval to the bottom of the water meniscus until 5mL was added. The distance between each marking was then measured (3mm) and seven additional markings were added to each tube; 1mL was equal to one mark. Direct volume measurements were performed every 0.03-0.04 seconds (as per frame of video) in order to obtain corresponding measurements to the 3D echocardiographic exam; each 3D ECHO volume of the dynamic heart phantom was 0.04-0.05 seconds apart. The volume changes in the tubes were recorded using a video camera with a digital clock. The video was reviewed using Microsoft Windows Live Moviemaker which allowed for frame-by-frame analysis.

Ultrasound Equipment and Settings

Three-dimensional datasets were recorded with a Philips IE33 ultrasound machine using an X5-1 matrix array three-dimensional transducer. The volume rate was 20Hz, the depth 17cm and the sector width 80 x 80 degrees which allowed inclusion of the entire heart into the sector. Gain, time gain compensation and compression were optimised in order to provide similar signal intensity of the myocardium at all depths and to reduce echoes from the fluid. Acquisition was performed using full volume setting which created a single beat dataset by "stitching" 4 sub-volumes. The datasets were analysed offline using a commercially available software application (Philips QLAB v8.1) specifically designed for clinical 3D dataset processing. This application has two sub-programs for analysis of three-dimensional (3D) datasets for measurement of LV volumes (3DQ and 3DQadv); both were used in this study.

4.2 Methods: 3D ECHO Ejection Fraction and Volume Calculation in a Dynamic Heart Phantom

There are three methods that have been incorporated into the Philips QLAB v8.1 LV analysis platform. The first is a semi-automatic contour detection algorithm (method A1) which requires minimal input by the user (5 landmarks – lateral, septal, anterior and

inferior mitral hinge points, and apex) and automatically detects the 3D contour of the structure while calculating the residing volume. This method comes with two sub routines (methods A2 and A3) which allow for manual correction at different stages of volume and contour processing. The method B utilises the 2D Simpson's biplane method on the two orthogonal long axis views of the 3D dataset – the benefit is that the user can fully optimise the datasets with the complete cardiac structure present within 3D pyramidal image array, avoiding possible foreshortening which occurs often in 2D ECHO LV assessment. The third method is the manual method of discs technique (method C) whereby the LV is sliced into 16 short axis slices, of which the contours are available for manual area tracing by the user. The distance is then measured and the volume of each individual disc calculated and summed to provide the LV volume.

Methods A1, A2, A3 and C were performed in five different 3D datasets of the anthropomorphic dynamic heart phantom, and method B was performed in one dataset. The five datasets were acquired using the Phillip IE33 ultrasound scanner at different positions on the phantom viewing window; each position fell within a 3cm radius of the previous position, and all were random in their movement patterns. Each dataset contained 34 3D ultrasound volumes per recording; a 3D volume is defined as a single 3D frame of an ultrasound recording. Of these 34 recordings, only the nine volumes that existed between the largest and smallest volume were used for analysis and volume calculation.

4.2.1 Volume Measurements Using Three-Dimensional Contour Finding (Methods A1-3)

In the phantom, only the LV and right ventricle (RV) are included; therefore, we have only a two chamber view corresponding to a 4CV in humans, and a single chamber view corresponding to a 2CV. Prior to volume calculations, the orientation of the ventricle in the two and four chamber views was optimised to allow accurate border delineation by the user when using the 2D Simpson's biplane QLAB tool (3DQ), or by the 3D voxel semi-automatic contour detection algorithm (3DQ advanced). Optimisation of the phantom dataset in the quad screen involved magnifying the image and orientating the window so that the short axis view was in the bottom left viewing window, the four chamber view (minus the left and right atria in the phantom heart) in the top left and the two

chamber (minus the left atrium in the phantom heart) in the top right. Figure 4.7 represents the default orientation of the 3D dataset in the quad screen following initiation of the QLAB software application. Reorientation was performed by rotating the green axis (top left window) clockwise 90 degrees in the two chamber window (Fig. 4.8) and rotating the blue axis (bottom left window) using the same method (Fig. 4.9).

The subprogram 3DQadv (method A) has been developed to identify the borders of the LV semi-automatically (70). Once the ventricle is delineated, the 3DQadv program calculates the volume by summing the voxels within the selected borders. The measurements are performed on the quad screen, which the program 3DQadv automatically opens when a 3D dataset is selected for analysis (Fig. 4.7). The right and left upper sections represent two orthogonal 2D planes of the 3D dataset corresponding to a four and two chamber view – as in the 3DQ subprogram. The operator reviews the size of the LV during the cardiac cycle by scrolling through the two orthogonal 2D views; the 3D volumes displaying the smallest and largest areas of the LV are visually identified. Five landmarks are positioned by the operator at the mitral hinge points: in the two orthogonal long axis views and in one view at the apex in order to initiate the endocardial contour finding algorithm (Fig. 4.10a). The results can be displayed in a shell view of the LV and a display of the calculated borders in the 2D cross sections of the ventricle (Fig. 4.11a-c). The accuracy of delineation can be assessed by reviewing the fit of the calculated LV contours with the borders of the ventricle in the 2D cross-sections. For method A1, no manual corrections of the endocardial contour were performed (Table 4.1).

Methods A2 and A3 included manual corrections of the initial endocardial contour after positioning the landmarks (pre-processing, method A2) or of the endocardial contours obtained after processing the entire 3D dataset (post-processing, method A3) (Table 4.1). Manual correction was performed when the calculated endocardial border was more than 2 mm away from the LV border in one or both orthogonal 2D views of the dataset. In method A2, additional landmarks were set on the true endocardial border and the contour finding algorithm was repeated (Fig. 4.10). If the resulting contours still deviated from the true endocardial border, the entire procedure was performed a

second time. No further corrections were performed when the second endocardial contours still deviated from the true endocardium.

Manual correction after processing the entire 3D dataset (method A3) was also performed on two orthogonal 2D views of the 3D dataset by dragging the contours provided by the algorithm to the desired endocardial borders (Fig. 4.10 a-f). This procedure was applied to all volumes throughout the entire cardiac cycle. Like in method A2, the entire procedure was repeated. The resultant time-volume curves for all three semi-automatic methods were subsequently compared with the true volume curve.

Table 4.1 Methods for measurement of LV volumes in a 3D dataset

A1	Semi-automated volumetric method – without manual correction	The time points of the smallest (end-systolic) and largest (end-diastolic) LV volumes were visually identified by reviewing consecutive apical 2D planes. Semiautomatic contour finding was initiated by placing markers at the base of the LV and the apex. No further adjustment was performed
A2	Semi-automated volumetric method + manual correction on end-systolic and end-diastolic volumes, before processing the entire 3D dataset	Correction/adjustment of the initial contour provided by the 3DQadv program in the end-systolic and end-diastolic volumes. Additional markers were placed on the true endocardium in two orthogonal apical views
A3	Semi-automated volumetric method + manual correction at all time points after processing the entire 3D dataset	Correction/adjustment of the final contours calculated the 3DQAdv program
B	Simpson's biplane method of discs on optimised orthogonal 2D planes of a 3D dataset	Manual tracing of the endocardial contour and measurement of length on two orthogonal 2D planes obtained from the 3D dataset using the 3DQ program
C	Manual method of discs technique using short axis slices	Manual tracing of a stack of short axis discs provided by the QLAB iSlice tool (located in the subprogram 3DQ)which allows the user to divide the ventricular chamber into a maximum of 16 discs for manual contouring of the endocardial border

LV = left ventricle, 2D = two-dimensional, 3D = three-dimensional

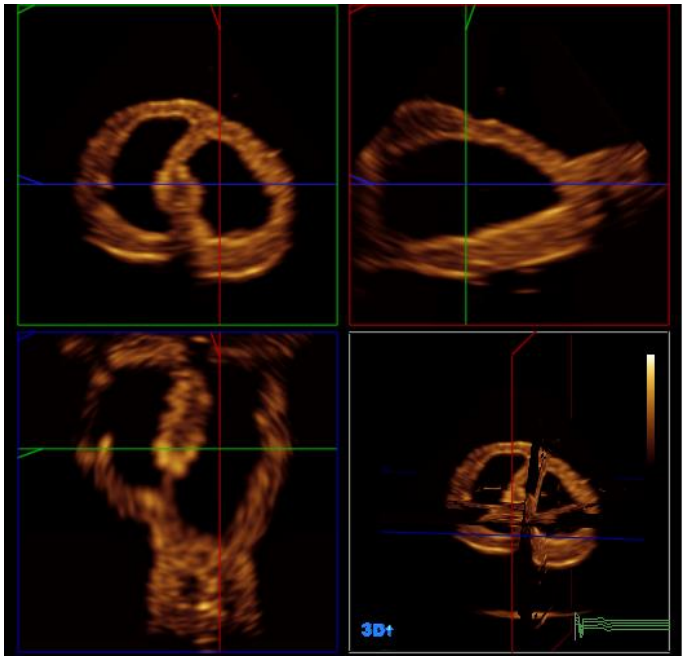

Figure 4.7 Initial orientation of phantom dataset in a quad screen demonstrating two orthogonal long axis views of the phantom heart in the top left and right windows, a short axis view in the bottom left window. On the bottom right the three orthogonal planes are shown together – this allows the operator to control and adjust the planes, in particular, to assure the longitudinal planes cut the true apex.

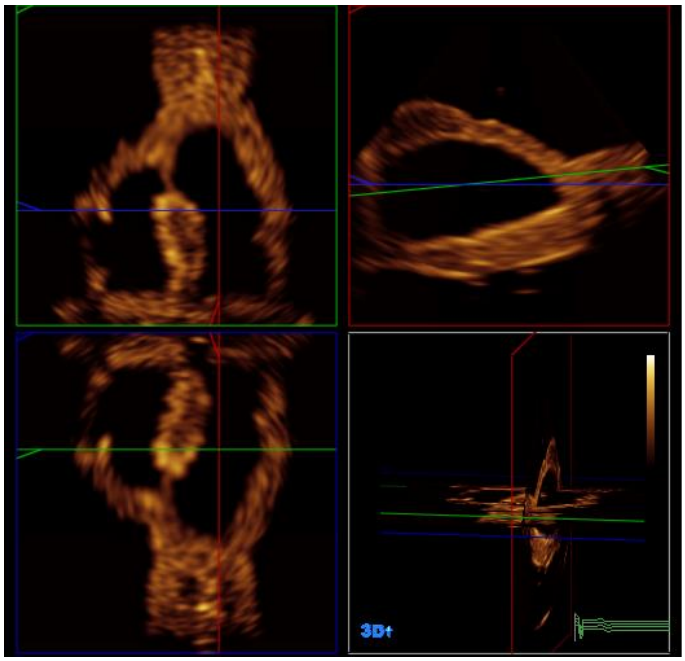

Figure 4.8 Orientation of phantom dataset following clockwise rotation of the green axis to approximately 90 degrees in the top right long axis view.

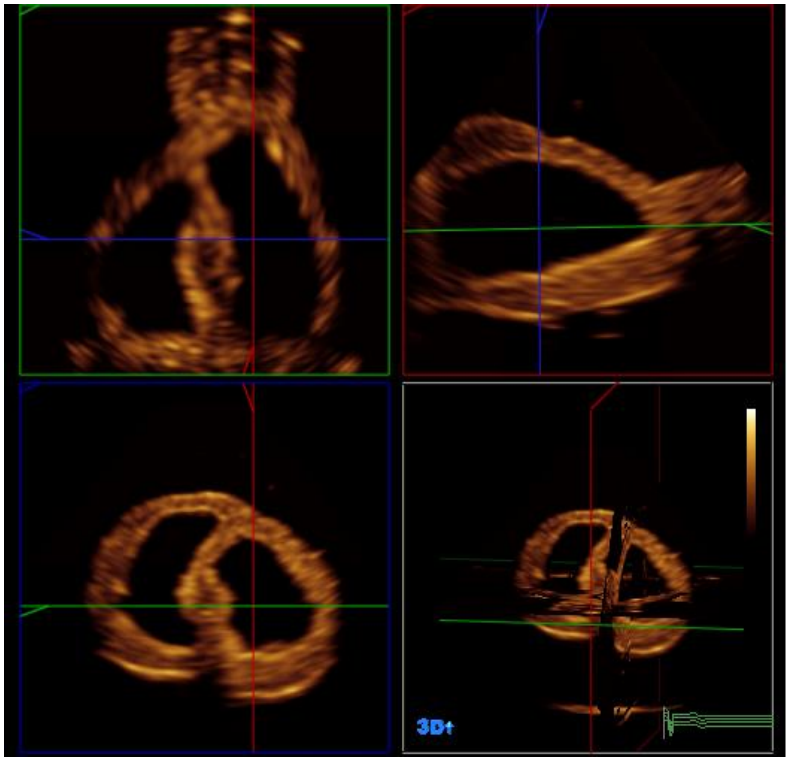

Figure 4.9 Final orientation of phantom dataset following approximately 90 degree clockwise rotation of blue axis in the top right long axis window.

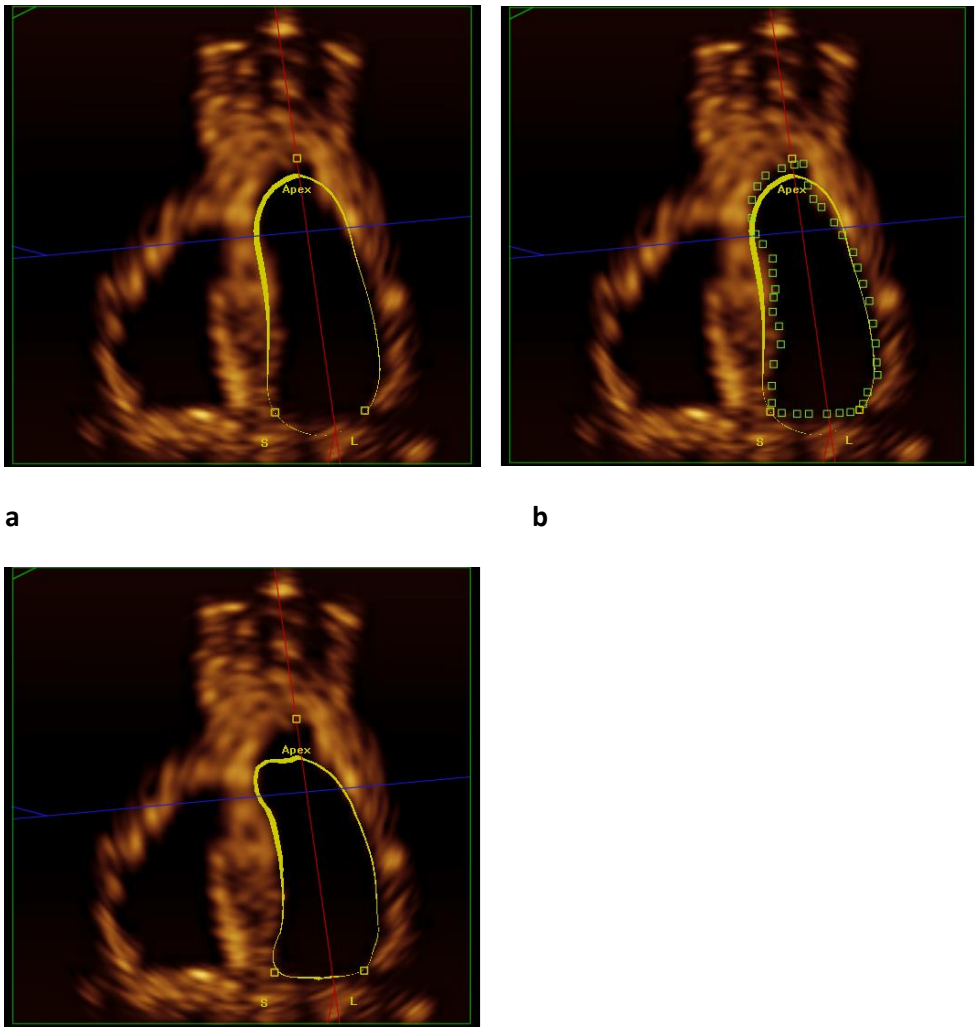

a **b**

c

Figure 4.10 Endocardial tracing of the left ventricle in the four chamber long axis view with a superimposed yellow border constructed by the 3DQadv automatic contour detection algorithm. Three markers are placed at the apex, and the hinge points of the anterior and posterior mitral leaflets (in addition two markers are placed at the hinge points of the mitral valve in the two chamber view). This is required to initiate the contouring algorithm (a). The border does not align well along the septal, apical and lateral borders. The green square markers indicate the points where the user has selected manual correction to occur and correct the misalignment of the yellow border (b). Zoomed view of the 4 chamber view window showing the recalculated yellow border following manual correction of the automatic contour detection algorithm – the manual correction algorithm performed well in aligning the septal and basal borders of the ventricle but failed to adequately follow the green corrective markers in the apical territory (c).

Method A1 Method A3

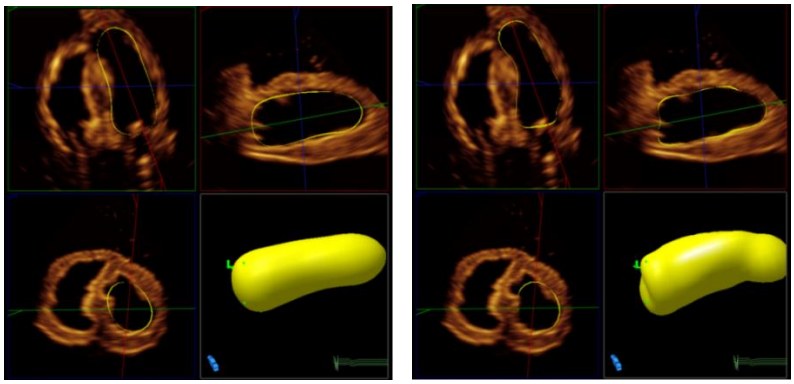

a d

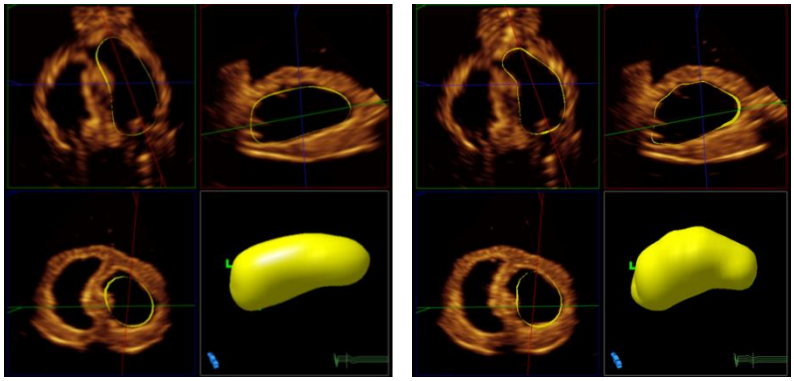

b e

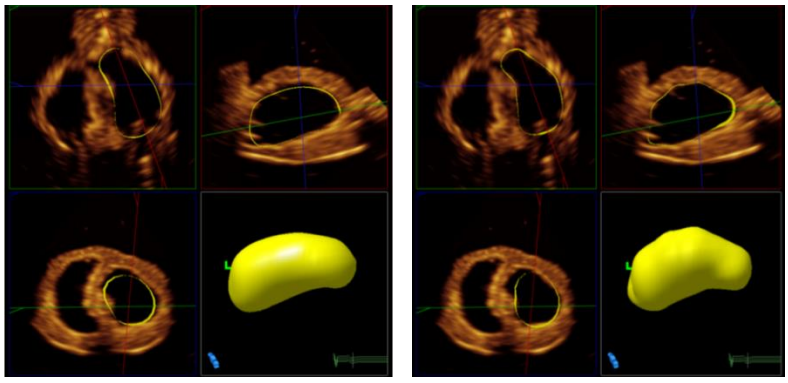

c f

Figure 4.11 Method A1 applied to three different volumes of the cardiac cycle (a - c). The corresponding results of method A3 are shown on the right (d – f). These are represented by volume 1 (0.0secs) (a & d), volume 5 (0.21secs) (b & f) and volume 8 (0.37secs) (c & f) of dataset 1.

4.2.2 Volume Measurements Using Two-Dimensional Method of Discs (Method B) from Three-Dimensional Datasets

Simpson's biplane is the standard technique for assessing volumes in two-dimensional echocardiography, but can also be applied on 2D planes from a 3D dataset (subprogram 3DQ – method B – Table 4.1 - Fig. 4.12). The LV volume is calculated from two orthogonal cross sections through the LV representing the four and two chamber views (70). The volume calculation is performed by summing up the volumes of a stack of 20 discs piling from the base of the ventricle to the apex. An ellipsoid shape is assumed for each disc and the diameter of the ellipse is the width of the ventricle in the four chamber and two chamber views. The position of the four and two chamber views are optimised in order to find the planes with the minimal difference in LV length measured from the middle of the base to the apex of the ventricle. In these views, measurements were performed according to the guidelines of the American Society of Echocardiography and the European Association of Echocardiography (71). By placing markers at the mitral hinge points and the apex of the ventricles, a shape was deployed which in most cases still had to be manually adjusted in order to follow the endocardium at the inner border.

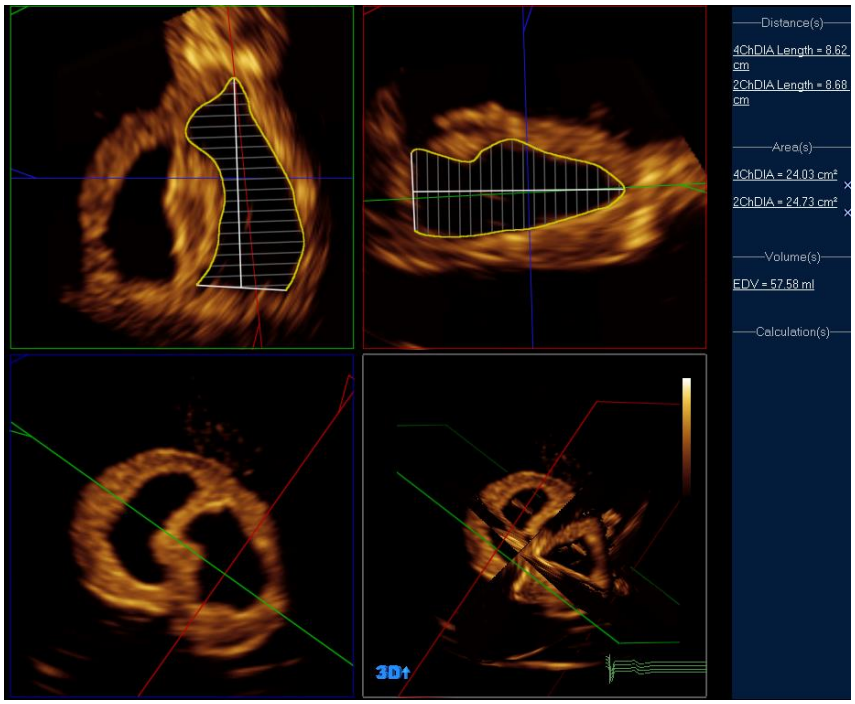

Figure 4.12 Screenshot of Philips QLAB 3DQ application measuring end-diastolic volume in a three-dimensional dataset with the Simpson's biplane method (method B).

4.2.3 Volume Measurements Implementing the Manual Method of Discs (MOD) Technique (Method C)

The subprogram 3DQ of the Philips QLAB LV analysis program allowed for the calculation of volume measurements using manual contouring of the short axis views with a slicing application (iSlice). This option slices the 3D LV dataset into 16 short axis slices with an area tracing function available for tracing the endocardial boundaries. However, an algorithm for volume calculation using this method does not exist, and so all measurements were entered into a Microsoft Excel spreadsheet and calculated by summing the volume of the total number of slices.

Following image optimisation as performed in methods A1-3 and method B, the left ventricular volumes were computed using the MOD technique (method C) aligned from the three-dimensional dataset (71). The LV volume was calculated from the sum of volumes in the stake of 14 short axis slices (16 – 2 end slices void of any chamber volume) (Fig. 4.13 & 4.14). The volume of each slice was calculated from the area, manually traced in the short axis view, multiplied by the total length of the ventricle (the longest length between both views), and divided by 14 (the number of slices with

traceable volumes). The area was manually traced at the inner border of the myocardium (Fig. 4.15).

The ventricular volumes of five different datasets were calculated. The volumes were calculated over the course of the phantom contraction between the largest and smallest volume, per 3D echocardiographic volume.

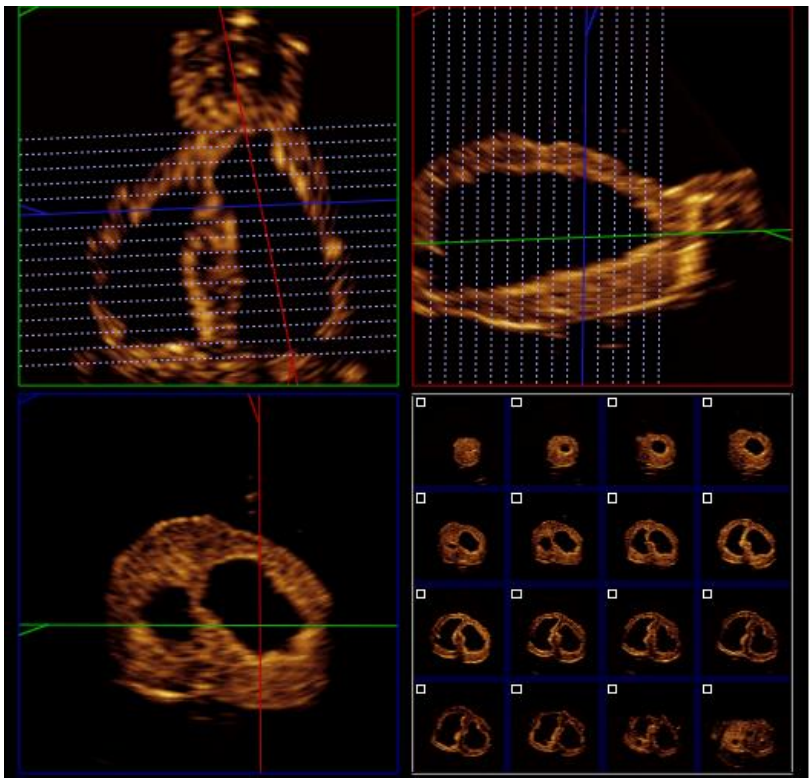

Figure 4.13 Example of the iSlice tool (used in method C) in the Philips QLAB software in a phantom heart model designed for ultrasound interrogation shown in the quad screen.

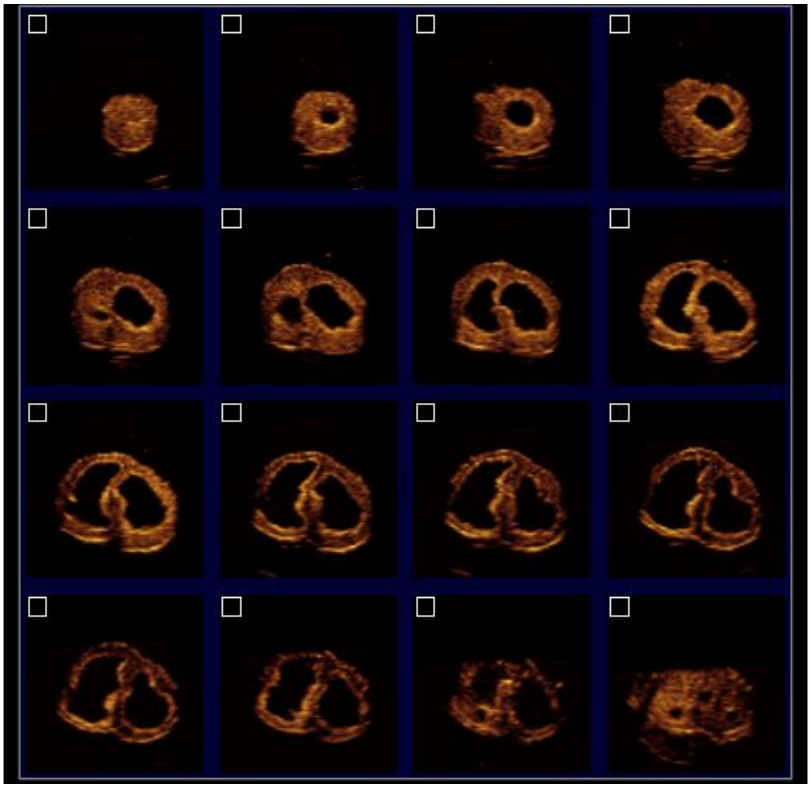

Figure 4.14 Enlarged view of the iSlice window displaying 16 short axis cross sections (used in method C) through the left ventricle of the phantom heart. Note that the first and last slice contains no visible volume allowing for identification of the end borders of the chamber.

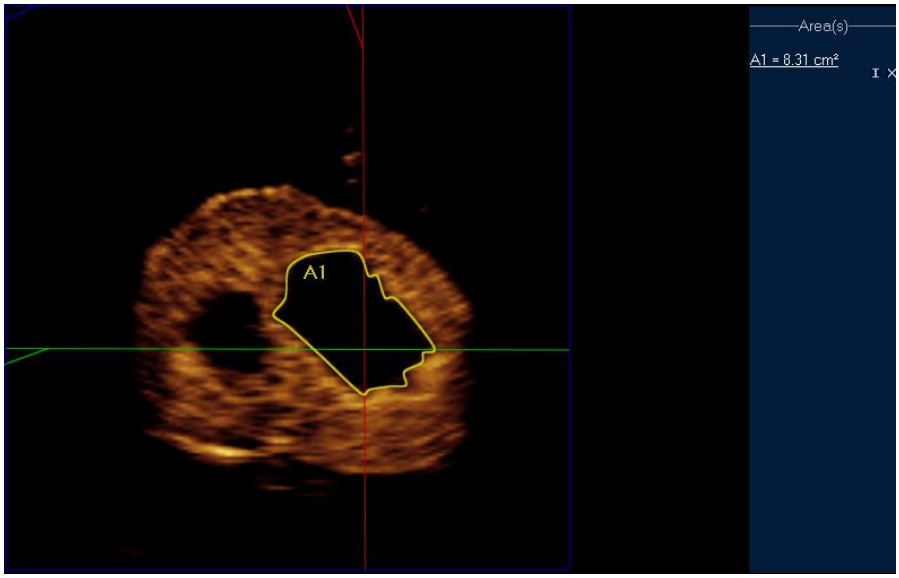

Figure 4.15 Enlarged view of the 5th slice with a manually traced area overlaying the border during implementation of method C. Note the area is available i n the right column.

The MOD volume calculations were performed in five different datasets by reader one and in one dataset by reader two to assess inter-observer variability.

Statistics

Descriptive statistics were used for measurements between datasets and the true volumes; measurements were presented as mean values and standard deviation for the true volume measurements. For further comparison of the MOD measurements with the true volumes in the phantom and the assessment of the inter-observer variability, the Bland-Altman test was used.

4.3 Three-Dimensional Echocardiography Ejection Fraction and Volume Calculation in a Dynamic Heart Phantom: Results

The true volume measurements were repeated twice in two different datasets to assess the reproducibility of the true volumes in the phantom. The largest standard deviation over the course of four datasets was 0.87mL (Fig. 4.16). The volume varied from 73.00mL at the beginning of the heart cycle to 61.00mL at the end.

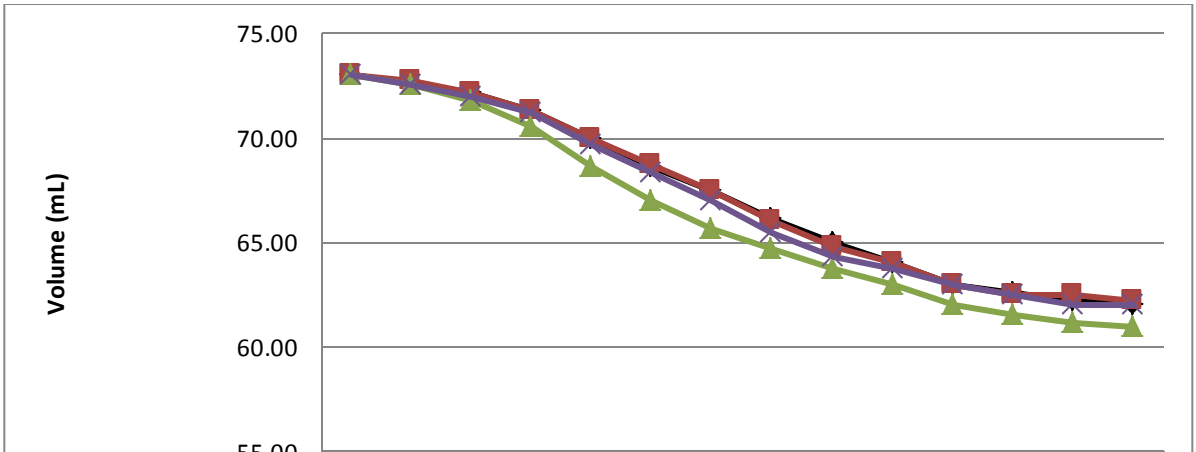

	0.00	0.03	0.06	0.09	0.12	0.15	0.18	0.21	0.24	0.27	0.30	0.33	0.36	0.39
True Volume D1 A1	73.00	72.63	72.17	71.33	70.00	68.67	67.50	66.13	65.00	64.00	63.00	62.63	62.17	62.00
True Volume D1 A2	73.00	72.75	72.19	71.33	70.00	68.75	67.50	66.00	64.75	64.00	63.00	62.50	62.50	62.17
True Volume D2 A1	73.00	72.50	71.75	70.50	68.67	67.00	65.67	64.67	63.75	63.00	62.00	61.50	61.13	61.00
True Volume D2 A2	73.00	72.50	72.00	71.25	69.67	68.33	67.00	65.50	64.33	63.75	63.00	62.50	62.00	62.00
Mean	73.00	72.59	72.03	71.10	69.58	68.19	66.92	65.57	64.46	63.69	62.75	62.28	61.95	61.79
SD	0.00	0.12	0.20	0.40	0.63	0.81	0.87	0.66	0.55	0.47	0.50	0.52	0.59	0.53

Figure 4.16 Comparison of repeated measures of the true phantom volume during the cardiac cycle between the largest and smallest volume. D1 = Dataset 1; D2 = Dataset 2; A1 = Analysis 1; A2 = Analysis 2. The x axis denotes time in seconds.

In all experiments, high quality recordings could be obtained without dropouts. Each recorded 3D dataset included a full cardiac cycle with 34 consecutive 3D volumes. The QLAB software documents the time value of each 3D echocardiographic volume which allows for comparison of volume curves (0.4-0.5seconds per 3D volume) .In the following graphs only the 3D volumes between the largest and smallest LV volume are displayed. The heart phantom provided an asymmetric shape during most parts of the cardiac cycle. Only when the anthropomorphic heart was stretched was the LV shape was close to a symmetric ellipsoid shape. During that phase, the contour calculated by the 3DQadv algorithm followed the true endocardium with minor deviations (<2 mm). The agreement between two readers measured in 20 different datasets using a normal ellipsoid shaped ventricle was very high (bias = 0.59mL) with small variability (limits of agreement = -2.58 to 3.75mL) using method A1. When a comparison between readers was made using the abnormal ventricular shape, the bias was 1.79mL and the limits of agreement were -1.57 to 5.19mL.

Compared to the true volumes measured, using method A1 resulted in an underestimation of up to 19.3ml (31% of the true volume) (Fig. 4.17). There were considerable differences between multiple measurements in different 3D datasets. On average, the difference between the true volume and A1 measurements was 18% ± 6.5%. However, all volume curves showed a similar decline from the largest to the smallest volume.

When manual correction was performed on the initial contours (method A2), less deviation from the true volumes was found, and there was both under- and over-estimation (Fig. 4.18). The maximum difference was 14 ml (21% of the true volume). With method A3, which consisted of manual correction after the 3D dataset had been completely processed, the differences to the true volume were similar to those found with method A2. However, the measurements do not smoothly follow the true volume curve. There are outliers which distort the volume curves and do not indicate the gradual decline of the volumes (Fig. 4.19).

With method A1, it was not possible to achieve an endocardial contour that followed completely the true LV border (Fig. 4.22 & 4.24a): without manual correction there was misalignment of the calculated endocardial contour seen mainly at the apex (long axis views) and in short axis views (SAX). That was not different with pre-processing correction (Fig. 4.23 & 4.24d). Using post-processing correction, the best alignment was achieved in long axis planes, but in SAX there was still considerable deviation of the calculated endocardial contour from the true endocardium (Fig. 4.11). In the SAX view, the contour never fit to irregular shapes and was restricted to an ellipsoid shape.

Figure 4.20 shows the comparison of the volume measurements obtained with method B (biplane Simpson) with the true volume. There was a discrepancy between the measurements of both readers and the true volume, which reached a maximum difference of 13.7 ml (19% of the true volume); however, fewer measurements were performed. One reader (reader 2) had a good agreement with an average difference of 6.5%. Reader 1 had an average difference of 12.8%. The volume curves obtained with method B do not represent the true volume change.

Figure 4.21 displays the volume changes over time of the true volumes and the calculated volumes performed using method C in 5 datasets and a second read by an independent observer of dataset one. The volume calculations performed using method C corresponded very closely with the true volume measurements. Only one volume curve did not follow the trend of the true volumes. The largest difference with the true volumes was 6.5mL (9%) (Fig. 4.21).

Bland-Altman analysis showed that limits of agreement were narrowest in method A1, when the results of reader 1 were compared with the true volumes (Fig. 4.25a). The limits of agreement were similar for method B in comparison with methods A2 and A3, which was unexpected considering the geometrical assumptions associated with the method (Fig. 4.25b & 4.26); they were worst in method A3. The bias was largest in method A1. When the measurements were compared between both readers, the best results were obtained for method A1 (bias = 4.4 mL; LOA = 3.35 to 5.4mL). When manual correction was used, the limits of agreement for the inter-observer variability became worse (A2 bias = 6mL, LOA = -2.3 to 14.4mL; A3 bias 3.4mL; LOA = -9.8 to 16.7mL). Similar results were obtained when comparing both readers for method B against the true volume (bias = -6mL; LOA = -4.1 to 16.3mL). When the agreement between the method C measurements and the true volumes was calculated using Bland-Altman analysis, there was an excellent agreement (bias = -0.46mL; limits of agreement of -6.3 to 5.4mL) (Fig 4.2a). The same statistical analysis was performed to compare both readers to assess inter-observer variability (bias = 0.9mL; limits of agreement -2.3 to 4.1mL) respectively.

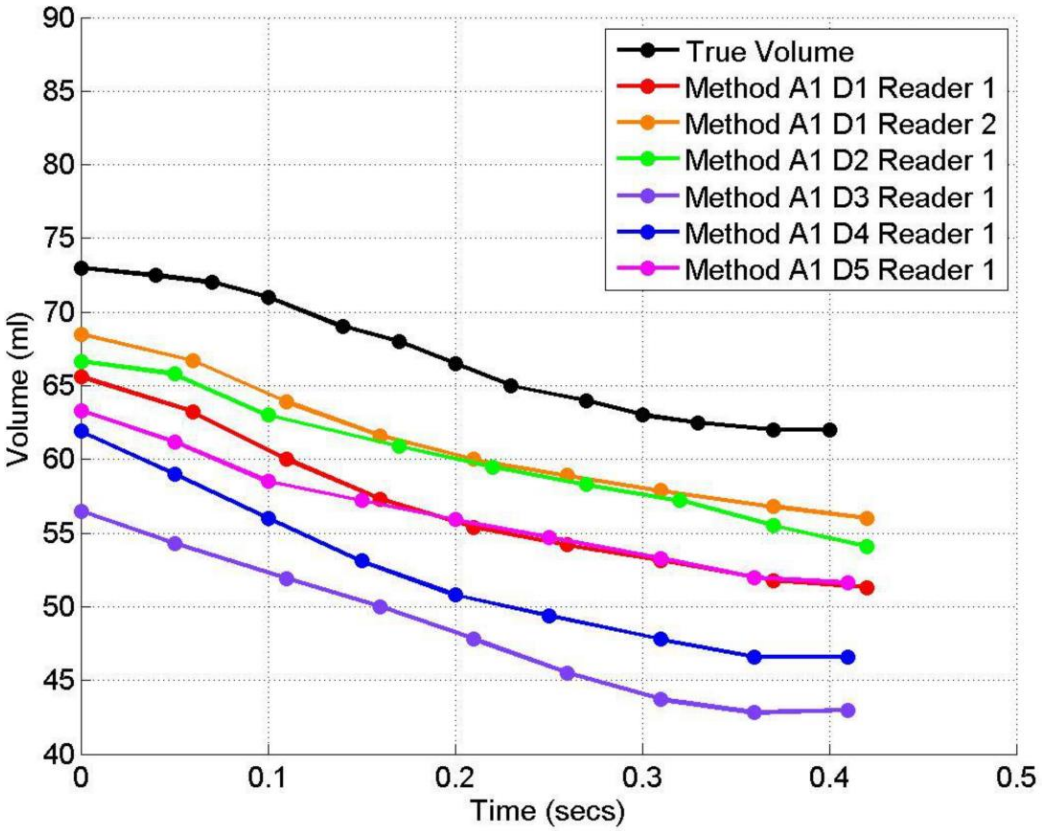

Figure 4.17 Comparison of method A1 from different datasets taken at different positions in the phantom viewing window with the true volumes. Method A1 = semi-automated volumetric method with no manual correction. D1 = dataset 1; D2 = dataset 2; D3 = dataset 3; D4 = dataset 4; D5 = dataset 5.

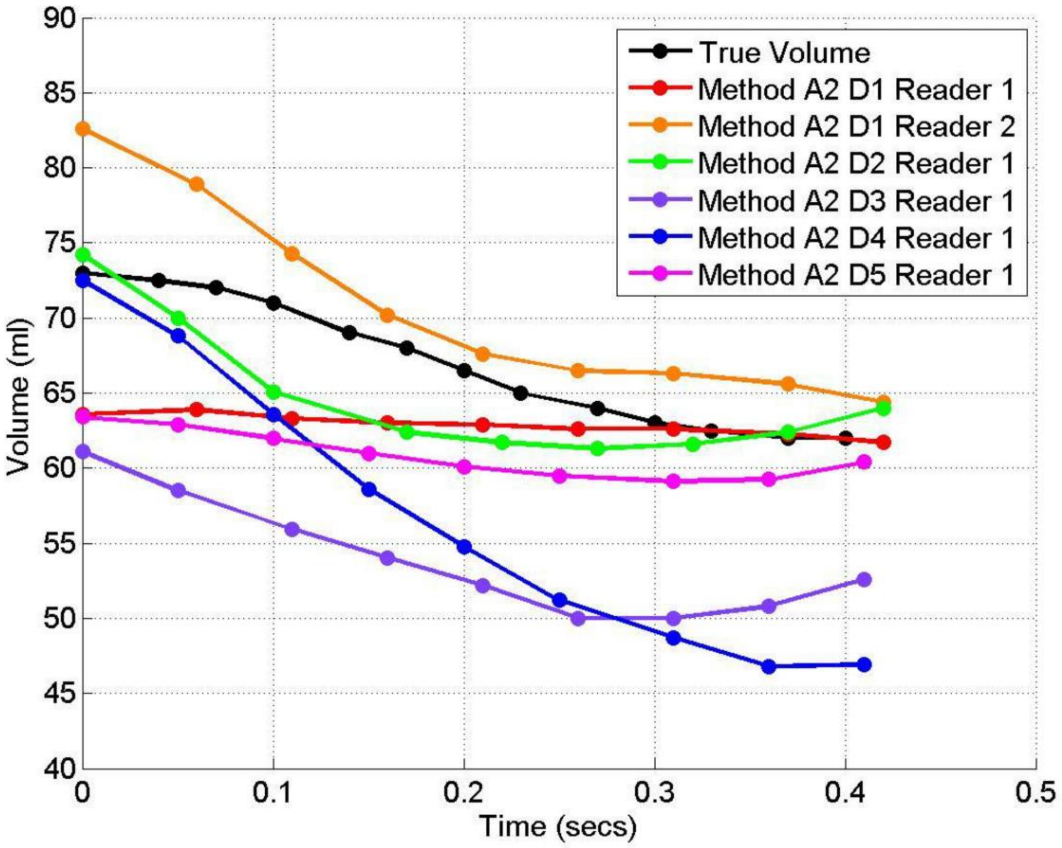

Figure 4.18 Comparison of method A2 from different datasets taken at different positions in the phantom viewing window with the true volumes. Method A2 = semi-automated volumetric method with pre-processing manual correction. Abbreviations as in 4.17.

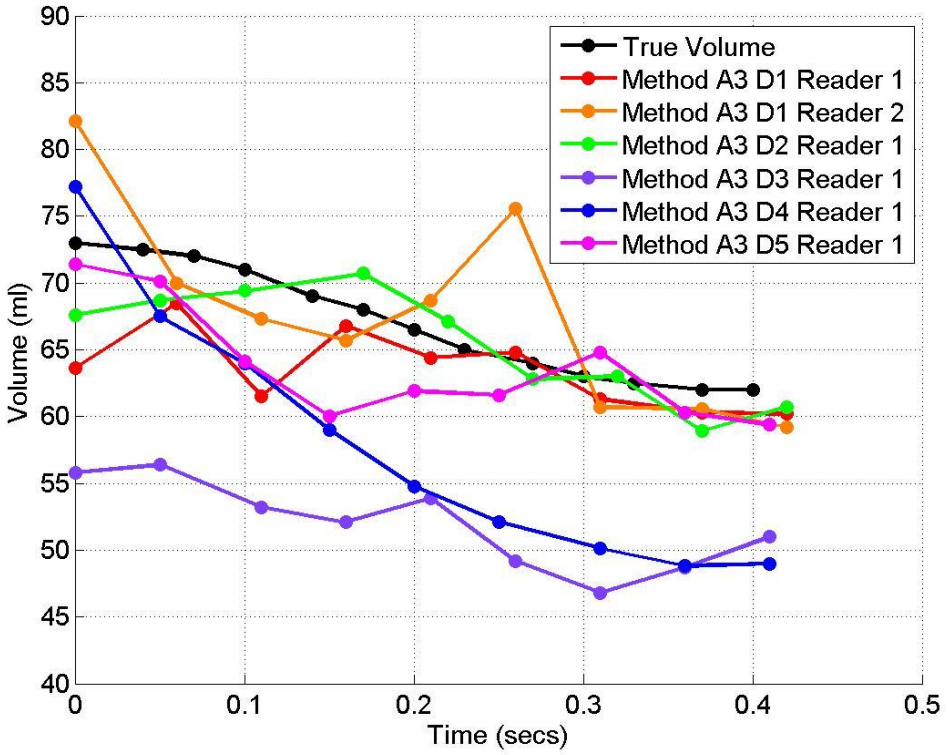

Figure 4.19 Comparison of method A3 from different datasets taken at different positions in the phantom viewing window with the true volumes. Method A3 = semi-automated volumetric method with post-processing manual correction. Abbreviations as in Fig. 4.17.

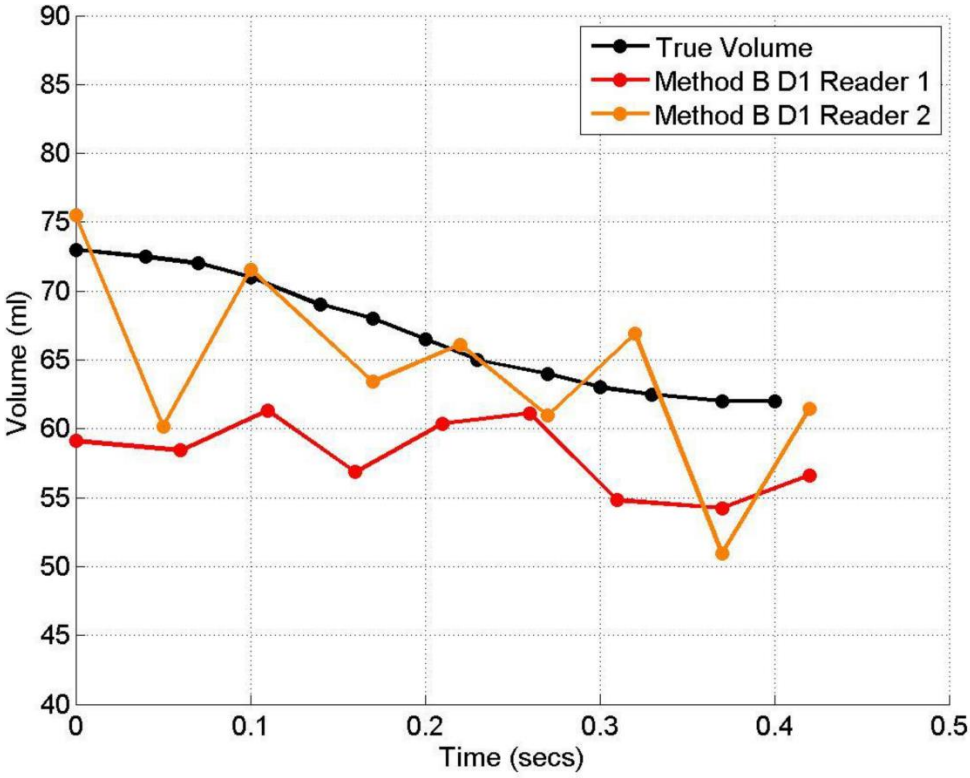

Figure 4.20 Comparison of method B from two different readers with the known volume. Method B = Simpson's biplane method of discs. Abbreviations as in Fig. 4.17.

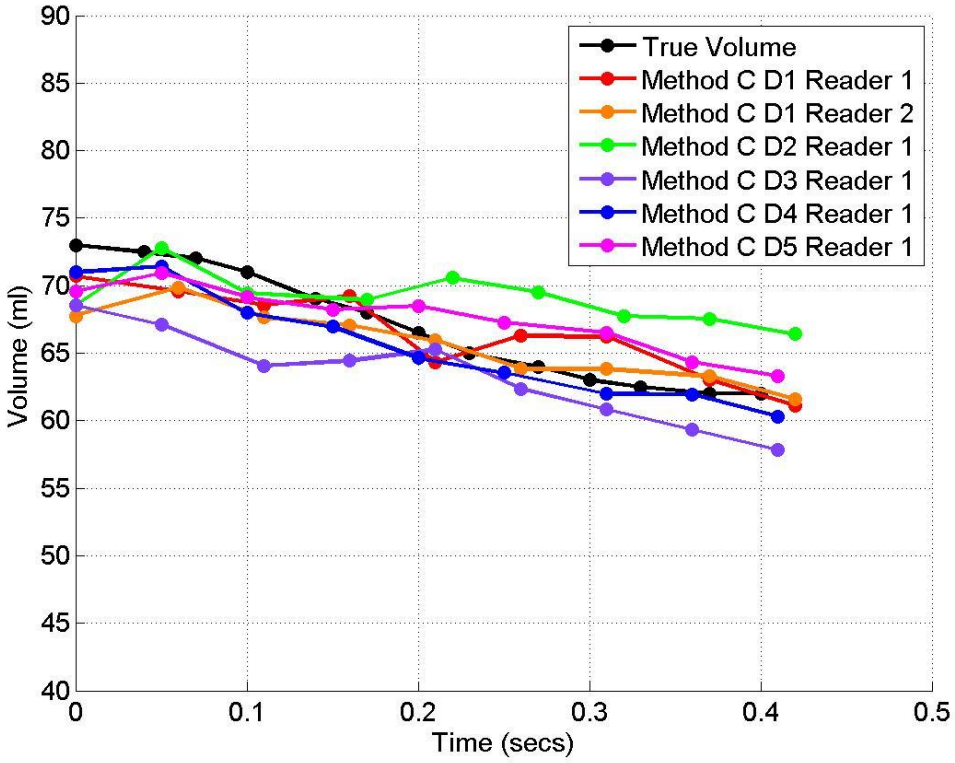

Figure 4.21 Comparison of method C for three-dimensional echocardiography left ventricular volume calculation in five different phantom datasets. Method C = manual tracing of a stack of short axis discs. Abbreviations as in Fig. 4.17.

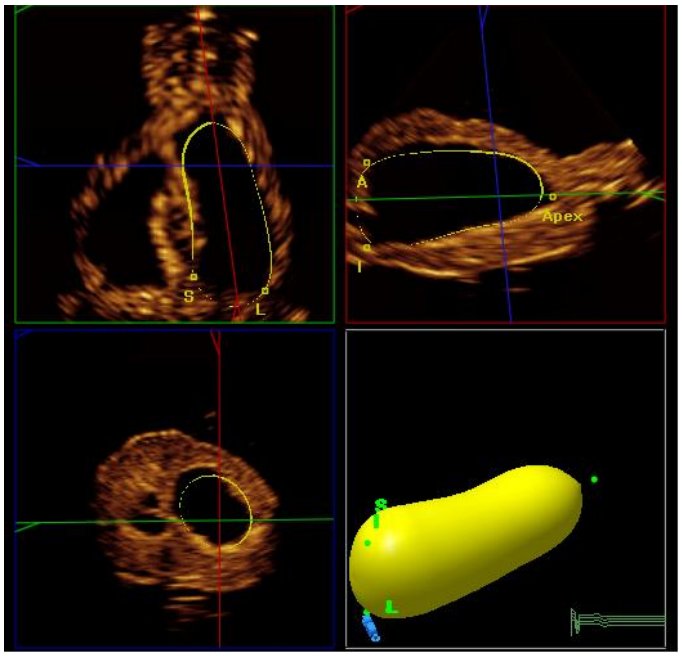

Figure 4.22 Quad screen view of method A1 semi-automatic contour detection algorithm before manual correction.

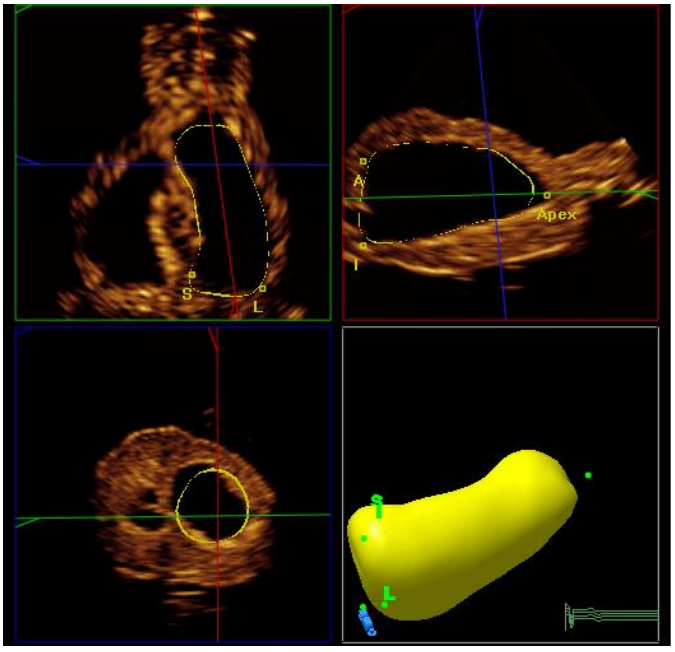

Figure 4.23 Quad screen view of method A2 with good border delineation in four and two chamber views.

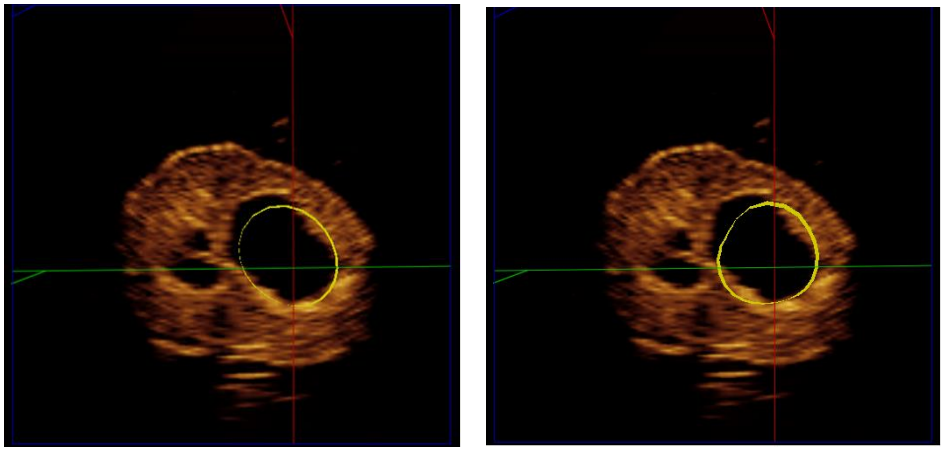

a **b**

Figure 4.24 Zoomed image of method A1 border detection in the short axis view, before manual correction, of a model with an overall good fit; note, even in a good fitting ventricle, the misalignments seen in the short axis view (a); enhancement of the short axis view of method A2 displaying misalignment (b).

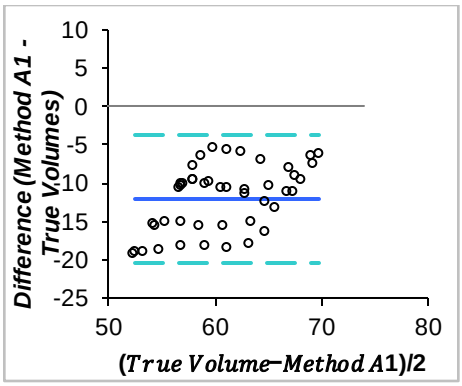

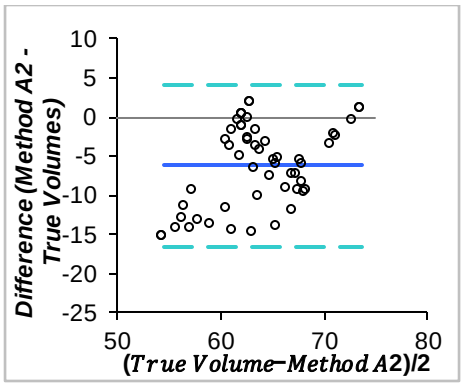

a **b**

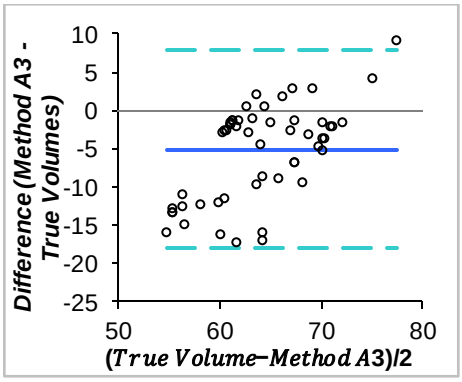

c

Figure 4.25 Comparison of the method A volume measurements with the true volumes using Bland-Altman analysis: A1 (a), A2 (b), A3 (c).

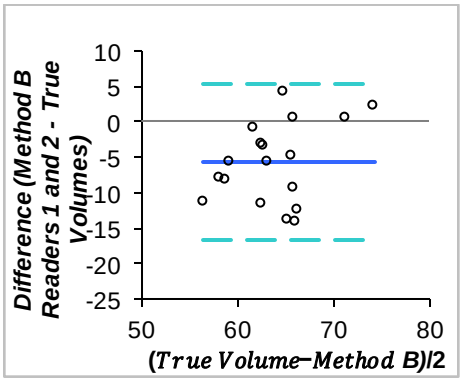

Figure 4.26 Comparison of the volume measurements performed with method B Readers 1 and 2 versus the true volume.

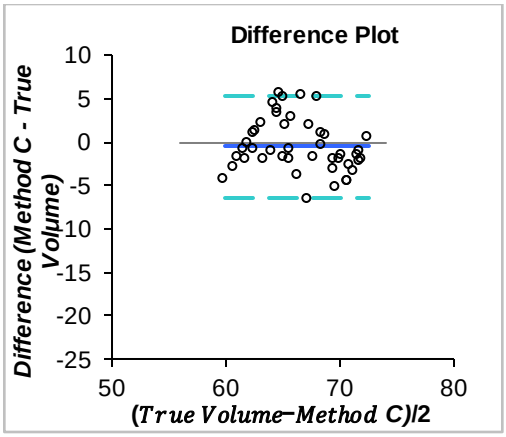

Figure 4.27 Bland-Altman analysis between the method C technique and the true volumes of five different datasets.

4.4 Three-Dimensional Echocardiography Ejection Fraction and Volume Calculation in a Dynamic Heart Phantom: Discussion

After completing the experimental and statistical analysis portions of this study, the following were concluded in relation to the proposed hypotheses: 1. the semi-automatic contour detection algorithms had great difficulties fitting to the asymmetrical shape of the LV; 2. there was documented underestimation in calculated LV volumes using the semi-automatic techniques in which reproducibility worsened with manual correction (this is likely a result of the inaccuracies in chamber contouring); 3. the manual method of discs is the most accurate and reproducible method for assessing LV volume.

In order to evaluate the quality of a contour finding algorithm, a ventricle is needed which changes in shape during the cardiac cycle. This could be achieved with our phantom by using an axle which pushes the apex of the heart phantom towards the base. A downside of this model is that it only allowed for minor volume changes, which are not representative of the volume changes in a normal heart. However, we aimed to investigate the quality of an LV contour finding algorithm. For this purpose, it was advantageous to have no major volume changes.

We could show that none of the semi-automatic methods for endocardial contour finding completely fit with the endocardial borders, although the image quality was excellent in all experiments when asymmetric volumes were analysed (Fig. 4.10 & 4.11).

This is in agreement with findings of Jacobs et al. who reported difficulties in applying semi-automatic contour algorithms to patients with LV aneurysms (39). After setting the initial contour, the computer algorithm performs a sequence analysis to find the contours of the other volumes within the cycle (72). The reason for preselecting the lowest and highest volumes is probably that it allows the system to perform a process of interpolation instead of "finding" the contours of the entire endocardium during the cardiac cycle. There is another commercially available software which can be used offline (TomTec 4D LV-Analysis). This software allows the operator to vary the amount of automatic interpolation that the system performs. This may be particularly helpful in the irregularly shaped ventricle. With the software available for our experiments, we were not able to control the amount of interpolation.

The endocardial contours provided by the semiautomatic algorithm can be corrected manually in different ways (Table 4.1); although, this did not allow an optimal fit of the calculated contour with the endocardium. With the current software, it is possible to draw a contour in two orthogonal long axis views after auto-detection has occurred. The algorithm, however, does not completely follow directly the original tracing in the desired positions of the ventricle. The Philips QLAB 8.1 user manual describes the 3DQadvanced (method A) method of volume calculation as being completely independent of geometric assumptions; our study findings suggest, that this is not entirely the case, as the borders created by the automatic contour detecting algorithm seem to be limited by an ellipsoid shaped framework to which even the manual correction algorithm is bound (73). In particular, reviewing the short axis views show that the completed contour deviates from the endocardium in many parts of the LV; this demonstrates that the algorithm is limited in its ability to follow abnormal shapes (Fig. 4.23 & 4.24).

How does this affect volume measurements? Compared with the true volume of the LV, the volumes measured with method A1 were smaller, equalling a maximum error of 31% and mean error of 18% ± 6.5%. This error was higher than a static phantom study carried out by Herberg et al., who reported an error of -6.7±2.5% (63). Mor-Avi et al. were able to show in their static phantom study a difference between selected borders in short axis tracings. By using a balloon with a known volume of 150mL, three SAX

tracings were taken of the inner, outer and midline of the border, showing a difference of 57ml in volume from tracing between the inner and outer border; the most accurate tracing reported to be in the centre of the border calculating a volume of 148mL (35). However, in the heart phantom the borders were placed as close as possible along the inner side of the myocardium using manual correction, and that resulted in a smaller error (A2 bias = 6.2mL; A3 bias = 5.1mL) compared to volumetric measurements without manual correction.

The reproducibility in methods A1 (LOA = -20 to -3mL), A2 (LOA = -16 to 4) and A3 (LOA = -18 to 8), although poorer than would have been expected with such high image quality, were still better than the majority of clinical studies reported in the literature review (*see Chapter 3*). These limits of agreement were further reduced by implementing method C (LOA = -6 to 5mL) for which volumes were attained via direct contouring of the short axis slices. For accurate and reliable assessment of LV volumes, it is also necessary to reconstruct unforeshortened 2D planes for the initial contour finding; this is now available with the 3D ECHO technology. However, the available program includes no tools to actually confirm optimal orientation of the 3D dataset by measuring the long axis of the two orthogonal views. In particular, placing the apical marker is more variable in an asymmetrically shaped LV. This limitation could have affected the measurements and further study is needed to address this problem; however, this would require a modification of the current software, which also should be adapted to non-ellipsoid shapes.

There is only one study, to our knowledge, that focused solely on comparing 3D ECHO LV volume measurements with CMR in a population of patients with LV aneurysms. When compared to other studies of patients with symmetrical ventricles, as reported in Figure 3.2 (see *Chapter 3.0*), Marsan et al. reported an EDV bias (-21.6mL) in the same range; however, the limits of agreement (-102.4 to 59.2mL) were among the largest of the 18 study cohort (40). This suggests that the authors had difficulty generating accurate volume measurements in patients with an asymmetrically shaped ventricle.

Method of discs (method C) was one of the first techniques adopted for three-dimensional volume calculation in echocardiography, but with earlier ultrasound instrumentation and technology, the image quality did not allow for the levels of

accuracy now seen with the current semi-automatic contour detecting and volume calculation algorithms (57,74). This is the first study to reintroduce this method for volume calculation using contemporary ultrasound technology.

The method of discs technique is the method of choice in CMR imaging for the calculation of left ventricular volumes; it has been repeatedly validated and is now the accepted reference standard (15). The high level of accuracy in CMR was demonstrated in a phantom mould taken from an excised dog heart, in which Childs et al. reported an excellent agreement (bias = 4.94mL; limits of agreement = -8.83 to 17.05mL) (58). In the current study, the same level of accuracy was demonstrated under ideal imaging conditions using a phantom heart (bias = -0.45mL; limits of agreement = -6.15 to 5.31mL) (Fig. 4.27). This was further demonstrated graphically where 4 of the 5 datasets analysed by reader 1 followed the same trend over time as the true volumes (Fig. 4.21); this was in agreement with hypothesis 3. The anthropomorphic dynamic heart phantom model represents near perfect image quality whereby the methodology of the MOD technique can be assessed under controlled settings using the true volumes measured directly from the phantom during its cardiac cycle.

Before development of the matrix array transducer which allows for full volume echocardiographic image acquisition, groups experimented with the computational construction of a 3D echocardiographic matrix from multiple acquisition of 2D images with use of ultrasonic spatial locators fixed to the transducer. With knowledge of the location of the transducer in 3D space, the 2D images could be aligned and a 3D matrix constructed (74-76). This technique allowed the users to perform short axis tracing and volume calculation in echocardiography for the first time without any geometrical assumptions. This technique was largely developed and tested by Gopal and colleagues, who were able to show good correlations in volume calculations between this technique and cardiac magnetic resonance imaging in normal subjects (75). In a follow-up study by the same group in patients with abnormal ventricles, using the same comparison, a bias of -28.4mL with limits of agreement of -95 to 38.2mL for end-diastolic volume were reported, with a bias of -13.1mL and limits of agreement of -66.7 to 40.5mL for end-systolic volumes (74). Although the bias is reasonably good in comparison to modern techniques, the limits of agreements for the measurements are considerably wide,

demonstrating a lack of reproducibility. This is most likely due to reduced image quality and errors in the interpolation of a 3D matrix from 2D images.

Overall, the widely documented underestimation of 3D ECHO semi-automatic volume calculation has been reported to be associated with an inability to distinguish between the comprehensive networks of muscle trabeculations that line the internal cavity of the left ventricle with that of the actual endocardial smooth muscle wall (51). However, in the dynamic phantom model, a consistent underestimation was still documented, particularly in the method void of manual corrections, even though the border was well defined with no trabeculations present. It is believed that the error reported from these experiments is due to an inability of the contour to fit to the abnormal shape of the phantom ventricle; this is an error in 3D ECHO volume calculations which has not previously been reported.

4.5 Limitations

In the dynamic heart phantom the true volumes were only measured between the largest and smallest volume of its cycle, indicating the volume changes between end-diastolic and end-systolic volumes. In clinical investigations, these are the two most important volumes used for diagnosing disease and monitoring disease progression; it was believed that these volumes and those in between would be the most important to focus on.

Throughout this study, the primary reader (reader 1) was of a novice experience level. This could have potentially underestimated the accuracy and reproducibility of the methods tested. However, in method A1 where the worst agreement was observed, the process of border contouring and volume calculation was largely automatic, which reduces the potential for reader variability. Furthermore, in method C the agreement was the highest, which is the technique most likely to be affected by user experience.

The anthropomorphic hydrogel heart was the only one used in the dynamic heart phantom for these experiments; thus, the data is limited to this particular sized ventricle. Future investigations would require testing in different sized and shaped ventricles to determine more specifically where limitations in the methods exist. There was also a limited cardiac output to the programmed routines used in this experiment.

The ejection fraction calculated by the true volumes was 15%, which is in the classification range of severely abnormal according to the American Society of Echocardiography and European Association of Echocardiography guidelines (23,24).

The heart rate used in the experiments was also fixed and not programmable, limiting the range of the current results. Future investigations should focus on different heart rate ranges, in particular the higher heart rates, where the temporal resolution is lower relative to the patient's intrinsic heart rhythm.

As with all ultrasound measurements, the accuracy of the volume calculations is subject to the quality of the image. In this study, the quality of image was excellent with near zero artefacts and very clear border delineation. However, there was evidence of signal quality reduction in the periphery of the sector–potentially affecting method C measurements in particular. This was the case due to the position of image acquisition (which resembles the parasternal long axis view in human studies) where the ultrasound beam is perpendicular to the LV wall at the centre of the sector and become more tangential towards the periphery of the sector (Fig. 4.28). In human studies, the image quality is worse in the basal planes when images are performed in the apical views. This is caused by a diversion of the scan lines at greater depths; most often a problem in the basal territory of human studies where by the view used to acquire images for MOD volume analysis would almost exclusively be the apical long axis position; the signal intensity also reduces as the depth of the signals increase, thus the territories (i.e. base) which are farthest away from the transducer will result in the poorest image quality.

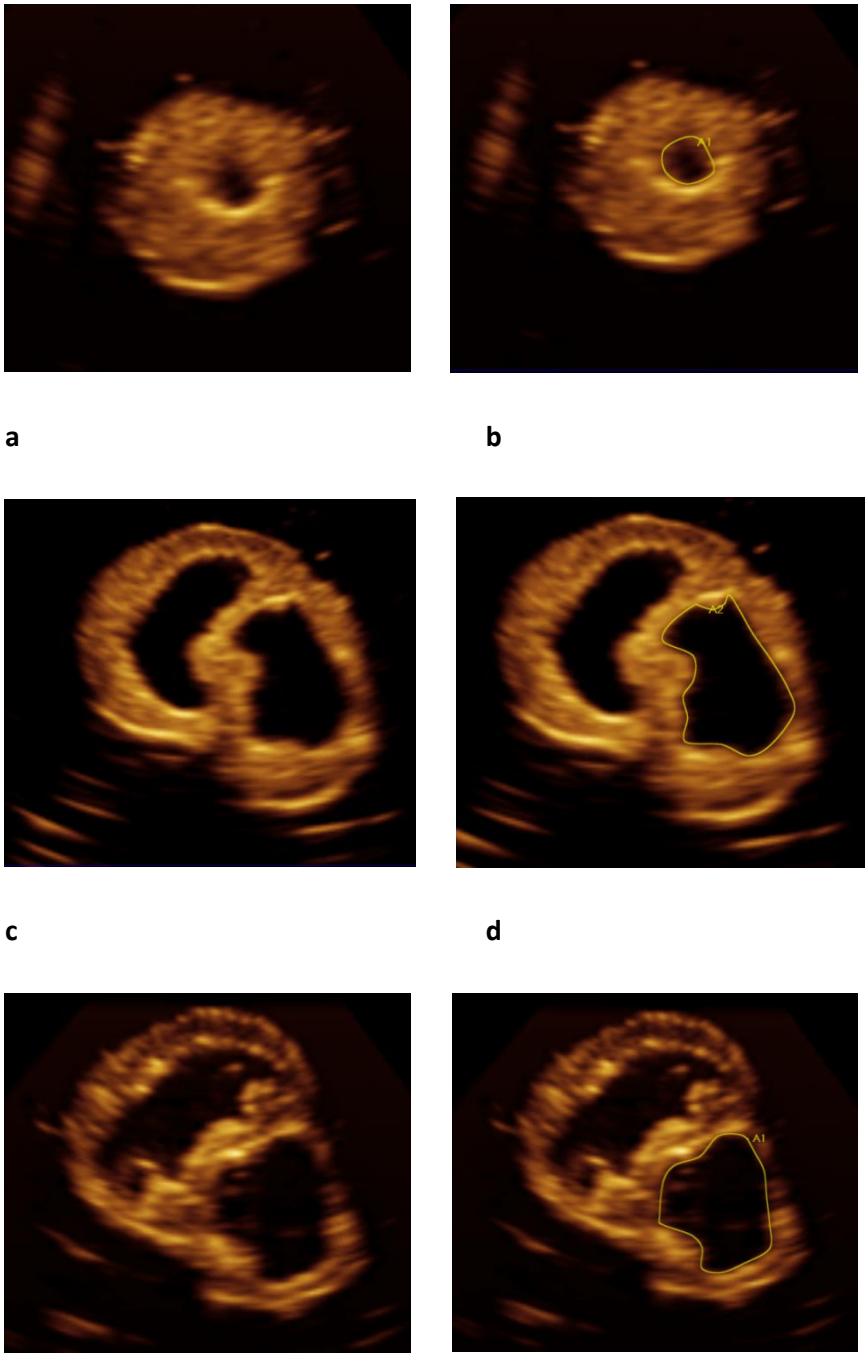

Figure 4.28 Short axis views demonstrating the difference in image quality between the slices from the centre of the ultrasound beam to the slices taken towards the periphery of the ultrasound sector. The endocardial definition is best in the centre, which facilitates manual tracing (c & d). Note the drop outs in the slices taken in the periphery (e & f) and the blurred display (a & b).

A limitation of method C in the human population will also be the identification of the basal border. In the phantom study, this was an easy task as the border is straight and flat. However, in a human study, the border is concave and may not be clearly identifiable in at least one of the long axis views, even in the higher quality images. Furthermore, the exact anatomical landmark at which to place the end basal slice will need to be identified. A comparison of studies between CMR and MOD would allow optimal methodology to be designed in human studies by assessing whether the basal slices should be placed inferior, in line with, or anterior to the mitral annulus.

MOD is a time consuming technique. It took approximately two hours to perform the volume calculations of one dataset for all volumes between and including the end-diastolic and end-systolic volumes. This equates to approximately 12 minutes per volume, which is too long for a period of analysis to add to the overall process of echocardiographic reporting; especially in light of the workload that the average echocardiography laboratory faces. In order to make 3D MOD work in clinical practice, the manual tracing needs to be replaced by an automated contour finding algorithm (see page 87).

4.6 The First Experimental Study: Conclusions

In a heart phantom with abnormal LV shape none of the tested methods for automated endocardial contour finding showed a complete fit with the endocardial borders despite optimal image quality. This is due to the fact that the algorithms used for automatic contour finding and manual correction seem to allow only ellipsoid shapes. Furthermore, the overall agreement with the true volumes worsened when manual correction was applied. This lack of agreement despite excellent image quality in an asymmetrical LV is a new error previously not identified by the literature or the governing bodies of echocardiography. Caution should be taken when using semi-automatic contouring algorithms in patient populations with large asymmetrical left ventricular aneurysms, as the underestimation in volume calculations is likely to be larger and less reproducible. The manual method of discs technique could be a potentially accurate technique in these patient groups, however, further studies need to be performed in human subjects.

Reference:

(1) Mor-Avi V, Jenkins C, Kühl HP, Nesser H, Marwick T, Franke A, et al. Real-Time 3-Dimensional Echocardiographic Quantification of Left Ventricular Volumes: Multicenter Study for Validation With Magnetic Resonance Imaging and Investigation of Sources of Error. J Am Coll Cardiol: Cardiovascular Imaging 2008 7;1(4):413-423.

(2) Herberg U, Brand M, Bernhardt C, Trier HG, Breuer J. Variables Influencing the Accuracy of 2-Dimensional and Real-time 3-Dimensional Echocardiography for Assessment of Small Volumes, Areas, and Distances. Ultrasound Med Biol 2011 July 01;30(7):899-908.

(3) Caiani EG, Corsi C, Zamorano J, Sugeng L, MacEneaney P, Weinert L, et al. Improved Semiautomated Quantification of Left Ventricular Volumes and Ejection Fraction Using 3-Dimensional Echocardiography with a Full Matrix-array Transducer: Comparison with Magnetic Resonance Imaging. J Am Soc Echocardiogr 2005 8;18(8):779-788.

(4) Jenkins C, Moir S, Chan J, Rakhit D, Haluska B, Marwick TH. Left ventricular volume measurement with echocardiography: a comparison of left ventricular opacification, three-dimensional echocardiography, or both with magnetic resonance imaging. Eur Heart J 2009 January 01;30(1):98-106.

(5) Coon PD, Pollard H, Furlong K, Lang RM, Mor-Avi V. Quantification of Left Ventricular Size and Function Using Contrast-Enhanced Real-Time 3D Imaging with Power Modulation: Comparison with Cardiac MRI. Ultrasound Med Biol 2012 Nov;38(11):1853-1858.

(6) Corsi C, Lang RM, Veronesi F, Weinert L, Caiani EG, MacEneaney P, et al. Volumetric Quantification of Global and Regional Left Ventricular Function From Real-Time Three-Dimensional Echocardiographic Images. Circulation 2005 August 23;112(8):1161-1170.

(7) Heyde B, Cygan S, Choi HF, Lesniak-Plewinska B, Barbosa D, Elen A, et al. Regional cardiac motion and strain estimation in three-dimensional echocardiography: a validation study in thick-walled univentricular phantoms. IEEE Trans Ultrason Ferroelectr Freq Control 2012 Apr;59(4):668-682.

(8) Lesniak-Plewinska B, Cygan S, Kaluzynski K, D'hooge J, Zmigrodzki J, Kowalik E, et al. A dual-chamber, thick-walled cardiac phantom for use in cardiac motion and deformation imaging by ultrasound. Ultrasound Med Biol 2010 Jul;36(7):1145-1156.

(9) P1E-1 Left Ventricular Phantom with Pulsatile Circulation for Ultrasound Strain Rate Imaging. Ultrasonics Symposium, 2006. IEEE; 2006.

(10) A new thick-walled hydraulic model of the left heart for the assessment of blood-wall interaction using ultrasound. Computers in Cardiology, 2004; 2004.

(11) Leeson P, Augustine D, Mitchel ARJ, Becher H. Echocardiography: Oxford Specialists Handbooks. 2012.

(12) Pattynama PMT, De Roos A, Van der Wall EE, Van Voorthuisen AE. Evaluation of cardiac function with magnetic resonance imaging. Am Heart J 1994 9;128(3):595-607.

(13) Jacobs LD, Salgo IS, Goonewardena S, Weinert L, Coon P, Bardo D, et al. Rapid online quantification of left ventricular volume from real-time three-dimensional echocardiographic data. Eur Heart J February 2006 February 2006;27(4):460-468.

(14) Leung KY, Bosch JG. Automated border detection in three-dimensional echocardiography: principles and promises. Eur J Echocardiogr 2010 Mar;11(2):97-108.

(15) Phillips Ultrasound. QLAB Advanced Quantification Software User Manual: Release 8.1. USA: Philips Medical Systems; 2010.

(16) Marsan NA, Westenberg JJ, Roes SD, van Bommel RJ, Delgado V, van der Geest RJ, et al. Three-dimensional echocardiography for the preoperative assessment of patients with left ventricular aneurysm. Ann Thorac Surg 2011 Jan;91(1):113-121.

(17) Gopal AS, Schnellbaecher MJ, Shen Z, Boxt LM, Katz J, King DL. Freehand three-dimensional echocardiography for determination of left ventricular volume and mass in patients with abnormal ventricles: Comparison with magnetic resonance imaging. J Am Soc Echocardiogr 1997 10;10(8):853-861.

(18) Zomorano JL, Bax JJ, Rademakers RE, Knuuti J. The ESC Textbook of Cardiovascular Imaging. Dordrecht, The Netherlands: Springer; 2010.

(19) Childs H, Ma L, Ma M, Clarke J, Cocker M, Green J, et al. Comparison of long and short axis quantification of left ventricular volume parameters by cardiovascular magnetic resonance, with ex-vivo validation. J Cardiovasc Magn Reson 2011 Aug 11;13:40-429X-13-40.

(20) Gopal AS, King Jr. DL, King DL, Keller AM, Rigling R. Left ventricular volume and endocardial surface area by three-dimensional echocardiography:

Comparison with two-dimensional echocardiography and nuclear magnetic resonance imaging in normal subjects. J Am Coll Cardiol 1993 7;22(1):258-270.

(21) Gopal AS, Shen Z, Sapin PM, Keller AM, Schnellbaecher MJ, Leibowitz DW, et al. Assessment of Cardiac Function by Three-dimensional Echocardiography Compared With Conventional Noninvasive Methods. Circulation 1995 August 15;92(4):842-853.

(22) Thavendiranathan P, Liu S, Verhaert D, Calleja A, Nitinunu A, Van Houten T, et al. Feasibility, Accuracy, and Reproducibility of Real-Time Full-Volume 3D Transthoracic Echocardiography to Measure LV Volumes and Systolic Function: A Fully Automated Endocardial Contouring Algorithm in Sinus Rhythm and Atrial Fibrillation. J Am Coll Cardiol: Cardiovascular Imaging 2012 3;5(3):239-251.

(23) Lang RM, Bierig M, Devereux RB, Flachskampf FA, Foster E, Pellikka PA, et al. Recommendations for chamber quantification. Eur J Echocardiogr 2006 Mar;7(2):79-108.

(24) Lang RM, Bierig M, Devereux RB, Flachskampf FA, Foster E, Pellikka PA, et al. Recommendations for Chamber Quantification: A Report from the American Society of Echocardiography's Guidelines and Standards Committee and the Chamber Quantification Writing Group, Developed in Conjunction with the European Association of Echocardiography, a Branch of the European Society of Cardiology. J Am Soc of Echocardiogr 2005 12;18(12):1440-1463.

5 Final Discussion and Summary

Echocardiography is the most cost-effective and available method of assessing left ventricular function in clinical diagnostic cardiology. The most important parameter that can be derived from this assessment is left ventricular ejection fraction, calculated from end-diastolic and end-systolic volume measurements. Due to the reliance of good acoustic windows and operator experience, the accuracy and reproducibility of echocardiography has been stringently validated; as is evident in the 18 scientific studies that were reviewed in Chapter 3.0. However, in recent years, with the development of 3D ECHO, evidence has demonstrated levels of accuracy and reproducibility much closer to that of the reference standard, cardiac magnetic resonance imaging (CMR).

The initial aim of this project was to determine the findings of the most recent literature comparing volume and ejection fraction calculations of all echocardiographic methods and CMR. A comprehensive review of the literature was already available by Dorosz and co-authors. Dorosz et al., however, did not include the absolute latest studies available; also absent was an assessment and discussion of the normal values of all techniques. The current review was able to determine clinically important disparities between different imaging modalities for normal LVEF and indexed (body surface area) volume ranges. These differences demonstrated an important lack of interchangeability of these measurements between different cardiac diagnostic modalities as well as different analysis packages within the same imaging modality, highlighting the necessity for use of the same diagnostic tool for follow-up measurements.

Following the literature reporting the normal values, studies investigating the accuracy of echocardiographic techniques were reviewed. As was expected, studies comparing 3D ECHO with CMR reported a higher accuracy than those looking at 2D ECHO. In order to improve the impact of the review, only studies including 30 patients or more were included. There were only three studies where a comparison of contrast 2D ECHO was made. Thus, a clear difference between contrast 2D ECHO and 3D ECHO was unable to be defined; however, it appears that 3D ECHO may be more accurate. There were only two multi-centre studies that had been performed: the first comparing contrast 2D ECHO (Hoffman et al.) and the second 3D ECHO (Mor-Avi et al.). Interestingly, the Mor-Avi study showed a worse agreement to CMR than the Hoffman study (Fig. 3.1-3.3). This was attributed to the lower experience levels by some of the centres, and highlighted the importance of user training and experience. The experience level of the users was most evident in end-diastolic volume (EDV) measurements, where a bias of -37mL (limits of agreement = -91 to 17mL) was reported by the most experienced group, which worsened to -89mL (limits of agreement = -155 to -23mL) in the least experienced group.

None of the studies calculated 3D ECHO volume in an anatomically accurate dynamic heart phantom where the method could be entirely scrutinized void of the common

limitations associated with all echocardiographic techniques, such as poor acoustic windows, soft tissue attenuation and unclear visualisation of endocardial borders. Furthermore, with the exception of one study, no studies investigated thoroughly the accuracy of the 3D ECHO volume calculation methods in irregularly shaped ventricles. This provided opportunity for the second part of this project: challenging the contour finding algorithm in 3D ECHO volume calculations using a dynamic heart phantom with an irregularly shaped left ventricle.

The anthropomorphic dynamic heart phantom, designed specifically for ultrasound interrogation, generated perfect image quality for testing of the 3D ECHO volume algorithms. The phantom provided small volume changes due to the nature of its hydrogel material (polyvinyl alcohol and graphite). However, this turned out to serve the purpose of the experiment further as it provided a multitude of asymmetric shapes throughout its contractile cycle. The four algorithms, which are described in Table 4.1 were quantitatively assessed on their accuracy in calculating volumes, and qualitatively assessed as to how well they fit to the endocardial border in all three windows of the quad screen display. A very good inter-observer variability was observed in both ventricular shapes that were severely asymmetric (bias = 1.79mL; limits of agreement = -1.57 to 5.19mL) and in shapes that were closer to a symmetrical (bias = 0.59mL; limits of agreement = -2.58 to 3.75mL) ellipsoid shape, likely due to the automatic nature of the algorithms. There was a good agreement in method A1 with the true volumes (bias =-12; limits of agreement = -20.4 to -3.6mL) in comparison with the clinical studies reviewed; however, this reduced with the introduction of manual correction. There was an overall lower agreement in the semi-automatic methods than one would expect in images of such high quality. These results, though, made sense when compared to the qualitative analysis, since in none of the studies did the contouring algorithm fit well to the inner border of the phantom. This is true even in the manual correction data where the border was made to fit reasonably well in the long axis views, yet still fit poorly in the short axis view. Thus, in the absence of poor endocardial border definition it is believed that a new error has been discovered which stems from the algorithms inability to deal with asymmetrically shaped ventricles.

It is clear that the error associated with poor endocardial border definition coupled with this newly discovered error resulting from the fixed framework of the contouring algorithms will compound the inaccuracy of 3D ECHO in patient groups, for example, those with large anterior infarcts. Thus, an alternative measurement tool needs to be investigated which would be most accurate in these patient groups. This led to the third study of the project: reintroduction of the manual method of discs technique (MOD). This technique, using the Philips QLAB software's ability to selectively slice the 3D volume into up to 16 difference partitions, allows direct contouring of the short axis slices identical to the CMR method of volume calculation.

MOD demonstrated high levels of accuracy in the phantom model both graphically (Fig. 4.21) and statistically (Bias =-0.42mL; limits of agreement = -6.15 to 5.31mL) in comparison with the true volumes (Fig. 4.27); furthermore, it showed excellent agreement between readers (Bias = 0.9mL; limits of agreement = -2.3 to 4.1mL). The possible limitations in human studies were discussed in Chapter 4.0, however, the phantom model experiments proved that the principle methodology is feasible and accurate; thus, human studies are warranted to identify the specific limitations and strengths of this technique in the clinical arena as a feasible LV volume measurement tool in patient types that have asymmetrical ventricles.

6 Future Investigations

Chapter 4.0 identified a newly discovered error in a commercially available semi-automatic contour algorithm which is a recommended tool for 3D ECHO LV volume and ejection fraction calculation by the American Society of Echocardiography and European Association of Echocardiography (1). This error demonstrates a limitation in the software to correctly follow the contour of a LV chamber of asymmetrical geometry. For this tool to be accurate in patient groups with cardiac anatomy reflective of the chamber structure of the phantom heart, the algorithm must be redesigned to be more accommodating of various shapes, instead of the ellipsoid shape which is mostly representative of healthy hearts. There is current work being performed by the Computer Science Department of the University of Alberta which will allow both contouring and volume calculations of any shape (Fig. 6.1). Semi-automatic contouring of this malleability would also allow accurate volume calculations of structures such as the right ventricle and both atria, to which the complex shape and structure of these chambers have proven difficult for accurate assessment using ultrasound (2-4).

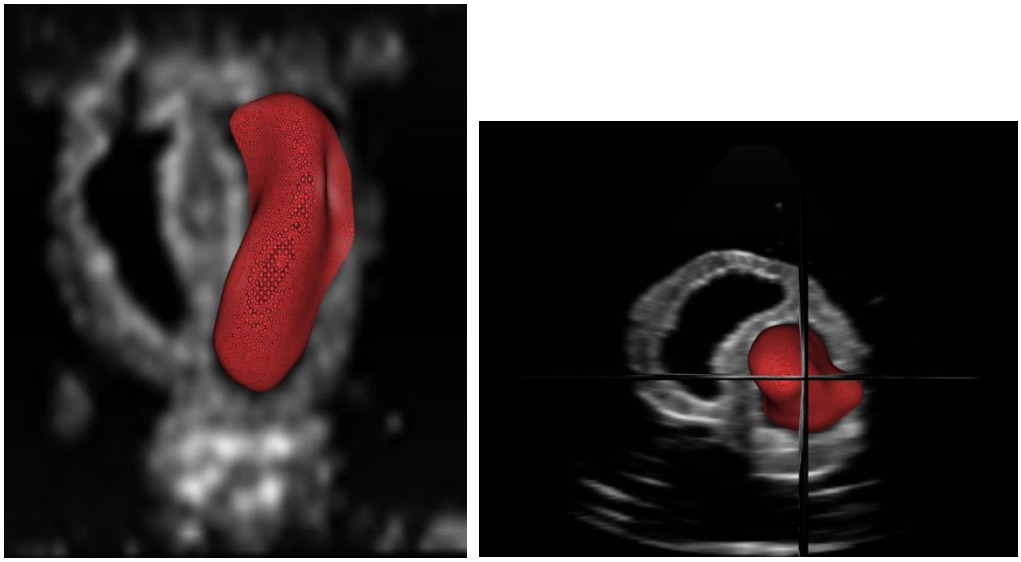

a **b**

Figure 6.1 Image of a segmentation algorithm for three-dimensional volume calculations which has no geometrical limitations to shape as displayed in the phantom dataset. a = Long axis view; b = short axis view. Image courtesy of Dr. Kumaradevan Punithakumar, Operational and Computational Director of the Servier Virtual Cardiac Centre at the Mazankowski Alberta Heart Institute.

Most importantly in the focus for future developments in echocardiography should be for the improvement of image quality in three-dimensional echocardiography (3D ECHO). A method which has been demonstrated, and is still being developed by our research group, is 3D ECHO image fusion (5-7). The premise is to improve image quality

by combining two or more 3D datasets. This has so far demonstrated two promising outcomes in its approach: 1) the fusion (i.e. summing of images) of specific structure focused images to create a dataset with a heart of high quality complete structures (as many 3D ECHO human images have wall drop-outs) and, 2) improvements in signal-to-noise ratio, which will assist in strengthening the clarity of borders and structures (Fig. 6.2).

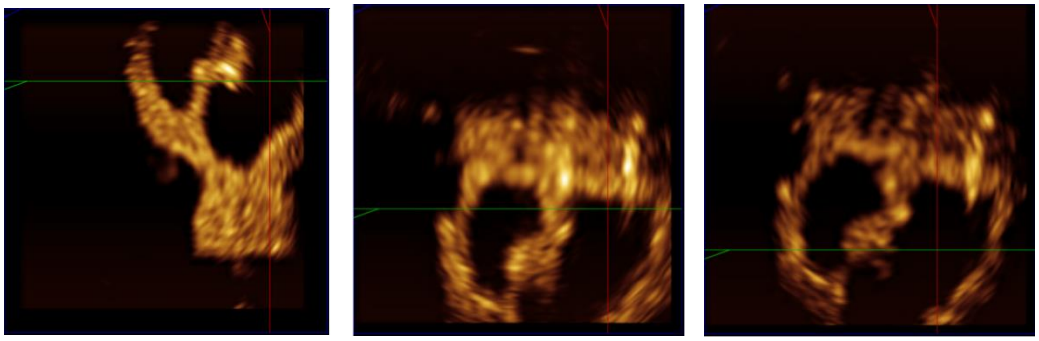

a **b** **c**

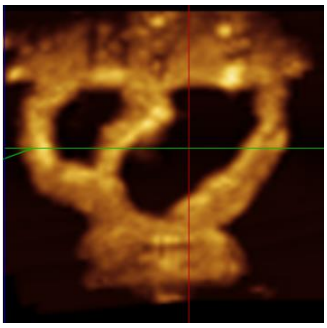

d

Figure 6.2 Fusion of three incomplete datasets (a-c) acquired in an anthropomorphic dynamic beating heart phantom and fused together to create a structurally complete image (d) of the heart. Images courtesy of Dr. Kashif Rajpoot (Assistant Professor, School of Electrical Engineering and Computer Science, National University of Science and Technology, Islamabad, Pakistan).

However, for the experiments on image fusion with the described heart phantom, the high level of image quality we have observed would be a limitation. A reduction in image quality was possible through two methods: the first involving reduction in the power of the scanner (Fig. 6.3b); the second used a thin (3mm) commercially available silicone layer (General Electric Silicone 2 Clear: Premium Waterproof Silicone) commonly used for sealing of home tiles and other home renovations (Fig. 6.3c &d) (8). The latter allowed excellent levels of ultrasound absorption while inducing no artefacts**.** In earlier trials of attenuation, layers of a gelatin-based material were tested; however, strong reverberation artefacts were generated from this material (Fig. 6.3e) (9). This was likely

due to a large difference in acoustic impedance between the gelatin layer and the plastic film used for the mimicking of an epidermal layer in the phantom viewing window. The silicone layer likely had an acoustic impedance much closer to that of the film leading to a significantly smaller amount of artefact. Using these methods of image attenuation in the phantom model will allow experimental testing of the fusion method for improving image quality, in turn, increasing the accuracy of volume calculations and other quantitative measures of cardiac function and performance.

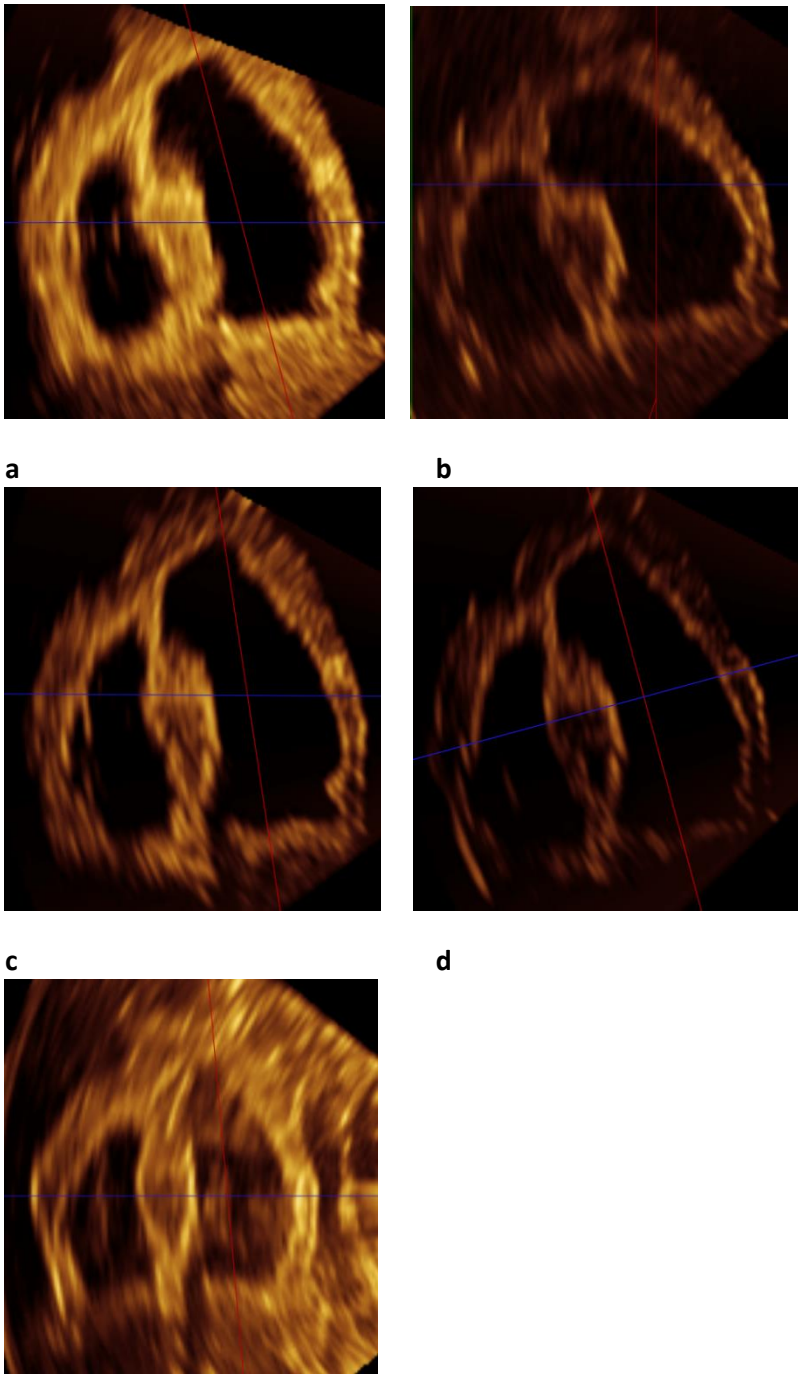

Figure 6.3 Images comparing the visual differences in image clarity between an image with a mechanical index of 1.2 and no attenuation layers (a), an image with a mechanical index of 0.1 and no attenuation layers (b), an image with a mechanical index of 1.2 and 3mm of 100% silicone attenuation layer (c), an image with a mechanical index of 1.2 and 6mm of 100% silicone layer (d) and an image with a mechanical index of 1.2 and 1.35cm of gelatin attenuation layer (e).

Finally, development of an automatic segmentation algorithm would prove advantageous for the MOD technique in order to reduce the amount of time taken in performing volume calculations using this method. Automatic segmentation of the 14 slices partitioned by the Philips QLAB software would not be a difficult algorithm to design as it would be asked to segment two-dimensional images. As a result, this tool would increase the utility of the software to the echocardiographer.

Reference:

(1) Lang RM, Badano LP, Tsang W, Adams DH, Agricola E, Buck T, et al. EAE/ASE recommendations for image acquisition and display using three-dimensional echocardiography. Eur Heart J Cardiovasc Imaging 2012 Jan;13(1):1-46.

(2) Rudski LG, Lai WW, Afilalo J, Hua L, Handschumacher MD, Chandrasekaran K, et al. Guidelines for the echocardiographic assessment of the right heart in adults: a report from the American Society of Echocardiography endorsed by the European Association of Echocardiography, a registered branch of the European Society of Cardiology, and the Canadian Society of Echocardiography. J Am Soc Echocardiogr 2010 Jul;23(7):685-713; quiz 786-8.

(3) Lang RM, Bierig M, Devereux RB, Flachskampf FA, Foster E, Pellikka PA, et al. Recommendations for Chamber Quantification: A Report from the American Society of Echocardiography's Guidelines and Standards Committee and the Chamber Quantification Writing Group, Developed in Conjunction with the European Association of Echocardiography, a Branch of the European Society of Cardiology. J Am Soc Echocardiogr 2005 12;18(12):1440-1463.

(4) Lang RM, Bierig M, Devereux RB, Flachskampf FA, Foster E, Pellikka PA, et al. Recommendations for chamber quantification. Eur J Echocardiogr 2006 Mar;7(2):79-108.

(5) Rajpoot K, Grau V, Noble JA, Becher H, Szmigielski C. The evaluation of single-view and multi-view fusion 3D echocardiography using image-driven segmentation and tracking. Med Image Anal 2011 Aug;15(4):514-528.

(6) Rajpoot K, Grau V, Noble JA, Szmigielski C, Becher H. Multiview Fusion 3-d Echocardiography: Improving the Information and Quality of Real-Time 3-D Echocardiography. Ultrasound Med Biol 2011 7;37(7):1056-1072.

(7) Szmigielski C, Rajpoot K, Grau V, Myerson SG, Holloway C, Noble JA, et al. Real-time 3D fusion echocardiography. J Am Coll Cardiol Cardiovasc Imaging 2010 Jul;3(7):682-690.

(8) Development of silicon-based materials for ultrasound biological phantoms. Ultrasonics Symposium (IUS), 2009 IEEE International: IEEE; 2009.

(9) Bude RO, Adler RS. An easily made, low-cost, tissue-like ultrasound phantom material. J Clin Ultrasound 1995 May;23(4):271-273.

Appendix A

Visual Show Automation (VSA): Operation Protocol

Remove protective cover from phantom servo and control console.

Attach power cables to appropriate ports – making sure everything is switched on and battery is connected.

Connect USB cable from PC computer where the VSA software is installed to the RAPU USB port (Fig. A).

- Tab next on remote advanced playback unit (RAPU) LED console screen (located on top of the phantom motor hub and control board) until the USB link is reached – hit enter (Fig. B). This should begin connection between workstation and console indicated by USB software installation and recognition at bottom right hand corner of computer screen.

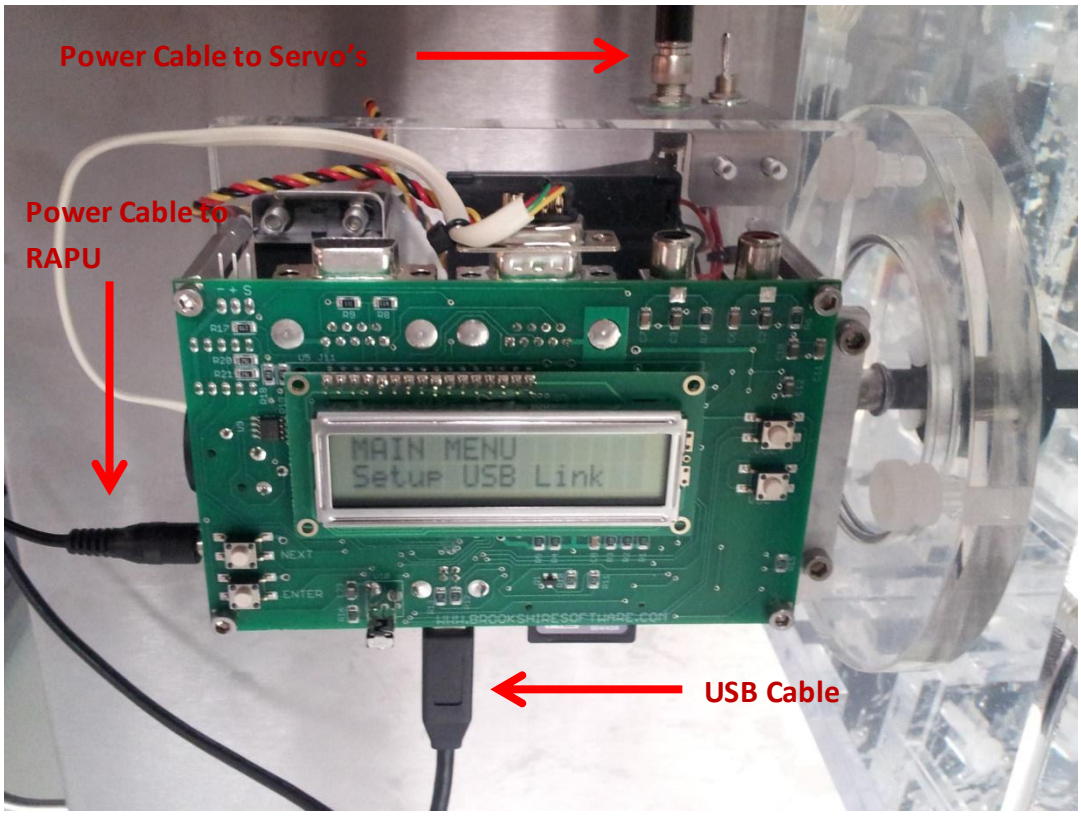

Figure A. Cable configuration for control hub. RAPU = Remote Advanced Playback Unit

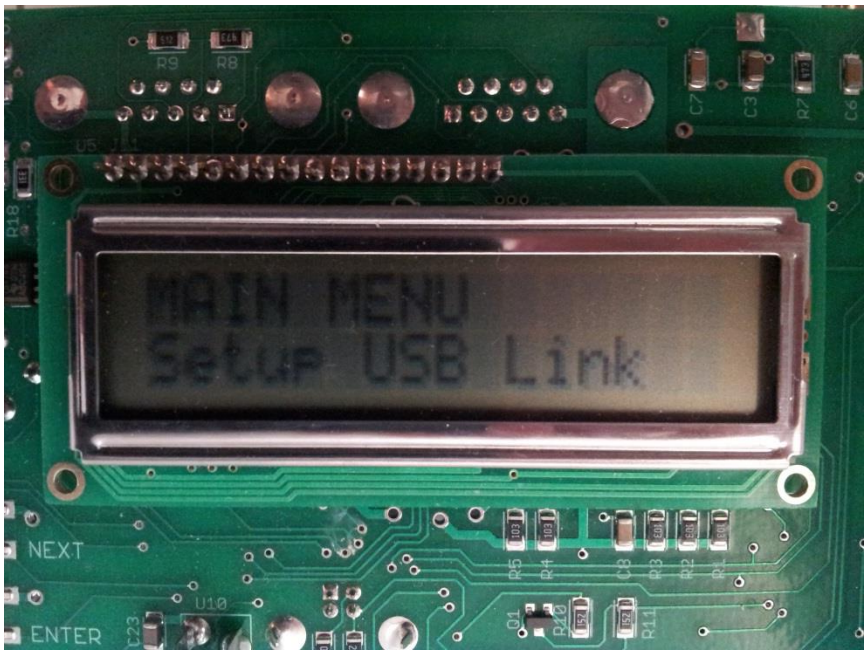

Figure B. Image of the remote advanced playback unit (RAPU) LED display.

Open VSA software on workstation:

- Under tools menu click on Settings
- Click on the device settings tab
- Lower left corner click on the hammer tool and select *invert enable*, unchecking all devices.
- Check device 0 and 1. Device 0 = Compression. Device 1 = Torsion.
- Change port setting for both devices by double clicking on column window and selecting RAPU1.
- Click ok.

Setting up workflow:

- Devices are shown in top left corner.
- Create your first phase by clicking next to Device 0 and dragging for an allotted period of time (shown below the phase windows).
- Double click on the highlighted bar to access event properties.
- By the dial control the position of the phantom is changed. In order to program the different steps of movement (event) click on stop position and select the desired angle on the clock face which correlates with the desired movement; click capture to set process.
- Repeat as many times as are required to create a full cardiac cycle. (You may cut and paste events accordingly)
- Repeat for device 1 in order to program torsion.